15:25:53 OCA PAD INITIATION - PROJECT HEADER INFORMATION 05/08/89

Active

Project #: E-25-565 Cost share #: E-25-215 — Rev #: 0
Center # : 116P5072-0A0 Center shr #: 111C5072-0A0 OCA file #:
Work type : SS
Contract#: LETTER DTD 4/11/89 Mod #: Document : GRANT
Prime #: Contract entity: GTRC

Subprojects ? : N
Main project #:

Project unit: ME Unit code: 02.010.126
Project director(s):
JETER S M ME (404)894-3211

Sponsor/division names: AM SOC HEAT REF AIR CON ENGR / ATLANTA, GA
Sponsor/division codes: 500 / 001

Award period: [illegible] to 900630 (performance) 900630 (reports)

Sponsor amount	New this change	Total to date
Contract value	6,000.00	6,000.00
Funded	6,000.00	6,000.00
Cost sharing amount		6,000.00

Does subcontracting plan apply ?: N

Title: APPLICATION FOR GRANT-IN-AID

PROJECT ADMINISTRATION DATA

OCA contact: David B. Bridges 894-4820

Sponsor technical contact

MARK FALLEK
(718)403-2628
GAS ENERGY
166 MONTAGUE STREET
BROOKLYN, NY 11201

Sponsor issuing office

WILLIAM W. SEATON
(404)636-8400
1791 TULLIE CIRCLE, N.E.
ATLANTA, GA 30329

Security class (U,C,S,TS) : U ONR resident rep. is ACO (Y/N): N
Defense priority rating : N/A supplemental sheet
Equipment title vests with: Sponsor GIT X

Administrative comments -
PROJECT INITIATION, $6000 FROM SPONSOR AND $6000 COST-SHARE FUNDS FROM MECH. ENGR.;

GEORGIA INSTITUTE OF TECHNOLOGY
OFFICE OF CONTRACT ADMINISTRATION

NOTICE OF PROJECT CLOSEOUT

RE527

Closeout Notice Date 07/19/90

Project No. E-25-565 Center No. 116P5072-0A0

Project Director JETER S M School/Lab MECH ENGR

Sponsor AM SOC HEAT REF AIR CON ENGR/ATLANTA, GA

Contract/Grant No. LETTER DTD 4/11/89 Contract Entity GTRC

Prime Contract No.

Title APPLICATION FOR GRANT-IN-AID

Effective Completion Date 900630 (Performance) 900630 (Reports)

Closeout Actions Required:	Y/N	Date Submitted
Final Invoice or Copy of Final Invoice	N	
Final Report of Inventions and/or Subcontracts	N	
Government Property Inventory & Related Certificate	N	
Classified Material Certificate	N	
Release and Assignment	N	
Other	N	

Comments

Subproject Under Main Project No.

Continues Project No.

Distribution Required:

Project Director	Y
Administrative Network Representative	Y
GTRI Accounting/Grants and Contracts	Y
Procurement/Supply Services	Y
Research Property Managment	Y
Research Security Services	N
Reports Coordinator (OCA)	Y
GTRC	Y
Project File	Y
Other	N
	N

Transient and Steady State Simulations of an Advanced Desiccant Enhanced Cooling and Dehumidification System Progress Report

by

Eileen Elizabeth Chant

Project No. E-25-565

June 29th 1990

TABLE OF CONTENTS

SUMMARY

In many air conditioning applications, the cooling and dehumidification coil is unable to properly meet the dehumidification requirements of the load. In any air conditioning process, the enthalpy change of moist air can be considered to have two components, the "latent" component at constant temperature, and the "sensible" component at constant moisture. The latent heat ratio of the load is defined as the ratio of the latent load to the total load. The latent heat ratio of the system is the ratio of the latent cooling to the total cooling performed by the cooling equipment. The latent heat ratio of a conventional cooling and dehumidification coil is often smaller than the latent heat ratio of the load. This mismatch is often ignored, which degrades the comfort conditions, or compensated with reheat, which degrades energy efficiency. The most efficient means of increasing the latent heat ratio is currently a heat pipe to exchange heat from the return air (upstream of the coil) to the downstream, supply air. A proposed cycle to be investigated, desiccant enhanced cooling (DEC), utilizes moisture exchange in a similar way that heat pipes use heat exchange to provide a better match between the latent load of the space and the latent load capabilities of the equipment. A rotary desiccant wheel, or moisture exchanger, is placed between the supply and return air. The return air picks up moisture from the wheel and the supply air deposits moisture to the wheel. Since the return air stream is now nearer to its dew point when it reaches the cooling coil, the coil performs increased dehumidification. After exiting the cooling coil, the supply air stream undergoes additional dehumidification as it passes through the desiccant wheel. The adsorption process in the wheel releases energy, thus effectively

providing free reheat to the moist air. The air leaving the desiccant wheel, headed for the conditioned space, now has the proper supply air conditions of low humidity and moderately low temperature which allow it to absorb the heat and humidity load of the space. In addition, the evaporating temperature of the vapor compression unit can be raised, increasing its efficiency.

Proper materials selection and design of this innovative technology require realistic simulations. It is anticipated that a various desiccant materials will be investigated for the proposed system. The current work considers methods to improve both the accuracy and efficiency of the needed simulation. A parabolic moisture concentration profile assumption that has proven to agree well with experimental adsorption data will be used to model the diffusion process inside the desiccant particle. This contrasts with an existing model, the pseudo-gas-side controlled model, which uses an empirically degraded lumped transfer coefficient approach to solve for the rate of adsorption. The use of the parabolic concentration profile is more suitable in modeling the adsorption process for a variety of materials than the lumped capacitance method as it proceeds from first principles after the concentration profile assumption. It is expected to increase the accuracy of the solution as the parabolic profile assumption more closely approximates the physics of the adsorption process. In addition, the resulting system of partial differential equations retains the same number of independent variables as the lumped transfer coefficient method. Both the transient and the periodic steady state solutions are of interest. The two solutions will be investigated to determine the most efficient way of simulating the system comprising the desiccant wheel,

cooling coil, and refrigeration cycle. If the integrated system proves through use of the transient model to respond much more quickly to changes in load than the rate at which the load changes, then it will be possible to use the periodic steady state solution to simulate the DEC system. The advanced model of this innovative concept will be used to assess desiccant enhanced cooling as an alternative to heat pipe technology and to evaluate preliminary design parameters.

The following reports on the state of the project. Development of the rotary desiccant wheel model is in its final stages. The development of the governing equations for the parabolic concentration profile model and the implementation of the model is described in Chapter 3. The model validation procedure is covered in Chapter 4. The first phase of the validation procedure was to compare the model with simple systems. The model was first compared with a rotary heat exchanger and a counterflow heat exchanger by setting the mass transfer coefficient to zero and setting the speed of rotation high in the case of the counterflow heat exchanger. The agreement with published heat exchanger performance data was excellent. The model was then compared with fixed bed adsorption experimental data and simultaneously compared with two other models; the pseudo-gas-side controlled model, and a model that accounts for solid side diffusion. The parabolic concentration profile shows good agreement with the experimental data and the solid side diffusion model. The commonly used pseudo-gas-side controlled model also shows favorable agreement. However, the parabolic concentration profile model has the advantage of incorporating a commonly available

property, the effective diffusivity, to account for the solid side diffusion process. The pseudo-gas-side model's empirically degraded mass transfer coefficient has been determined for a very few systems. As the research will investigate the effect of a variety of innovative desiccant materials on the proposed system's performance, the pseudo-gas-side controlled model is not feasible for the current study.

The model is then compared to the considerably more complex case of a rotary heat and mass exchanger. The results of this comparison were fairly favorable, however further work is required to quantify the results. Various convergence routines were attempted in order to speed up convergence to periodic steady state. None of the routines tried thus far have been entirely successful. The convergence routine attempts will not be addressed in this report. The results will be reported at a later date when this phase of the project is completed.

1. INTRODUCTION

1.1 Concepts

Use of desiccants for dehumidification purposes in air conditioning systems has been investigated in recent years. Desiccants are materials which upon contact with moist air at moderate temperatures exhibit a great affinity for water vapor. There are two main groups of desiccants: solids and liquids. Solid desiccants are porous materials. The water vapor molecules condense and adhere to the surface of the pores. This surface effect is called physical adsorption. Liquid desiccants incorporate the condensed water vapor molecules into their bulk. This volumetric effect is physical absorption. The term sorption has been adopted to describe both processes. Internal energy is released during the sorption process; consequently, warm humid air passed through a desiccant exits hot and dry. When the bed, or the solution in the case of liquid desiccants, has become saturated, hot air must be brought into contact with it to regenerate the desiccant.

The most common desiccant dehumidifier configuration is the rotary desiccant wheel. The current state-of-the-art rotary wheel consists of a spoked hub with tape wound around spacers, forming a parallel passage geometry. The surface of the tape is coated with a thin layer of a solid desiccant or impregnated with a liquid desiccant solution. See Fig 1. for illustration of the geometry of the parallel passage rotary desiccant wheel. This particular configuration along with laminar moist air flow is desirable due to [37] its relatively high mass

transfer to pressure drop ratio. Various research groups have directed considerable resources towards mathematical and experimental investigation of these systems. As a result of this effort, desiccant assisted cooling systems have proven to be economically beneficial in certain specialty applications as well as demonstrating an improved capacity to handle large latent loads compared with conventional vapor compression (VC) dehumidification equipment.

1.2 Applications

In many air conditioning applications, the cooling and dehumidification coil is unable to properly meet the dehumidification requirements of the load. The enthalpy change of moist air can be considered to have two components, the "latent" component at constant temperature, and the "sensible" component at constant moisture. The latent heat ratio of the load is defined as the ratio of the latent load to the total load. The latent heat ratio of the system is the ratio of the latent cooling to the total cooling performed by the cooling equipment. The latent heat ratio of a conventional cooling and dehumidification coil is often smaller than the latent heat ratio of the load. VC technology requires the coil temperature to be below the dew point of the moist air in order to perform dehumidification. In commercial applications, reheat is often applied to the cool and wet leaving air stream in order to maintain prescribed comfort requirements of the air-conditioned space. In residential applications, the mismatch of the system to the load is usually ignored.

The coil apparatus dew point (ADP) of the VC unit is determined by constructing a line on

the psychrometric chart through the return air state (state #2) and the supply moist air state (state #3) and extending the line to the saturation curve (See Fig. 12). A common model used to describe cooling coil performance considers the supply air state as a mixture of bypass air, which remains at the return air state, and the moist air that has passed through the cooling coil and has reached equilibrium with the cooling coil. In reality, the coil temperature varies along the length of the coil and the ADP is not the average temperature of the coil. It is a function of various parameters such as velocity of the air, coil depth, refrigerant temperature and entering air state. The ADP is actually an upper temperature limit for the cooling coil. Only in an ideal heat exchanger will the moist air reach equilibrium with the coil. In order to maintain prescribed comfort conditions, the actual coil temperature will be lower than the ADP temperature. As the ADP increases, the coefficient of performance (COP = cooling effect produced/work input) of the VC unit increases. It is desirable to have a VC unit operating at the highest possible ADP as this will increase the system efficiency.

When large latent loads are present, the VC equipment is incapable of meeting the space conditioning requirements. For example, a standard VC unit processing 50% relative humidity air falls short of providing the space dehumidification requirements when the latent load fraction is 0.4 [14]. Even with an ADP of 40°F, the VC system does not meet the latent load and overcools the air. In addition to not properly meeting the load requirements, lowering the ADP causes the VC unit to operate at a low COP. For this reason, desiccant assisted cooling systems (DACS) have demonstrated technical feasibility and have been found to provide better humidity control than VC units in situations where large latent loads occur

[19], and [44].

Achieving lower humidity in a conditioned space is desirable in many industrial applications and processes. Product quality improves with lower relative humidity in production and storage of many items. For example, relative humidities of 10% are required for manufacture and storage of some pharmaceuticals [3]. Other industries, such as food and beverage production, electronics, chemicals, rubbers, plastics, metals, glass, cosmetics, and many others use depressed humidity levels during manufacture and storage of their products.

Supermarkets applications of DACS have achieved a fair amount of success. Some of the reasons that supermarkets are good candidates for DACS include the high latent-to-sensible load that the supermarket experiences due to the sensible heat absorbed by the open food refrigeration cases and the large amount of traffic experienced by the supermarket. Lower humidity levels reduce frost buildup on the food, require less work for the refrigeration cases and fewer defrost cycles, and increase the shelf life of food. Cargocaire Corporation began marketing a commercial hybrid desiccant cooling system designed for supermarkets applications in 1985. There are currently 135 of these units operating in supermarkets around the nation. Table 1.1 lists some supermarket chains which install the hybrid desiccant cooling system in all new supermarkets and major renovations in the regions indicated [20], [5] and [42]. In 1988, Cargocaire's hybrid desiccant system sales were 250 percent higher than those of 1987 [5].

Table 1.1 Supermarkets which routinely install hybrid desiccant cooling systems in all new stores [5]

Chain	Location
Winn-Dixie	Florida
H.E. Butt	Texas
Big Bear	Columbus, Ohio
Bormans	Detroit, Michigan
Allied	Detroit, Michigan
Pick and Save	Michigan
Air Force Commissary	Hybrid systems are chosen depending on location

Desiccants have been found to act as a good filter for contaminants [40]. In addition to removing particulate contaminants, vapor contaminants are condensed out of the air. Desiccants are effective in removing carbon monoxide, nitrogen dioxide, and sulfur dioxide [40]. The adsorption capacity that desiccants have for pollutants and the subsequent effect on performance will be further quantified by research underway at the Solar Energy Research Institute and the University of Wisconsin. This attractive feature of desiccants increases the motivation to use them in HVAC systems as indoor air quality is an emerging important topic in space conditioning. As air-tightness increases, which is the current trend in energy efficient architecture, the contaminant problem as well as the moisture problem will be exacerbated.

2. RELEVANT PRIOR WORK

2.1 Developments in Desiccant Technology

There are two major types of desiccant systems described in the literature: hybrid and Pennington cycles. The Pennington cycle, first developed by Neal Pennington in 1952 [52], consists of a desiccant dehumidification stage followed by heat exchange with the ambient air. The purpose of these initial stages is to artificially increases the wet bulb depression. A stage of direct evaporative cooling is applied to the warm, dry air to supply cool, moist air to the conditioned space. The hybrid cycles incorporate a VC unit with a desiccant wheel to provide independent control of wet bulb and dry bulb temperature. The hybrid cycles sometimes use evaporative cooling to minimize compressor work, and also have the option of using compressor and/or condenser waste heat to partially supply regeneration energy to the desiccant. The Pennington and hybrid cycles vary in the amount of recirculation and ventilation air that is processed. See Fig. 2a and 2b for illustrations of a Pennington cycle and a hybrid cycle.

The previously discussed desiccant hybrid cooling system for supermarket applications was developed with GRI support and marketed by Cargocaire [1] and [48]. The system integrates a downsized conventional VC unit with a desiccant wheel. The sensible load is carried by the VC unit as well as an indirect evaporative cooler, and the latent load is carried by the dehumidifier wheel. Gas fired heat is used to regenerate the bed.

Calton [11] completed a field analysis of one of these systems in a 56,000 sq-ft store. The airflow requirements in the store from use of the system was reduced from 1 to 0.42 cfm/sq-ft. This lower airflow rate resulted in initial ductwork installation and materials savings that suggest immediate payback in installation of this type of system.

Burns, Mitchell and Beckman [10] considered three different hybrid desiccant systems and performed a computer simulation of each system's performance in a supermarket application. The three cycles have variations on the amount of recirculation air that is processed as well as usage of waste condenser heat for regeneration of the bed. In this study, all the cycles examined were discovered to be strong alternates to VC space conditioning.

Manley, Bowlen and Cohen [30] formulated and performed a computer simulation using field testing results in order to extend the performance of the supermarket systems to various climates, desiccant system types, and store types. The gas fired desiccant system was found to be attractive in humid climates. A gas fired desiccant HVAC system optimization was discussed. All of the optimization suggestions have since been incorporated into Cargocaire's hybrid system.

Significant effort has been expended in minimizing pressure drop through a solid desiccant dehumidifier. A rotary desiccant wheel with highly uniform passages is desirable as it will have a lower pressure drop than a wheel with a wide variation in the passage size. The ratios of the Stanton number for heat (St_h) and mass (St_m) transfer to friction factor (f) are often

used as one of the preliminary design consideration in a desiccant bed. The St_h/f and the St_m/f are dimensionless parameters which represent the ratio of heat transfer to pressure drop and the ratio of mass transfer to pressure drop, respectively. The desired effect is high ratios. Table 2.1 lists the St/f ratios that have been obtained for various configurations at different facilities:

Table 2.1 Experimental St_h/f and St_m/f By Various Researchers [37]

Researcher	Desiccant Bed Description	St_h/f	St_m/f
Pla-Barby et. al	Packed thin particle bed	0.06	0.02
IGT	Corrugated fiber material impregnated with molecular sieve particles	0.32*	0.21*
IIT	Parallel wall configuration silica gel sheets	0.49*	0.20
UCLA/SERI	Parallel passage config. with silica gel bonded to polyester tape	0.49*	0.40**

* Constant heat flux conditions

** Projected value

The COP of DACS such as the Pennington cycles in recent years have become similar to those of the absorption cycle COP. However, the desiccant assisted cooling systems have the advantage of requiring lower grade thermal energy than the absorption chiller. For silica gel, an adiabatic desiccant wheel often produces a maximum COP when the regeneration temperatures are 60°C to 80°C [44]. These temperatures are compatible with flat plate solar collector technology and can partially be supplied by waste condenser heat.

Table 2.2-COP's experimentally obtained for Pennington cycle DACS [43] and [55]

Researcher	COP_{th}	COP_{elec}	Approximate Date
IGT Solar MEC I	.45	---	1970
IGT Solar MEC III	.46	8.0	1970's
AiResearch	.60	5.8	1970's
IIT	.60	---	1970's
IGT HCOP	.95	6.2(Computer Projection)	1970's
ASK	1.00	---	1980
SERI	1.07	7.2(Computer Projection)	1980's
EXXON/GRI	1.05	5.4	1983

Table 2.2 lists experiment COP's for Pennington types cycles obtained various researchers. These results have been achieved in either field or laboratory conditions. Both SERI and EXXON project a COP of 1.3 [43] and [55] by about 1990. The improvements that SERI and EXXON plan to incorporate to achieve this include using other types of silica gel that are not currently commercially available, using unequal flowrates for the process and regeneration period, and recycling some of the hot process air for the regeneration period [55].

Yearly simulations were performed on a solar fired desiccant cooling system [34] by Nelson, Beckman, Mitchell and Close based on an effectiveness-NTU (NTU = number of transfer units, see Table 3.1) model for the dehumidifier wheel. This model is discussed in the following section. Component models of the recirculation and ventilation systems were developed for use with TRNSYS. Results of the six month simulation give a COP ranging from .67 to .79 with a variable collector area.

Significant gains have been made in optimizing the rotary desiccant wheel. Some general conclusions of the optimization studies are that a parallel passage laminar flow rotary

desiccant wheel with high passage uniformity is desirable for pressure drop considerations. Small desiccant particles such as microbead silica gel are also desirable as they effectively transfer moisture yet decrease pressure drop through the wheel. Many promising new desiccant materials have been recently introduced. Other performance advances have been achieved through the use of desiccants that minimize regeneration temperature. The currently marketed DACS do not use these optimized wheels, however a small market has been found for the commercially available rotary desiccant dehumidifiers. The fundamental design concepts of the rotary desiccant wheel have been developed. The technology is ready for development of innovative applications of desiccant technology such as the proposed desiccant enhanced cooling system.

2.2 Mathematical Models

The solid desiccant rotary wheel and the fixed bed have been modeled in a variety of ways. The mass and energy conservation equations are developed as well as the rate equations at the solid-moist-air interface. The models that account for gas and solid side resistance consider mass conservation equations for the fluid phase as well as diffusion in the solid. Many alternative models neglect the transfer process within the desiccant and consider the model to be gas side controlled. For the models that consider fluid phase resistance only, the mass transfer coefficient combines the effect of the air boundary layer mass transfer barrier and the intraparticle diffusion resistance in order to account for neglecting the gradients that surely exist in the solid phase. With this correction for solid side resistance in the gas phase, such a model is termed a pseudo-gas-side controlled model. Most of the models in the literature assume that the local rate of adsorption is proportional to the difference between

the free stream humidity ratio and the humidity ratio of a hypothetical moist air layer that is in equilibrium with the desiccant particle. This equilibrium model is valid [29] in modeling adsorption processes in which the particle is small and the mass flow rate of the air is low. Low flow rates allow more time for the moist air at the desiccant-moist-air-interface to approach equilibrium with the particle. Particles size is also important in the equilibrium theory as the particle diameters must be sufficiently small to neglect the concentration gradient that exists in the axial direction for both the desiccant bed and the moist air [42]. Both these requirements hold true for high performance rotary desiccant wheels designed to minimize pressure drop.

Carter [11] developed the conservation and rate equations for simultaneous heat and mass transfer in a desiccant bed. The rate equations are gas and solid side resistances for mass transfer and gas side for heat transfer. The diffusion equation is written for the desiccant granules. His numerical solution employed a modified Euler method. An experiment of a fixed bed was carried out and there was shown to be some discrepancy between theoretical and experimental results.

Bullock and Threlkeld [8] have developed a nonlinear numerical solution to the governing heat and mass transfer equations for pseudo-gas side controlled model. A predictor-corrector numerical procedure is utilized. The shapes of the experimental and theoretical outlet air state curves were similar.

R.B. Holmberg [21] considered the pseudo-gas-side controlled model and used a Crank-

Nicholson implicit numerical scheme for the periodic steady state case. The Gauss-Seidel convergence technique was used for iterative solution of the bed and fluid state.

Maclaine-cross developed a finite difference program called MOSHMX [46] for the pseudo-gas-side controlled model. The numerical scheme used is a second order Runge-Kutta for solution of the bed and fluid states. MOSHMX is also used to obtain periodic steady state through successive simulation of the wheel until steady state operation is reached. A Newton-Raphson method is sometimes used to speed up the rate of convergence [46].

Lavan and Mathiprakasam [32] obtained linearized solutions for the governing equations for the pseudo-gas-side controlled model. The linearized solutions are found to agree well with the nonlinearized numerical solutions. The linear model saves significant computing time. SERI has also developed several different types of models including a gas-side controlled model and a gas and solid side controlled model for an isothermal bed [37].

An upper limit of performance for the rotary dehumidifier wheel can be established by analysis of a dehumidifier wheel idealized with respect to transport phenomena. For the gas side controlled model, this idealization results in the assumption that the heat and mass transfer coefficients are infinite in the fluid. The model therefore assumes no temperature or concentration gradients perpendicular to the flow. The modeling for this ideal wheel was developed by Close and Banks of the Commonwealth Scientific and Industrial Research

Organization (CSIRO) in Australia. This model [4], [12] and [28] combines temperature and humidity ratio into two independent potentials. The potentials are functions of the state properties of the air-water vapor-matrix system. When the conservation equations are written in terms of these potentials, the two equations become uncoupled, two-dimensional hyperbolic wave equations. The resulting differential equations are solved via the method of characteristics. Lavan, Monnier, and Worek [26] also conducted an analysis in which a reversible desiccant cooling system was studied in order to determine upper limits on the performance of the system. The reversible thermal COP for the dehumidifier wheel coupled with evaporative cooling system was 4.66 for typical values of ambient humidity.

Van Den Bulck, Mitchell, and Klein [50] present the wave theory for the ideal dehumidifier and, using Jurinak's [23] independent potentials developed for silica-gel-air-water vapor, solve for the outlet regeneration and dehumidification states of an ideal dehumidifier. Operating charts were developed for various conditions. The independent potential charts have been developed by Maclaine-cross for lithium bromide, lithium chloride, and calcium chloride. Van Den Bulck, Mitchell and Klein [50] combined the results of the wave theory operating charts and developed expressions for enthalpy effectiveness and moisture effectiveness. The effectiveness expressions define the moist air outlet state of the real dehumidifier relative to the moist air outlet state of the idealized dehumidifier described in the preceding paragraph. Once the dehumidifier effectiveness is determined and the outlet state of the idealized dehumidifier is solved, the outlet state of the moist air is known. The

moisture effectiveness expressions are arrived at by analogy with an expression for effectiveness of a heat transfer alone rotary regenerator developed by Shah [45]. These correlations are reportedly valid [50] over a wide range of operating conditions.

The literature widely utilizes the pseudo-gas-side controlled model in the case of thin desiccant beds in which the lumped transfer coefficient is well known. This model, however, is not valid in cases where the performance of new desiccants is investigated. The solid and gas side controlled model is appropriate in the investigation of new materials. Yet consideration of the diffusion inside the particle adds a third independent variable to the problem. The solution is further complicated as the order of the system of partial differential equations increases from one to two due to the diffusion term in the solid phase.

3. RESEARCH PLAN

In recent years, there have been advances in gas-fired desiccant cooling technology. Minimal attention to electric specific applications has been seen. As previously demonstrated, gas fired desiccant cooling technology has attracted a small market. The continuing need to improve the efficiency of cooling equipment and to improve dehumidification performance of vapor compression equipment introduces unique and novel problems. A new and creative application of desiccant technology can potentially resolve some of the load mismatch that occurs in vapor compression technology between the latent load of the space and the latent load of the equipment.

The cycle to be investigated, DEC, places a desiccant wheel between the return and supply air stream in order to perform moisture exchange between the two air streams. The concept is analogous to heat pipe technology which performs heat exchange between the two air streams in order to provide a closer match between the latent load of the space and the latent load capabilities of the equipment. Evaluation of the DEC system via simulation requires modeling. The model used will assume a constant hourly heat and moisture load in the conditioned space. A constant load ultimately leads to a steady state operation of the system. Initially, a transient model will be developed for simulation of the system. If the transient model reveals that the load is massive and slowly changing compared with the response time of the DEC system, the periodic steady state solution will be sought as an additional simulation tool.

In modeling of the DEC cycle, it is anticipated that both transient and steady state system simulations will be necessary for this study. The transient simulation is an explicit problem, and the periodic steady state simulation is an implicit problem. In the periodic steady state problem, the bed state at the beginning of the process period is not known and must be assumed. When the integration of one revolution of the wheel is completed, a new state for the initial state of the desiccant bed has been calculated. If the calculated state differs from the assumed state, a new initial bed state is assumed and the integration is repeated until the calculated bed state equals the assumed state. A variety of algorithms are available to calculate the new "guess" of the bed state and these will be mentioned subsequently. The model developed will differ from the previous developed rotary desiccant dehumidifier wheel models in that a parabolic concentration profile assumption is used to model the mass transfer process in the solid phase. The model developed will be integrated into a VC model and system simulations performed. Preliminary design parameters will be investigated.

3.1 Solid Rotary Desiccant Wheel

i. Model Improvement-The Parabolic Concentration Profile Assumption

The most common model in the literature for thin desiccant beds is the pseudo-gas-side controlled model. An experimentally determined mass transfer coefficient is used which is somewhat lower than an air side mass transfer coefficient in order to account for the diffusion resistance in the desiccant particle. This type of model can produce significant [36] error, up to 30%, in outlet moisture concentration over time for regular density silica gel when

compared with the model that accounts for a concentration profile in the particle. It is proposed to model the diffusion in the silica gel particle with a parabolic concentration profile. The parabolic profile assumption is intuitive, remarkably simple, and has been observed experimentally. An assumed quartic [14] concentration profile has been investigated, but the conclusions were that the slight gains in accuracy were not sufficient to compensate for the lost simplicity. The parabolic concentration profile assumption in adsorption studies has been shown to produce excellent agreement with the exact solution [14] except for an initially small time period when the profile is developing. The parabolic profile assumption solution also has compared favorably with Rosen's dynamic, linear adsorption model which considers both film and intraparticle resistances. Rosen's rigorous solution, presented in 1951, is now considered the classical solution to fixed bed sorption [41].

The conservation of mass and energy equations for the gas side controlled parallel passage wheel are developed through the use of the following major assumptions and simplifications that are currently used in rotary desiccant wheel models:

Geometric symmetry allows the following two simplifications:

1. No radial variation in moist air properties are considered.
2. No radial variation in desiccant properties are considered.

General properties of desiccants and moist air support the next assumptions:

3. Free pore volume of the desiccant is negligible when compared with the passage volume. Hence storage capacity of moist air entrained in the

matrix is neglected.

4. Negligible axial conduction of heat or moisture compared with the forced convection rate.

5. The tranverse temperature gradients inside the desiccant bed are neglected.

6. Velocity of dry air is constant.

7. Heat transfer coefficients and density of moist air are constant.

8. Moist air is an ideal gas mixture.

The mass transfer process can be modeled with the following final assumptions:

9. A layer of moist air exists at the surface of the desiccant particle in equilibrium with the local moisture content of the desiccant particle.

10. Mass transfer potential can be described by local differences in humidity ratio (i.e. a modified Fick's Law approach).

Fig. A1 in the appendix illustrates the control volume used in development of the conservation equations and Table 3.1 describes the nomenclature. The appendix describes the development of the conservation equations. After application of the above assumptions and simplifications, the simplified conservation of mass equation is:

$$\frac{\partial w}{\partial z} + \beta_j \frac{M_{dd}/\theta}{\dot{m}_{da,j}} \frac{\partial W_d}{\partial \tau} = 0$$

and the simplified conservation of energy equation is:

$$\frac{\partial i}{\partial z} + \beta_j \frac{M_{dd}/\theta}{\dot{m}_{da,j}} \frac{\partial I}{\partial \tau} = 0$$

For the constant heat transfer coefficient assumption, the heat transfer rate equation is:

$$\partial i/\partial z = NTU_{q,j}\, c_p\, (T_e - T) + i_{fg}\, \partial w/\partial z \qquad (1)$$

Substituting the heat transfer rate equation into the conservation of energy yields the following expression for the rate of enthalpy change of the bed:

$$\partial I/\partial \tau = -1/(\beta_j\, \Gamma_j)\, \{\, NTU_{q,j}\, c_p\, (T_e - T) + i_{fg}\, \partial w/\partial z \,\} \qquad (2)$$

For a simplistic pseudo-gas-side controlled model, the mass transfer rate equation is:

$$\partial w/\partial z = NTU_{m,j}\, (w_e' - w) \qquad (3)$$

Substituting the mass transfer rate equation into the conservation of mass yields the following expression for the rate of change of moisture content of the bed:

$$\partial W_d/\partial \tau = -1/(\beta_j\, \Gamma_j)\, NTU_{m,j}\, (w_e' - w) \qquad (4)$$

Where $\Gamma_j = (M_{dd}\, /\dot{m}_{da,j}\, \theta)$. This expression, after converting all nondimensionalized independent variables to dimensional variables results in the following mass transfer rate equation:

$$\partial W_d/\partial t = -h_m'\, \alpha\, L/\, \beta_j\, M_{dd}\, (w_e' - w) \qquad (5)$$

As the variable α is the surface area of desiccant per unit length, the term α L is an effective surface area of the rotary desiccant wheel.

The proposed model differs from the pseudo-gas-side controlled model at this last equation. The additional assumption of the proposed model is that a parabolic concentration profile exists at all times in the desiccant particle. Fig. 3 illustrates the assumed concentration profile:

$$W = a_1 + a_2\, (r/R)^2$$

Where W denotes the local moisture content of the particle. The conservation of mass equation for diffusion of moisture in spherical coordinates assuming radial symmetry can be written as:

$$\partial W/\partial t = 1/r^2\, \partial\{r^2 D\, \partial W/\partial r\}/\partial r \qquad (6)$$

The boundary conditions are first from continuity of mass transfer at the surface of a spherical particle of radius R:

$$- \rho_p\, D\, \partial W/\partial r\big|_{r=R} = h_m\, (w_e - w)$$

and secondly from symmetry at the center of the sphere:

$$\partial W/\partial r\big|_{r=0} = 0$$

The initial condition can presume a uniform state:

$$W[r,t=0] = W_o[r]$$

Differentiating the assumed parabolic profile and inserting the first boundary condition into the results, the rate equation at the surface of the particle becomes:

$$\partial W/\partial r\big|_{r=R} = 2\, a_2\, (R/R^2) = 2\, a_2/R = - h_m\, (w_e - w)/(\rho_p\, D)$$

At the surface of the particle, the local moisture content is:

$$W[r=R] = a_1 + a_2 \qquad (7)$$

The average moisture content of the particle can be found through integration of the parabolic profile over the volume of the particle and dividing by the total volume of the particle and is:

$$W_d = a_1 + 3/5\, a_2$$

or rearranging:

$$a_1 = W_d - 3/5\, a_2$$

Substituting the above expression for a_1 into Equation (7), the new expression for local

moisture content at the surface of the particle becomes:

$$W[r=R] = W_d + 2/5\, a_2$$

The humidity ratio of the moist air in equilibrium with the surface of the desiccant particle is evaluated using the surface moisture content of the particle, i.e. $w_e = w_e[W_d+2/5a_2,T]$. Substituting this into the rate equation at the surface of the particle, a nonlinear expression for a_2 results:

$$a_2 = -(h_m R)/(2 \rho_p D) \{w_e[W_d+2/5a_2,T] - w\}$$

where a_2 must be solved for in order to find $\partial W/\partial r\big|_{r=R}$. Once a_2 is solved by iteration, then integrating Equation (6) over the volume of the particle to find the volumetric average of the rate of change of moisture content of the particle yields:

$$\partial W_d/\partial t = (3/R)\, D\, \partial W/\partial r\big|_{r=R} = (6/R^2)\, D\, a_2 \qquad (8)$$

Further substituting the nonlinear equation for a_2 into Equation (8) yields:

$$\partial W_d/\partial t = -(6/R^2)\, D\, h_m R/(2 \rho_p D) \{w_e[W_d+2/5a_2,T] - w\}$$

$$= -(3\, h_m/ \rho_p R) \{w_e[W_d+2/5a_2,T] - w\}$$

For a spherical particle, the particle density is:

$$\rho_p = M_{particle}/V = M_{particle}/(4/3\, \pi R^3)$$

Substituting this expression into the rate equation yields:

$$\partial W_d/\partial t = -(3\, h_m\, 4/3\, \pi R^3/ M_{particle} R) \{w_e[W_d+2/5a_2,T] - w\}$$

$$= -(4\, \pi R^2 h_m/ M_{particle}) \{w_e[W_d+2/5a_2,T] - w\}$$

Noting that the surface area of a spherical particle is $A_s = 4\, \pi R^2$ yields:

$$\partial W_d/\partial t = -(h_m A_s/M_{particle}) \{w_e[W_d+2/5a_2,T] - w\} \qquad (9)$$

Equation (9) is the nonlinear mass transfer rate equation which will be substituted for the widely used lumped capacitance constant coefficient rate equation. The analogy between Equation (5) and (9) is apparent when the two are compared. The parabolic profile

assumption has been reported to be valid in the modeling of adsorption processes [2], [15], [27] and [41]. This model proceeds from first principles after the initial assumption of the parabolic profile. The effects of diffusion are incorporated into the solution utilizing a method that has proven accurate, yet the computational cost of the solution of the system of equations increases very little when compared to the pseudo-gas-side model. The system of equations remains first order with two independent variables. The extra computational cost lies in the solution of a nonlinear rate equation versus a linear one.

The DEC system to be investigated operates under different regeneration conditions as a conventional desiccant assisted cooling system. As the DEC operating conditions vary greatly from the conventional desiccant enhanced cooling cycles, materials other than silica gel will be investigated to determine the type of desiccant that is most appropriate for DEC. An arbitrarily lumped mass transfer coefficient is of questionable accuracy and is also not available for many desiccants. As the diffusivity of adsorbents is a commonly available property, the parabolic profile model is more suited for this application.

Table 3.1-Nomenclature Used in Development of Governing Equations

$A_s = (4 \pi R^2)$ = Surface area of a spherical particle

c_p = Heat capacity of moist air

D = Effective diffusivity of desiccant particle

h_m = Air side convective mass transfer coefficient

h_q = Effective heat transfer coefficient

h_m' = Pseudo-gas-side controlled model lumped mass transfer coefficient

i = Enthalpy of fluid (moist air)

i_{fg} = Enthalpy of vaporization

i_{wd} = Enthalpy of wet desiccant

$\dot{m}_{da,j}$ = Mass flow rate of dry air for period j

M_{dd} = Total mass of dry desiccant

$M_{particle}$ = Mass of desiccant particle

$NTU_{q,j} = h_q A/(\dot{m}_{da,j} c_p)$ = Number of transfer units for heat transfer

$NTU_{m,j} = \hat{h}_m A/\dot{m}_{da,j}$ = Number of mass transfer units used in pseudo-gas-side model.

R = Radius of desiccant particle

r = Radial position inside desiccant particle

T = Temperature of moist air

T_e = Temperature of moist air in equilibrium with desiccant bed

w = Humidity ratio of moist air

w_e' = Humidity ratio of moist air in equilibrium with desiccant bed evaluated using the average moisture content of the particle.

w_e = Humidity ratio of moist air in equilibrium with desiccant bed evaluated using the surface moisture content of the desiccant particle.

W_d = Volumetric average moisture content of desiccant per unit mass dry desiccant

W = Local moisture content of desiccant per unit mass of dry desiccant

z = Nondimensional axial position

Greek:

α = Desiccant-moist air interface area per unit length

$\beta_j = \theta_j/\theta$ = Period fraction

θ = Time for wheel to complete 1 revolution

θ_j = Duration of period j

$\Gamma_j = (M_{dd}/\dot{m}_{da,j} \theta)$ = Period mass capacity ratio

ρ_p = Particle density

τ = Nondimensional time coordinate

The developed system of equations are coupled and nonlinear due to the nonlinear mass transfer rate equation, the nonlinear property relations, and the nonlinear adsorption isotherm. The adsorption isotherm is an expression for moisture content of the desiccant as a function of humidity ratio and temperature of the moist air in equilibrium with the desiccant. For example, the adsorption isotherm for regular density silica gel obtained by Brandemuehl through integration of the Clausius-Clapeyron equation and a regression analysis of Hubbard's [46] data yields the following relationship:

$$i_s/i_{fg} = 1 + .2843\, e^{-10.28\, W_d}$$

$$P_{wv,e} = 3387.7\, (2.112\, W_d\, P_{wv,sat}/3387.7)^{\,is/ifg}$$

where:

i_s = Heat of adsorption

$P_{wv,e}$ = Vapor pressure of water in equilibrium with the desiccant

$P_{wv,sat}$ = Saturation pressure of water vapor evaluated at the temperature of the moist air in equilibrium with the desiccant bed

The desiccant bed boundary conditions are the initial state of the bed in the case of the transient solution or the periodic steady state boundary conditions in the case of the periodic steady state solution (see Fig. 4). The boundary conditions at the inlet to the bed for both the regeneration as well as process air stream are specified. Knowledge of the initial values of the bed (or periodic steady state boundary conditions) and the inlet states of the moist air allow a numerical solution for the desiccant bed to be implemented. In summary, the numerical solution for the desiccant bed can be determined as a result of the knowledge of the following system of equations:

1. Conservation of mass expression

2. Conservation of energy expression

3. The two transfer rate equations

4. The expression for enthalpy of the desiccant as a function of the temperature and moisture content of the bed

5. The expression for enthalpy of moist air as a function of humidity ratio and temperature

6. The adsorption isotherm

7. The inlet moist air stream states, both process and regeneration

8. The initial values or periodic steady state boundary conditions of the bed

ii. Numerical Scheme-The Bulirsch Stoer Method

As previously developed, the system of equations for the pseudo-gas-side model are as follows:

$$\partial i/\partial z = NTU_q\, c_p\, (T_e - T) + i_{fg}\, \partial w/\partial z \tag{10}$$

$$\partial I/\partial \tau = -1/(\Gamma_j\, \beta_j)\, \{\, NTU_q\, c_p\, (T_e - T) + i_{fg}\, \partial w/\partial z \,\} \tag{11}$$

$$\partial w/\partial z = NTU_m\, (\hat{w}_e - w) \tag{12}$$

$$\partial W_d/\partial \tau = -1/(\Gamma_j\, \beta_j)\, NTU_m\, (\hat{w}_e - w) \tag{13}$$

The parabolic concentration profile model differs from the pseudo-gas-side model. While the particle temperature will vary along the flow, constant temperature in the particle perpendicular to the air flow is assumed. Therefore the temperature of the desiccant particle is equal to the temperature of the hypothetical equilibrium layer, T_e, and for a spherical particle equations (12) and (13) are replaced by the following mass transfer rate equations:

$$\partial W_d/\partial \tau = - (3\, h_m\, \theta/\rho_p\, R)\, \{w_e[W+2/5a_2, T_e] - w\} \quad (14)$$

$$\partial w/\partial z = \beta_j\, \Gamma_j\, (3\, h_m\, A_s\, \theta/\rho_p\, R)\, \{w_e[W+2/5a_2, T_e] - w\} \quad (15)$$

Analogous expressions can be developed for a planar geometry. This is a system of partial differential equations. However, these equations can be written in the following form:

$$\partial i/\partial z = f[T, w, T_e, W] \quad (10a)$$

$$\partial I/\partial \tau = - 1/(\beta_j\, \Gamma_j)\, f[T, w, T_e, W] \quad (11a)$$

$$\partial w/\partial z = g[W, T_e, w] \quad (15a)$$

$$\partial W_d/\partial \tau = - 1/(\beta_j\, \Gamma_j)\, g[W, T_e, w] \quad (14a)$$

Where the equations are numbered to correspond to the rate equation that they represent. Although the conservation of mass and conservation of energy equations are partial differential equations, the form of Equations (10a),(11a),(14a) and (15a) are ordinary differential equations. If the right hand side can be evaluated at a given location, the solution can be advanced a step in both the axial and temporal direction using an ordinary differential equation (ODE) method. The right hand side of Equations (10a),(11a),(14a) and (15a) depend on both the desiccant state (W_d, T_e) and the moist air state (w_f, T_f). In order for both states to be known at a given location, an alternating direction approach must be utilized in the solution: A step is taken in the axial direction and a step is taken in the temporal direction. Specifically, the desiccant state at $(t+\Delta t, x+\Delta x)$ is found using information from $(t, x+\Delta x)$, $(t-\Delta t, x+\Delta x)$ etc. while the moist air state at $(t+\Delta t, x+\Delta x)$ is found using information from $(t+\Delta t, x)$, $(t+\Delta t, x-\Delta x)$ etc. Information for the desiccant state comes only from previously temporal positions, while information for the moist air state only comes from previous axial positions and therefore the use of ODE methods can be implemented. The desiccant state

and the moist air state are coupled by the right hand side of the rate equations.

A variety of solutions for the rotary desiccant wheel exist in the literature. The numerical solutions seen include the following: modified Euler, predictor corrector, and Runge-Kutta with adaptive stepsize control. Both the transient and steady state solutions are of interest. The transient solution "marches" through the solution. One method of obtaining periodic steady state is via repeated integrations of the wheel until the state of the bed at the end of the rotation is equal to the state of the bed at the beginning of the rotation within a specified tolerance. A convergence routine can be utilized to speed up the rate of convergence. For example, Maclaine-cross obtained the steady state solution with a second order Runge-Kutta numerical integration method and used a Newton-Raphson algorithm to accelerate convergence to periodic steady state operation.

The parabolic concentration profile model will use a similar approach, yet with a efficient ODE integrator called the Bulirsch-Stoer (B-S) method. This method was proposed by its authors [7] in 1966. The three key features of the method are a multistep method with an even powered error function, adaptive stepsize control, and rational function extrapolation to a grid size of zero for the purposes of decreasing the truncation error. The multistep method used by the algorithm is called the modified midpoint method. It is a midpoint rule algorithm slightly modified by Gragg [18]. The modified midpoint method (MMM) procedure as applied to some ODE, $dy/dx = f(x,y)$, is as follows for an overall step of size H [18]:

$$x_{i+1} = x_i + h \qquad i=0,1,...,n-1$$

where $h = H/n$ is the adjustable secondary stepsize

The first step: $\eta(x_1,h) = Y_0 + h\, f(x_0,y_0)$

The second through nth step:

$$\eta(x_{i+1},h) = \eta(x_{i-1},h) + 2\, h\, f(x_i,\eta(x_i,h)) \quad i=1,2,...,n-1$$

The corrector (n+1)th step:

$$Y(h,x) = 1/2\, [\eta(x_{n-1},h) + \eta(x_n,h) + h\, f(x_n,\eta(x_n,h))]$$

Where Y(h,x), the final step, is the approximation to the solution at location x using a step size h.

The MMM integration algorithm's truncation error is of special interest in the context of the B-S method. Gragg [18] has shown that the asymptotic expansion of Y(h,x) has only even powers of x, i.e.:

$$Y(h,x) = y(x) + \alpha_2(x)\, h^2 + \alpha_4(x)\, h^4 + \alpha_6(x)\, h^6 + ... \qquad (16)$$

As the first step of the algorithm is a first order method, the expansion of $\eta(x,h)$ associated with the step which produces the largest error is of the form:

$$\eta(h,x) = y(x) + \alpha_1(x)\, h + \alpha_2(x)\, h^2 + \alpha_3(x)\, h^3 + \alpha_4(x)\, h^4 + ... \qquad (17)$$

As the errors associated with stepping from x to x+H has a first order truncation error step, this error propagates through to the final step. Therefore the approximation to y(x) has an expansion of the form:

$$Y(h,x) = y(x) + \alpha_1(x)\, h + \alpha_2(x)\, h^2 + \alpha_3(x)\, h^3 + \alpha_4(x)\, h^4 + ... \qquad (18)$$

However, Gragg has shown that $\eta(x,h) = \eta(x,-h)$ and subsequently $Y(h,x) = Y(-h,x)$. The only way that this can hold is for the odd powers of equation (17) and (18) to disappear, i.e. $\alpha_1(x) = \alpha_3(x) = \alpha_5(x) = ... = 0$. The result is equation (16). When the MMM integration technique

is used with an extrapolation technique to approximate the solution as $y(x)=Y(0,x)$, two orders of magnitude of truncation error are cancelled at a time.

The B-S method proceeds as follows: The differential equation is repeatedly integrated from x to x+H using a successively smaller secondary stepsize. Figure 5 illustrates the process. The solution converges with an increasing number of steps. Each time the solution $Y(h,x+H)$ is found, a rational function extrapolation to a grid spacing of zero is performed using the previous solutions. The rational function extrapolation procedure is preferred in some problems because of it's ability to model poles. For our application, it is preferred because there is evidence in the literature that rational function extrapolation is a slightly more efficient procedure than polynomial extrapolation [6a]. A rational function is the quotient of two polynomials:

$$Y_m(h_i) = \frac{P_\mu(h_i)}{Q_\nu(h_i)} = \frac{p_0 + p_1 h_i^2 + \ldots + p_\mu h_i^{2\mu}}{q_0 + q_1 h_i^2 + \ldots + q_\nu h_i^{2\nu}}$$

where $\mu = \nu$ for m odd
and $\nu = \mu + 1$ for m even

This is called a diagonal rational function extrapolation due to the manner in which μ and ν are defined. The function must satisfy the following:

$$Y_m(h_k) = Y(h_k,x) \qquad k=i,i+1,\ldots,i+m$$

In other words, for a given secondary grid spacing, h_k, the rational function is set equal to the solution of the differential equation obtained using that stepsize. $\{h_k\}$ is a decreasing sequence of MMM stepsizes tending toward zero. The desired solution, $Y_m(0)=P_0/Q_0$, is computed following each execution of the MMM algorithm by a recursion formula developed in [17]. Convergence is obtained when:

$$|Y_m(0) - Y_{m-1}(0)| < \epsilon$$

where ϵ is some specified tolerance. The formulas assume that the approximation is a function in h^2, which is the case for the MMM algorithm. Fig. 6 illustrates the extrapolation process. The five solutions, where $Y_m(0) = W_d(t=.08)$, are plotted versus the stepsize H/n used (The fifth integration, n=16, was not included on Figure 1 for clarity). Fig. 6 shows $T_m(0)$, where the independent variable is time, using the first 2 solutions, corresponding to m=2, and $Y_m(0)$ for m=3,4, and 5. In this example, convergence occurs at m=5, which uses five solutions. The method also incorporates adaptive stepsize. This allows the solution to take large steps in the region of the solution where constant gradients exist. The nature of the varying stepsize is illustrated in Fig. 7. During the region where the curvature of the slope changes, the algorithm takes smaller steps. When the slope of the curve is fairly constant, the stepsize continues to increase. The figure indicates for each step the number of MMM steps needed for the algorithm to converge. If the number of integrations (m in Figure 6) was large, the next suggested step size is smaller than the previous one, if the number of integrations was small, the next step size is increased. Specifically, the authors of the method suggest the following method in choice of the next stepsize given the previous overall stepsize, H_{did}:

$$H_{next} = H_{did} * (6/i) \qquad (19)$$

Where i indicates the number of times that the interval was reintegrated. In the application of the rotary desiccant wheel, it has been necessary to limit H_{next} to some $H_{next,max}$ due to stability problems which occur at very large stepsizes. The program calculates the maximum stepsize allowable due to stability considerations as an upper limit on the stepsize. In the rotary

desiccant wheel, changes in the rotation speed of the wheel, desiccant particle size, or mass flow rate of the dry air can have a profound effect on the gradients, or transfer rates, in both the temporal and axial directions. It is important to have a method such as this which does not rely on assumed appropriate grid sizes. The repeated evaluations provide a measure of confidence in the results.

In solution of the desiccant wheel, evaluation of the right hand side (RHS) of Equations (10), (11), (14) and (15), is the most time consuming portion of the solution process. The nonlinear parabolic profile rate equation, the nonlinear expression for the hypothetical equilibrium state and the property relations must be solved for each evaluation of the rate equation. Keeping the number of RHS evaluations down to the minimum without sacrificing accuracy is important in order to maximize computational efficiency. The B-S method compares well with other methods in this respect. For example, one suggested sequence of increasing number of steps to reach the same location is: 2,4,6,8,12,16,24... . For example, if the B-S method takes 2, 4 and 6 steps across the same distance, and converges at n=6, the number of RHS evaluations is (n+1 for each n) 3 + 5 + 7 = 15 evaluations. As we have achieved the accuracy of at least a grid size of 6, this is 15 evaluations/6 steps = 2.5 evaluations/step. With each successive extrapolation the order of error is a power of 2 higher. For this example, the order of truncation error is 6. This is a higher truncation error than 4th order Runge-Kutta but only requires 2.5 evaluations/step versus the 4th order Runge-Kutta's 4 evaluations/step. 2.5 evaluations/step is more work than if a second order method is used. However, a bigger step can probably be used as the truncation error is smaller than the second order methods,

thereby decreasing overall effort. In the above example, the new suggested step size as according to Equation (19): $H_{next} = H_{did}*(6/3) = 2*H_{did}$ or twice the previous overall stepsize. Use of the model reveals that large steps are used in portions of the wheel that have constant gradients.

In their 1966 paper in which Bulirsch and Stoer propose the method [7], a study was done comparing the B-S method with a fourth order Runge-Kutta (4 RHS evaluations per step), an Adams-Moulton-Bashforth predictor corrector method (2 RHS evaluations per step) and a polynomial extrapolation. The polynomial extrapolation is essentially the B-S method differing only in the extrapolation technique. Euler's equation of motion for a rigid body without external forces and the equation $y' = -y$ were solved through numerical integration using the four methods. As previously mentioned, the work involved in obtaining a solution can be represented by the number of RHS evaluations of the differential equation. Figures 8b and 9b show the results of the comparison for the 4 methods. The B-S method is superior in computational work performed for the examples here. As the exact solutions for the examples are known, the authors also computed the error associated with each method. Figures 8a and 9a show the error results for each of the methods. The B-S method generally produces the lowest error with the least number of function evaluations. The results of this paper are significant and indicate that the method is promising. Although the use of the B-S method requires more programming time for it's added complexity, it can reap benefits in terms of computational efficiency. It is concluded that method compares favorably with other commonly used ODE solvers and can provide the most computationally efficient algorithm

for numerical solution of the parabolic concentration profile model for the rotary desiccant dehumidifier.

iii. Information Flow for the DEC Model

a. Transient

Fig. 10a illustrates the information flow of the transient model. State #1 is the indoor or ventilation air and is specified. The initial state of the bed is specified as well. The integrated desiccant wheel model and cooling and dehumidification coil model will proceed in the following manner.

1. Calculate state 2 using rotary desiccant wheel model
2. Calculate state 3 using cooling and dehumidification coil model
3. Calculate state 4 using rotary desiccant wheel model

Repeat this procedure until periodic steady state is reached or load period has ended

b. Periodic Steady State

Once the transient rotary desiccant wheel model is completed, the model will be further developed for integration with a cooling coil model. Figure 10b illustrates the information flow for the periodic steady state model. State point 1 is the indoor or ventilation air and is specified. The initial state of the bed is unknown. For each load specification, or each hour in the case of a varying hourly load, the following procedure is followed:

1. The initial state of the bed is tentatively assumed
2. Calculate state 2 using explicit rotary wheel model
3. Calculate state 3 using cooling and dehumidification coil model
4. Calculate state 4 using explicit rotary wheel model

5. Choose a convergence technique to update the assumed initial state of the bed at the start of the process period and return to #2

This procedure will be repeated until the state of the bed at the beginning of the process period equals the state of the bed at the end of the regeneration period. There are several convergence techniques which have been investigated. These will be discussed in the next chapter.

3.2 Application of the Model

One proposed electric specific desiccant cooling technology, Desiccant Enhanced Cooling (DEC), has been proposed by Cromer of Florida Solar Energy Center (FSEC) [14]. The system uses moisture exchange in a similar way that heat pipes use heat exchange to enhance the performance of vapor compression cooling. The process air stream initially being moist and very warm is first passed through a desiccant bed and absorbs moisture from the bed, thereby raising the humidity ratio of the air and lowering the dry bulb temperature of the air stream. The cooling coil then performs more dehumidification as its inlet air is now closer to the dew point. Exiting the coil, the cold, wet air again passes through the wheel and deposits moisture. As the wheel performs essentially adiabatic dehumidification, heat is generated during the adsorption of water vapor that occurs. Therefore the air stream exits the wheel dryer and hotter (See Figure 11). As the return or "regeneration" stream is warmer and has a lower relative humidity than the supply or "process" stream, the potential exists for the transfer of moisture from the supply to the return air stream. The DEC concept promises to raise the efficiency of traditional vapor compression cooling equipment via increase of the evaporator temperature. Figure 11 illustrates the conventional vapor compression cycle with

reheat as well as the DEC cycle on a psychrometric chart. The path line 1-2-3-5 is the DEC process path. The path line 1-4-5 is the vapor compression with reheat process. Fig. 11 shows that the VC unit for the DEC cycle will have a higher ADP for the DEC system than for the VC with reheat system. As previously stated, currently the most efficient way of providing reheat is to place a heat pipe heat exchanger between the supply and return air stream. Heat pipe technology pays a performance penalty in that it requires a lower ADP than VC cooling. As a result of this, it is expected that the DEC system will allow a higher efficiency VC unit compared with both the VC with reheat system and the integrated heat pipe/cooling and dehumidification coil system.

4.0 MODEL VALIDATION

The validation process is an essential part of model development. Once the equations are developed and the code written, the model is used to simulate a known solution. This process validates the theory and the implementation of the theory. Successful completion of the validation procedure provides confidence in the results that the model produces. The validation procedure completed to date in the present work are simulation of the desiccant wheel as rotary and counterflow heat exchangers and comparison with heat exchanger theory, comparison of the model with fixed bed adsorption experiments, and simultaneous comparisons with both a pseudo-gas-side controlled and a diffusion resistance model. Finally the model is compared with experimental data from a heat and mass exchanger wheel that was tested at the Solar Energy Research Institute. The procedure and results of these tests are presented below.

4.1 Heat Exchanger Comparison

The rotary heat exchanger provides a solid surface which alternatively is rotated in the hot and cold stream (see Fig. 13). The solid matrix material is heated as it passes through the hot stream and cooled as it passes through the cool stream, thereby becoming a medium for heat to flow from the hot to the cold stream. Rotary heat exchangers are attractive for their compactness, inexpensive matrix mesh materials are frequently used and the periodic flow reversals tend to be self cleaning [24].

Converting the rotary desiccant wheel model to a rotary heat transfer alone exchanger was the first test applied to the model. This case was implemented by making the convective mass transfer coefficient zero. The moisture content of the air stream and the desiccant remain constant and sensible heat alone is transferred. The heat transfer wheel model was then run until periodic steady state obtained, and the resulting outlet states compared with the mean outlet state produced by the effectiveness-NTU method [24]. Periodic steady state is reached when the state of the desiccant at the beginning of the current rotation is equal to the state at the end of the rotation within some specified tolerance. For the rotary heat exchanger, the effectiveness of the heat exchanger is determined by the three dimensionless numbers, C_r/C_{min}, NTU_{hx}, and C_{min}/C_{max}. C_r is the matrix heat capacity rate and is defined as:

$$C_r = c_m M_m/\theta$$

The number of transfer units for the rotary heat exchanger is denoted as NTU_{hx}, where the subscripts are used to differentiate it from the NTU's defined for the rotary desiccant wheel model. The NTU_{hx} for a balanced flow regenerator with equal transfer coefficients in each period is:

$$NTU_{hx} = h_q A_s / (2 C_{min})$$

Table 4.2 at the end of this chapter describes the nomenclature used. The fluid heat capacity rates, C_{min} and C_{max} are:

$$C_{min} = \min\{ (c_{f,1} \dot{m}_{f,1}), (c_{f,2} \dot{m}_{f,2}) \}$$

$$C_{max} = \max\{ (c_{f,1} \dot{m}_{f,1}), (c_{f,2} \dot{m}_{f,2}) \}$$

where the subscripts 1 and 2 denote the periods of the regenerator. The effectiveness of the heat exchanger, which is a correlation of the dimensionless outlet fluid temperature based on numerical results of the governing equations for the case of balanced flow ($C_{min} = C_{max}$) is

defined as:

$$\epsilon = \frac{T_{c,o} - T_{c,i}}{T_{h,i} - T_{c,i}} = \frac{T_{h,i} - T_{h,o}}{T_{h,i} - T_{c,i}} \tag{3}$$

The effectiveness then is tabulated in [24] as a function of the three relevant variables:

$$\epsilon = \epsilon[C_r/C_{min}, NTU_{hx}, C_{min}/C_{max}]$$

These tables were produced from consideration of numerical results in the literature of Coppage and London [13], and Lambertson [26] as the major sources of information. The first heat exchanger simulation was run for $C_r/C_{min}=1$, $NTU_{hx}=2$, $C_{min}/C_{max}=1$. For this case, $\epsilon=.601$. Through the use of equation (3), the outlet temperature of the hot and cold fluid are found. These outlet temperatures are the mean outlet temperature for each period, which is the outlet temperature of the fluid averaged over the period. The periodic steady state solution of the model is plotted in Fig. (14) along with the effectiveness solution for that case. In addition, the inlet conditions, $T_{c,i}=35°C$ and $T_{h,i}=65°C$ are plotted. The agreement is excellent and shows that the model behaves well in the heat transfer only mode. Fig. 15 plots the results of the periodic steady state solution for the following case:

$$C_r/C_{min}=5,\ NTU_{hx}=3,\ C_{min}/C_{max}=1,\ \epsilon=0.746$$

The excellent agreement between the average period outlet temperature and the ϵ-NTU temperature is evident.

As the matrix heat capacity rate of a rotary heat exchanger becomes large, the behavior approaches that of a counterflow recuperator. The effectiveness of the rotary heat exchanger

is essentially equal to the effectiveness of the counterflow recuperator for $C_r/C_{min} > 5$. The correlation between the two is [24]:

$$\epsilon_{rotary\ hx} = \epsilon_{counterflow\ hx} \{ 1 - 1/(9\ (C_r/C_{min})^{1.93}) \}$$

The counterflow heat exchanger has a higher effectiveness than the rotary heat exchanger due to the fact that energy transfer occurs directly in the counterflow heat exchanger. At high matrix heat capacity rates, the matrix is either rotating very quickly, the mass of the matrix is large or the heat capacity is large. Each of these cases allows the matrix to transfer more energy from one stream to the next and the case of a counterflow heat exchanger, which is a direct-type heat exchanger, is approached.

Two counterflow heat exchanger simulations which were completed also produced excellent agreement with heat exchanger theory. The results are plotted in Fig. 16 and Fig. 17. A summary of the results of the heat exchanger validation procedure are tabulated in Table 4.1.

Table 4.1-Results of Heat Exchanger Simulation

Case	C_r/C_{min}	NTU_{hx}	C_{min}/C_{max}	$\epsilon_{literature}$	ϵ_{sim}
Rotary Heat Exchanger	1	2	1	.601	.612
Rotary Heat Exchanger	5	3	1	.746	.740
Counterflow Heat Exchanger	10	3	1	.750	.746
Counterflow Heat Exchanger	10	6	1	.857	.853

The comparison of the current model with the numerically based correlations for heat exchanger theory gave favorable results. This type of comparison indicated that the heat

transfer theory and the numerical procedure associated with the heat transfer theory have been implemented correctly. The next two validation procedures were implemented in order to test the mass transfer theory and implementation in the model.

4.2 Fixed Bed Adsorption

The next test to be applied to the wheel was comparison with fixed bed adsorption. The data which was used as a comparison is the PhD work done at UCLA by A.A. Peseran [36]. Peseran's work included a review of properties and modeling characteristics of water vapor adsorption on regular density silica gel for thin desiccant beds. His work compared experimental data against the pseudo-gas-side (PGS) model and a diffusion resistance model. Use of the experimental data and the two models in Peseran's thesis were ideal for validation of the parabolic concentration profile model. For these runs, the spherical particle concentration profile assumption was used as the moist air experiences contact with most of the particle surface area in a fixed bed. The adsorption isotherm and heat of adsorption used in the simulation were the same that Peseran used in his modeling. Regular density silica gel grade 01 were used in the experiments. Fig. 18 and 19 show example results of two of the completed runs.

The parabolic concentration profile model compares favorably with the experimental data in this run as well as the diffusion resistance model. The PGS controlled model compares favorably in these examples as well. However, the PGS controlled model uses an empirically degraded mass transfer coefficient correlation which is available for water vapor adsorption

on silica-gel as a result of extensive testing of this particular system. The parabolic concentration profile model uses a more commonly available property, the effective diffusivity, in modeling the resistance to mass transfer inside the desiccant particle. As the current work will investigate the effects of several desiccants on the DEC system's performance, the parabolic concentration profile model is more suitable for the current work. The PGS model would not be feasible as the empirically degraded mass transfer coefficient is not known for systems other than the silica-gel-water-vapor system.

The general conclusions of the fixed bed comparisons are that the parabolic profile assumption does well in approximating the diffusion inside the desiccant particle for thin desiccant beds. In a thin bed, which will always be the case for the current study due to pressure drop considerations, the parabolic profile develops quickly and the assumption becomes a good one for the current study. From these results, the parabolic concentration profile mass transfer model and numerical implementation of the model show promise of providing accurate solutions for the proposed system.

4.3 Rotary Desiccant Wheel Experimental Data

Extensive testing of various rotary desiccant wheels has been performed at the Solar Energy Research Institute (SERI). A graduate student at the University of Wisconsin, K.J. Schultz, has reported on the experimental results of three of the wheels in his PhD work [46]. These experimental results were used to compare the solution of the current model with the performance of a real rotary dehumidifier. Although the silica gel particles are spherical, the

planar parabolic concentration profile assumption was used due to the parallel passage geometry of the tested wheel. The silica gel particles are adhered to the passage walls of the wheel. One side of the particle will therefore be exposed to the moist air stream while the other side will be attached to the passage wall and will not experience contact with the moist air stream. This geometry seems more conducive to the planar assumption with the particle diameter as the thickness of the planar "slab" of desiccant. The use of the planar geometry also allows the model to run quite a bit faster using a stepsize many times larger than that of the spherical case. This is due to the lower amount of exposed surface area of the planar geometry and the resulting smaller number of transfer units. Fig. 20 and 21 give example performance results for two separate runs of one of the SERI wheels simulated.

The results of the simulation are fairly favorable. This indicates that the planar assumption does well in the parallel passage wheel. Fig. 21a is a plot of the outlet moisture content versus time for the simulation, and the experiment. The plot of the average outlet moisture content for the simulation reveals that periodic steady state has not been reached. This problem has occurred in several of the rotary desiccant wheel comparisons. The moist air outlet states approach periodic steady state up to a certain point and further rotations of the wheel does not change the outlet state any more. This problem is currently under investigation. However, the results of these comparisons appear to be very favorable once this problem is cleared up.

Table 4.2-Nomenclature for Heat Exchanger Theory

A_s - Surface area for each period
C_{min} - Minimum heat capacity rate
c_f - Heat capacity for fluid
M_m - Mass of matrix material
ϵ - Heat exchanger effectiveness
NTU_{hx} - Number of transfer units
rotation

C_{max} - Maximum fluid heat capacity rate
C_r - Matrix heat capacity rate
c_m - Heat capacity of matrix
m_f - Mass flow rate of fluid
h_q - Convective heat transfer coefficient
θ - Time of heat exchanger to complete i

Subcripts
1 - Period 1
2 - Period 2

5.0 REFERENCES

(1) "Advanced SuperAire Being Tested", Gas Research Institute Digest (GRID) 8, Winter 1985/1986, No.4, p. 36.

(2) Akulov, A.K., Ustinov, E.A., "Approximate Desorption Kinetics Equations. I. The Homogeneous Porous Grain Model", Russian Journal of Physical Chemistry, Vol. 55, p. 509, 1981.

(3) ASHRAE 1987 HVAC Systems and Applications Handbook, Temperature and Humidity Setpoints for Industrial Air Conditioning.

(4) Banks P.J., "Coupled Equilibrium Heat and Single Adsorbate Transfer in Fluid Flow Through a Porous Medium-I. Characteristic Potentials and Specific Capacity Ratios", Chemical Engineering Science, Vol 27, 1972, pp. 1143-1155.

(5) Banks, Nancy, Cargocaire marketing manager for Superaire products, phone conversation, July 1989.

(6) Booz-Allen and Hamilton Inc.,"Competitive Assessment of Desiccant Solar/Gas Systems for Single Family Residences", GRI-81/0063.

(7) Bulirsch, R., Stoer, J., "Numerical Treatment of Ordinary Differential Equations by Extrapolation Methods", Numerische Mathematik, Vol. 8, pp.1-13, 1966.

(8) Bullock, C.E., Threlkeld, J.L., "Dehumidification of Moist Air by Adiabatic Adsorption", ASHRAE Transactions, 1966, Vol. 72, No. 1986, pp 301-313.

(9) Burns, P.R., Mitchell, J.W., Beckman, W.A., "Hybrid Desiccant Cooling Systems in Supermarket Applications", ASHRAE TRANSACTIONS, Vol. 91, 1985, CH-85-09, No. 5, pp. 457-467.

(10) Calton, D.S., "Application of a Desiccant Cooling System to Supermarkets", ASHRAE TRANSACTIONS, Vol. 91, 1985, CH-85-09, No. 3, pp. 441-445.

(11) Carter, J.W., "A Numerical Method for Prediction of Adiabatic Adsorption in Fixed Beds", Transactions Instn Chem. Engineers, Vol. 44, 1966, pp. T253-T259.

(12) Close, D.J., Banks, P.J., "Coupled Equilibrium Heat and Single Adsorbate Transfer in Fluid Flow through a Porous Medium II-Predictions for a Silica Gel Air Drier Using Characteristic Charts", Chemical Engineering Science, 1972, pp. 1157-1169.

(13) Coppage, J.E., and London, A.L., "The Periodic-Flow Regenerator-A Summary of Design Theory", Transactions of the ASME, July 1953, pp. 779-787.

(14) Cromer, C.J., "Dehumidification Enhancement of Air Conditioners by Desiccant Moisture Exchange", Florida Solar Energy Center, Cape Canaveral, Fl., June 1988, DOE #DE-FC03-865F16305.

(15) Do, D.D., Rice, R.G., "Validity of the Parabolic Profile in Adsorption Studies", AICHE Journal, 32, No. 1, pp. 149-154, 1986.

(16) "Favorable Market Indicated for Residential Dehumidifiers", GRID 9, Spring 1986, No. 1, pp. 20-21.

(17) Gear, W., Numerical Initial Value Problems in Ordinary Differential Equations, pp.87-101, Prentice-Hall Inc., N.J., 1971.

(18) Gragg, W.B., "On Extrapolation Algorithms for Ordinary Initial Value Problems", Journal SIAM Numerical Analysis, Ser. B, Vol. 2, No. 3, 1965.

(19) Gregg, S.J., Sing, K.S.W., Adsorption, Surface Area and Porosity-Second edition, pp. 1-18, Academic Press, London, 1982.

(20) "H.E. Butt Tests Dry Air System", Chain Store Executive, July 1986, p.58.

(21) Holmberg, R.B., "Combined Heat and Mass Transfer in Regenerators with Hygroscopic Materials", ASME-Journal of Heat Transfer, Vol. 101, p. 205, 1979

(22) Hubard, S.S., "Equilibrium Data for Silica-Gel and Water Vapor", Industrial and Engineering Chemistry, 46, No. 2,pp. 356-358, February 1954.

(23) Jurinak, J.J., "Open Cycle Desiccant Cooling-Component Models and System Simulations", PhD Thesis, University of Wisconsin at Madison, 1982.

(24) Kays and London, Compact Heat Exchangers, Third Edition, McGraw-Hill, 1984.

(25) Lambertson, T.J., "Performance Factors of a Periodic-Flow Heat Exchanger", Transactions of the ASME, April 1958, pp. 586-592.

(26) Lavan, Z., Monnier, J.B., Worek, W.M., "Second Law Analysis of Desiccant Cooling Systems", Journal of Solar Energy Engineering, August 1982, Vol. 104, p 229-236.

(27) Liaw, C.H., Wang, J.S.P., Greenkorn, R.R., Chao, K.C., "Kinetics of Fixed Bed Adsorption: A New Solution", AIChE Journal, Vol. 25, No. 2, pp. 376, 1979

(28) "Maclaine Cross, I.L., Banks, P.J., "Coupled Heat and Mass Transfer in Regenerators-Predictions Using an Analogy with Heat Transfer", International Journal of Heat and Mass Transfer, Vol 15, pp. 1225-1242.

(29) Majumdar, P., Worek, W.M., Lavan, Z., "Heat and Mass Transfer in a Composite Desiccant Material", ASME Division of Heat and Mass Transfer, 1985, pp. 1-10.

(30) Manley, D.L., Bowlen, K.L., Cohen, B.M., "Evaluation of Gas Fired Desiccant Based Space Conditioning for Supermarkets", ASHRAE TRANSACTIONS, Vol. 91, 1985, CH-85-09, No. 4, pp. 447-455.

(31) Marciniak, T.J., et al, "Solid Desiccant Dehumidification Systems for Residential Applications", GRI85-198489.

(32) Mathiprakasam, B., Lavan, Z., "Performance Predictions for Adiabatic Desiccant Dehumidifiers Using Linearized Solutions", Journal of Solar Energy Engineering, Vol. 102, February 1980, pp. 73-79.

(33) McCallum, T.O., Russell, L. D., "Device to Reduce Air Conditioning Loads by Use of Waste Heat for Dehumidification.", Mississippi State, MI, DOE # DE-FG44-81R410486.

(34) Nelson, J.S., Beckman, W.A., Mitchell, J.W., Close, D.J., "Simulations of the Performance of Open Cycle Desiccant Systems using Solar Energy", Solar Energy, Vol. 21, pp. 273-278.

(35) Pesaran, A.A., "Heat and Mass Transfer Analysis of a Desiccant Dehumidifier Matrix", SERI/TR-252-2774

(36) Peseran, A.A., "Moisture Transport in Silica-Gel Particle Beds", PhD Thesis, University of California, Los Angeles, 1983.

(37) Pesaran, A.A., Zangrando, F., "Isothermal Dehumidification of Air in a Parallel Passage Configuration", ASME Division of Heat and Mass Transfer, 1985, 85-HT-72, pp. 1-11.

(38) Pesaran, A.A., Mills, A.F., "Moisture transport in silica gel packed beds-I. Theoretical study", International Journal of Heat and Mass Transfer, Vol 30, No. 6, pp. 1037-1049, 1987.

(39) Press, W.H., Flannery, B.P., Vetterling, W.T., Numerical Recipes, Cambridge University Press, 1986

(40) Relwani, S.M., "Indoor Pollution Control Capabilities of a Desiccant Dehumidifier System", IIT Research Institute, GRI-86/0200.

(41) Rice, R.G., "Approximate Solutions for Batch, Packed Tube and Radial Flow Adsorbers-Comparison with Experiment", Chemical Engineering Science, Vol. 37, No. 1, p. 83, 1982.

(42) Rosen, J.B., "Kinetics of a Fixed Bed System for Solid Diffusion into Spherical Particles", The Journal of Chemical Physics, Vol. 20, No. 3, p. 387, 1951.

(43) Schlepp, D, Schultz, K. J., "High Performance Solar Desiccant Cooling Systems", SERI/TP-252-2497.

(44) Schlepp, D, Barlow, R., "Performance of the SERI Parallel-Passage Dehumidifier", SERI/TP-252-1951.

(45) Shah, R.K., Thermal Design Theory for Regenerators. In Heat Exchangers: Thermal-Hydraulic Fundamentals and Design, pp.721-763. Hemisphere, N.Y., 1981.

(46) Schultz, K.J., "Rotary Solid Desiccant Dehumidifiers", Ph.D. Thesis, 1987, University of Wisconsin at Madison.

(47) Steele, W.A., The International Encylopedia of Physical Chemistry and Chemical Physics Topic 14. Properties of Interfaces, Vol. 3, pp.77-138, Pergamon Press, Oxford, 1974.

(48) "SuperAire Sales Mount-Advanced Unit Performance is Evaluated", GRID 10, Summer 1987, No. 2, pp. 20-22.

(49) Van Den Bulck, E., Mitchell, J.W., and Klein, S.A., "Design Theory for Rotary Heat and Mass Exchangers-I. Wave Analysis of Rotary Heat and Mass Exchangers with Infinite Heat Transfer Coefficients", International Journal of Heat and Mass Transfer, Vol. 28, 1985, pp. 1575-1586.

(50) Van Den Bulck, E., Mitchell J.W., Klein, S.A., "Design Theory for Rotary Heat and Mass Exchangers-II. Effectiveness- Number of Transfer Units Method for Rotary Heat and Mass Exchangers", International Journal of Heat and Mass Transfer, Vol. 28, 1985, pp. 1587-1595.

(51) Van Den Bulck, E., "Convective Heat and Mass Transfer in Compact Regenerative Dehumidifiers", Ph.D Thesis, University of Wisconsin, 1987.

(52) Watt, J.R. , Evaporative Air Conditioning Handbook, 2nd edition, Chapman & Hall, New York, 1986.

(53) Wepfer, W.J., Gaggioli, R.A., Obert, E.F., "Proper Evaluation of Available Energy for HVAC", ASHRAE Transactions, No. 2524, pp. 214-229.

(54) White, M.G., Heterogeneous Catalysis, pp. 41-56, Prentice Hall, NJ, 1990.

(55) Wurm, J., "Review of Open Cycle Desiccant Air-Conditioning Concepts and Systems", 1986 International Institute of Refrigeration (IIR) Meeting.

6.0 FIGURES

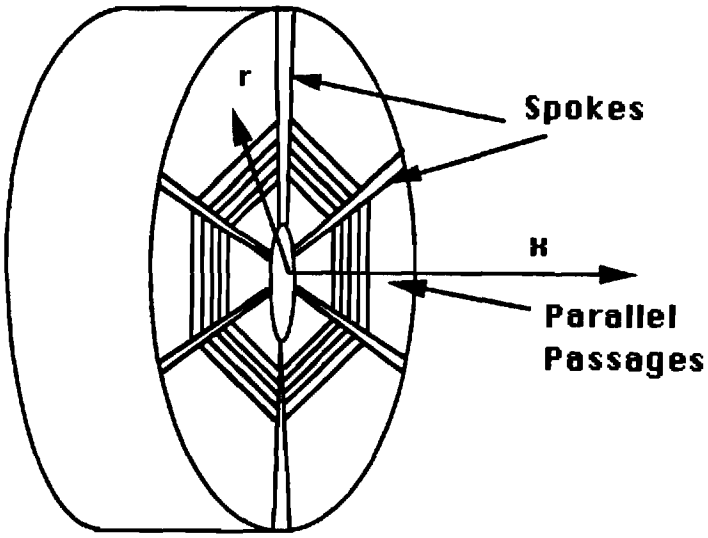

Fig. 1-Illustration of the Parallel Passage Rotary Desiccant Wheel

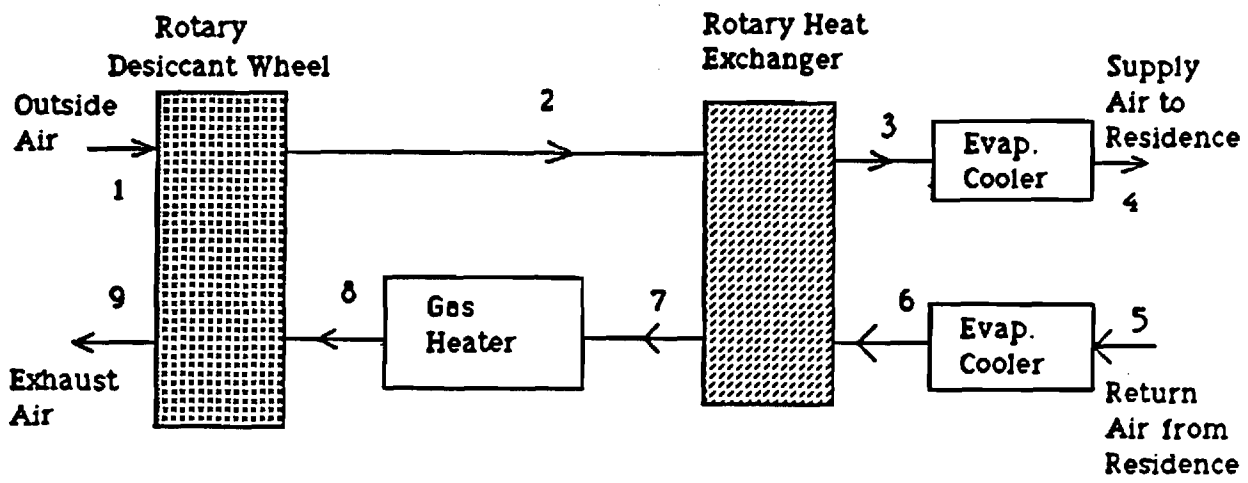

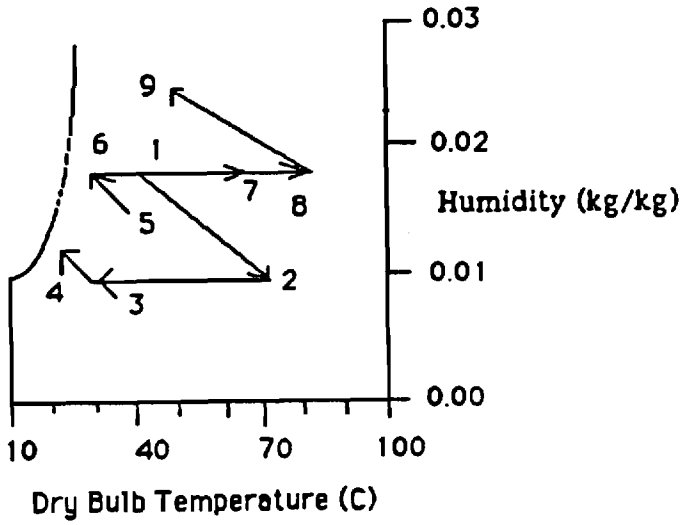

Fig. 2a-The Pennington Ventilation Cycle

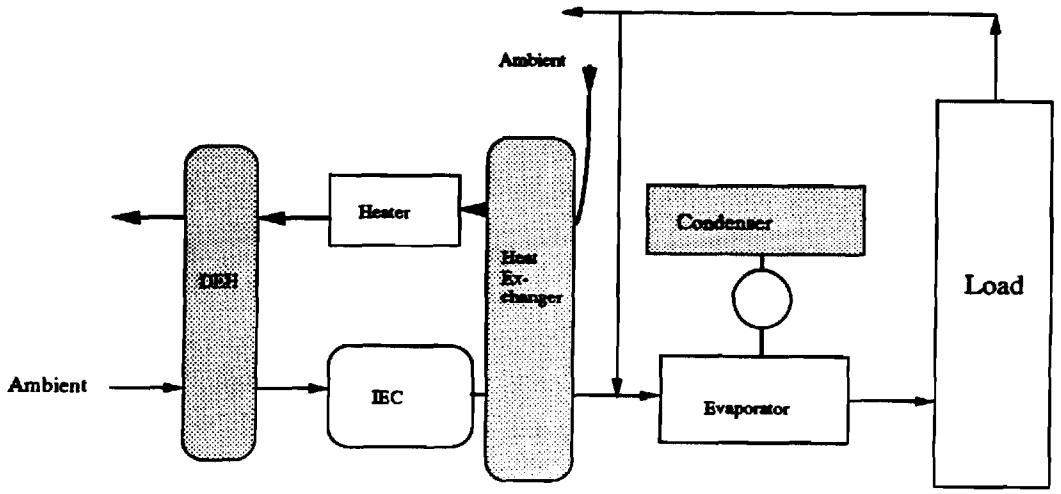

Fig. 2b-A Hybrid Desiccant Cooling Cycle

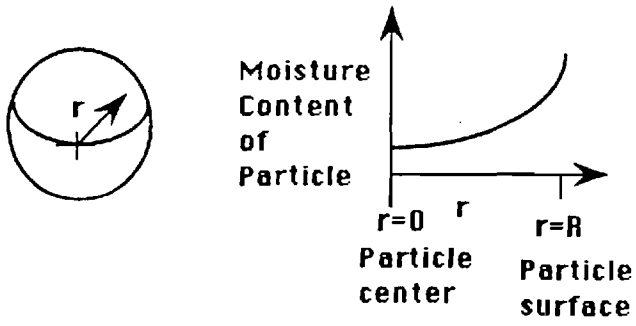

Fig. 3-Geometry of the Proposed Parabolic Concentration Profile Assumption for Spherical Particles

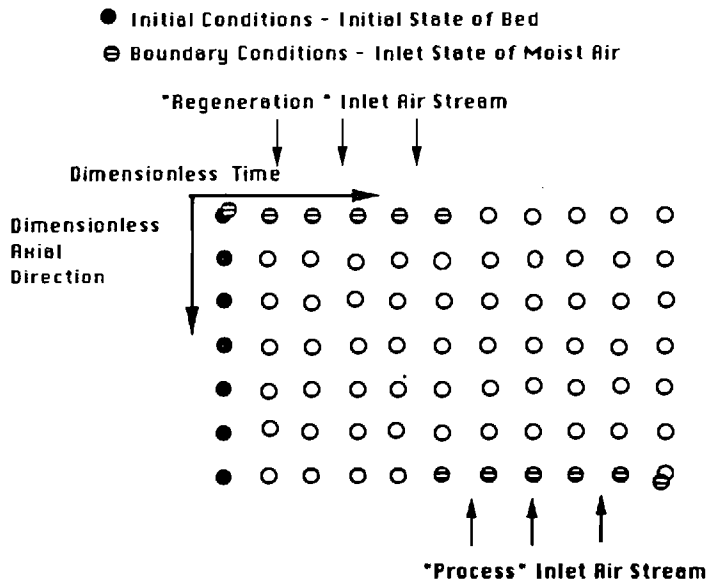

Fig. 4a-The Numerical Problem of the Transient Rotary Desiccant Wheel

Initial values are: $W_d(t=0) = W_o$ and $I_d(t=0) = I_o$

The Solution is obtained by "marching" from left to right

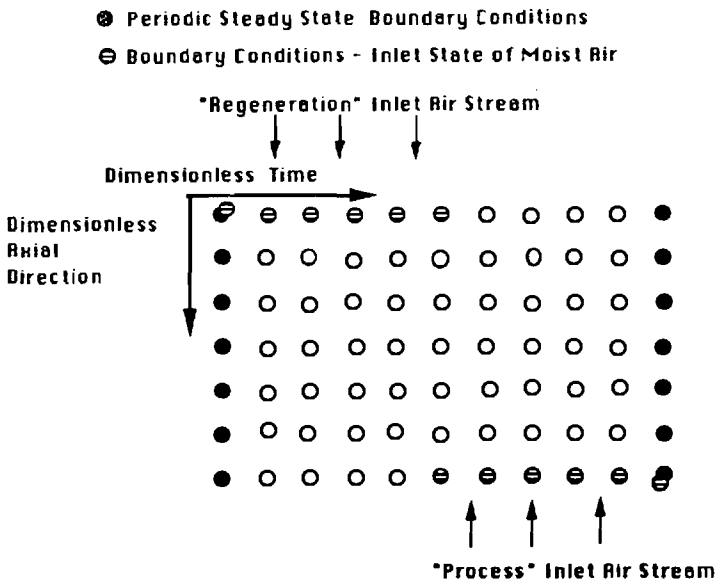

Fig. 4b-The Numerical Problem of the Periodic Steady State Rotary Desiccant Wheel

Periodic steady state boundary conditions are:

$$W_d(t=0) = W_d(t=t_2) \text{ and } I_d(t=0) = I_d(t=t_2)$$

Where t_2 denotes end of regeneration period

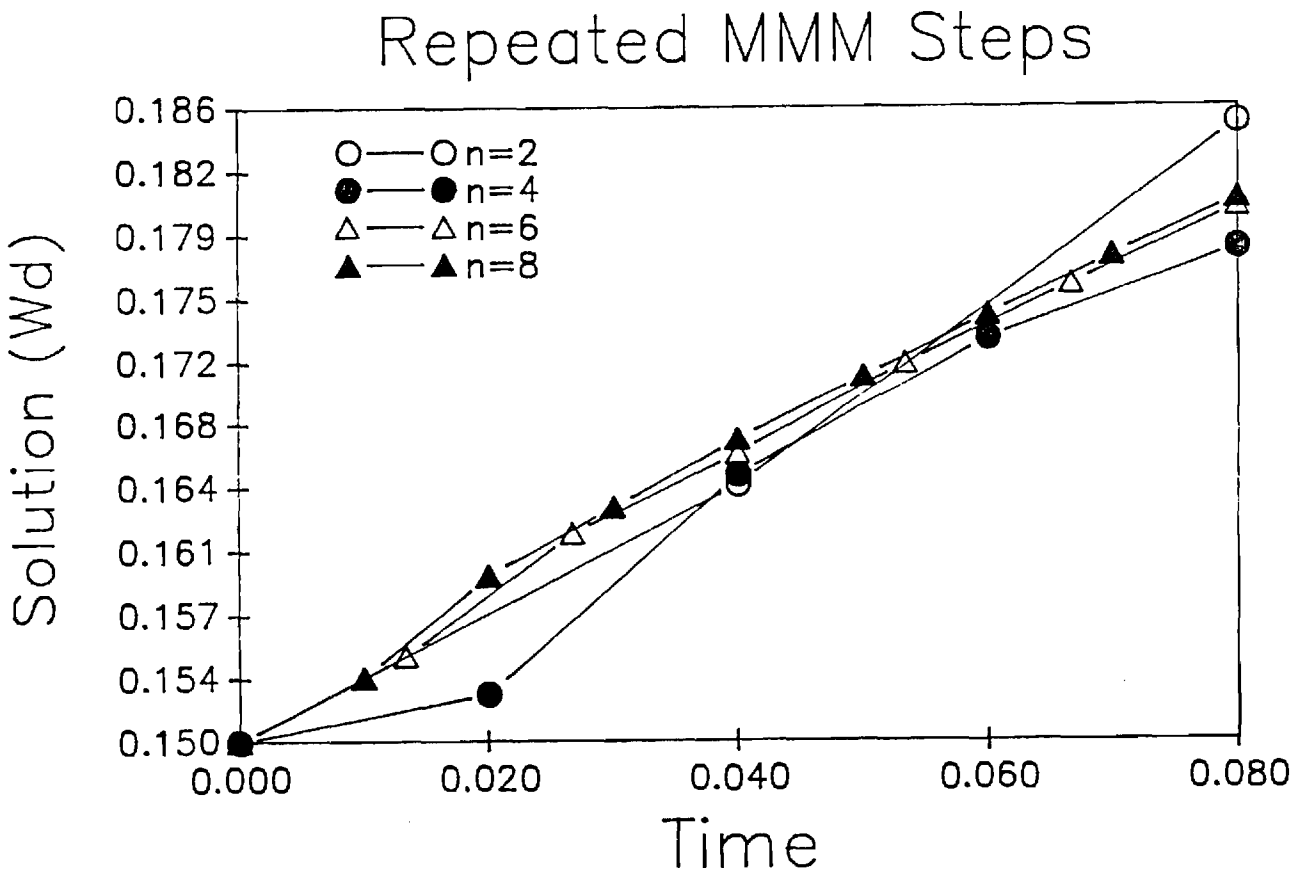

Fig. 5-Repeated Integration Using the Modified Midpoint Method

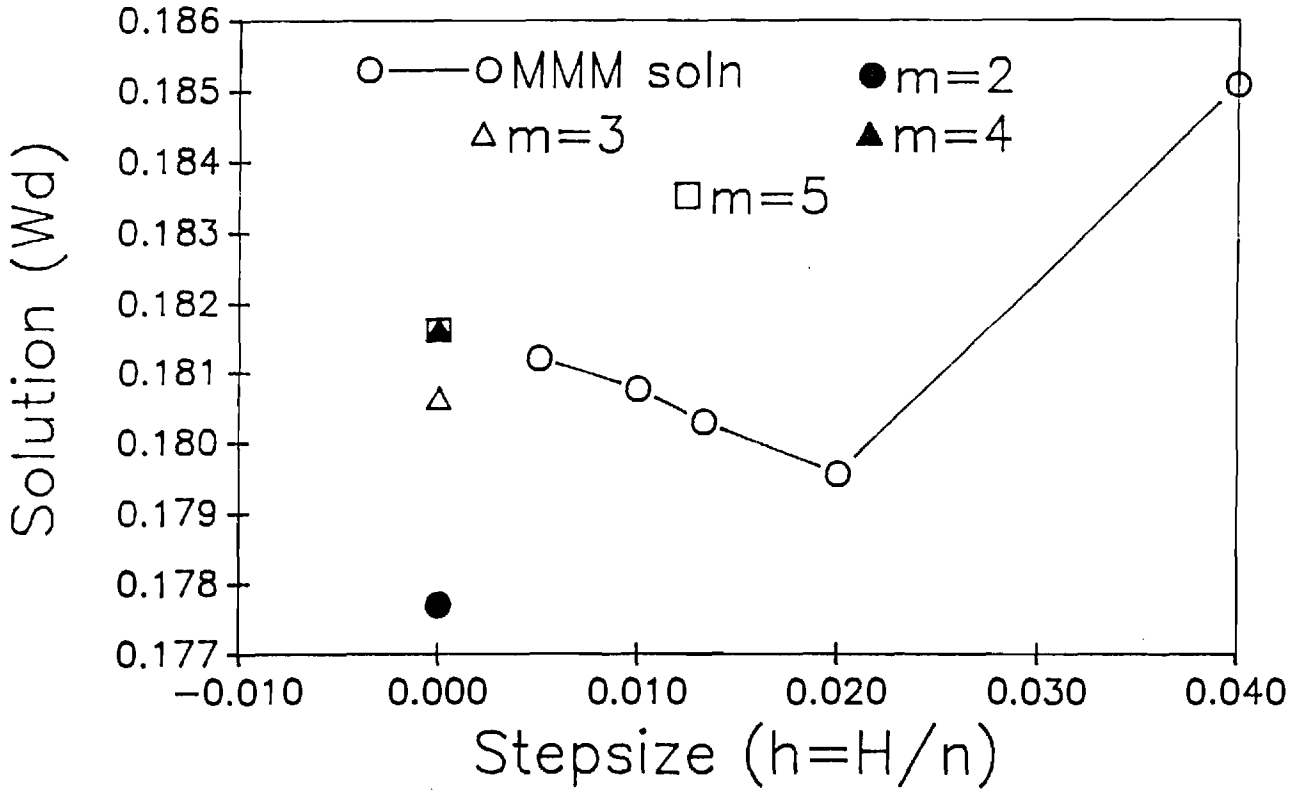

Fig.6-Illustration of Rational Function Extrapolation to Zero Stepsize

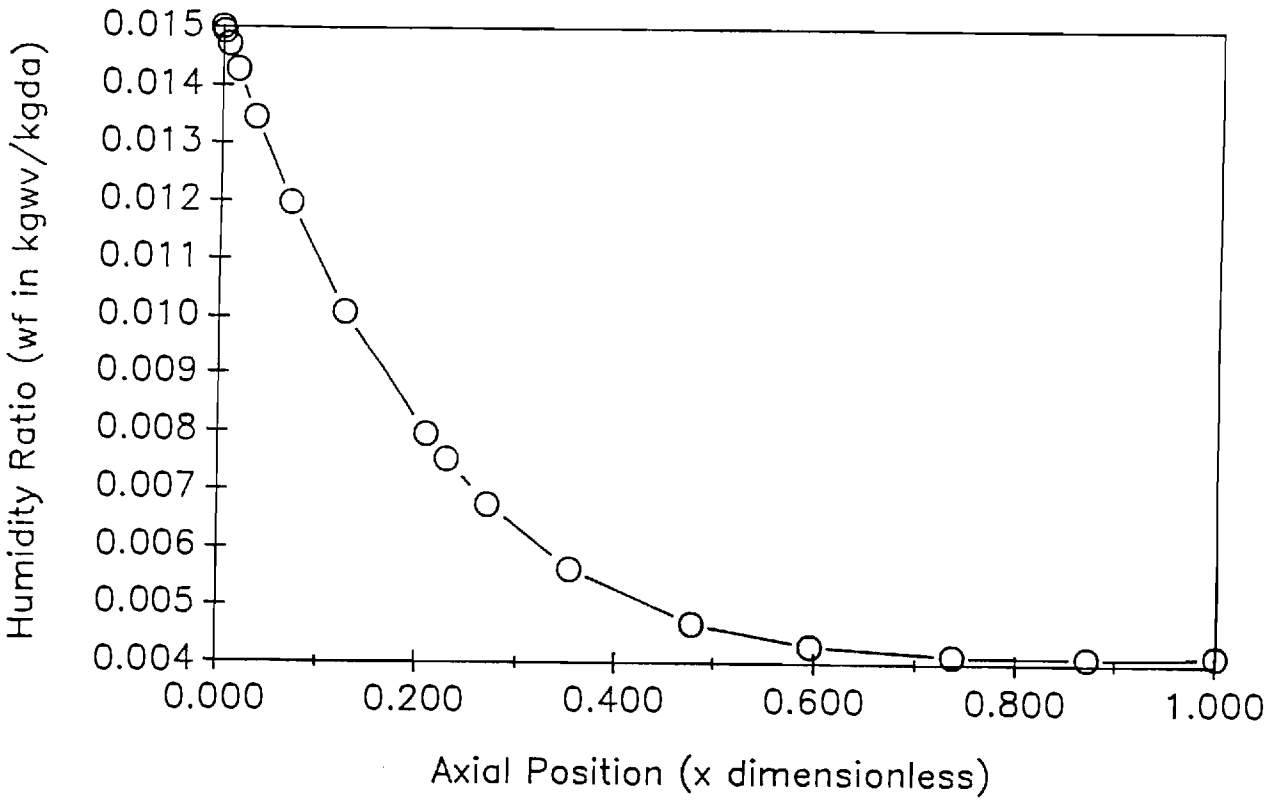

Fig. 7-Illustration of Varying Stepsize for the Bulirsch-Stoer Method

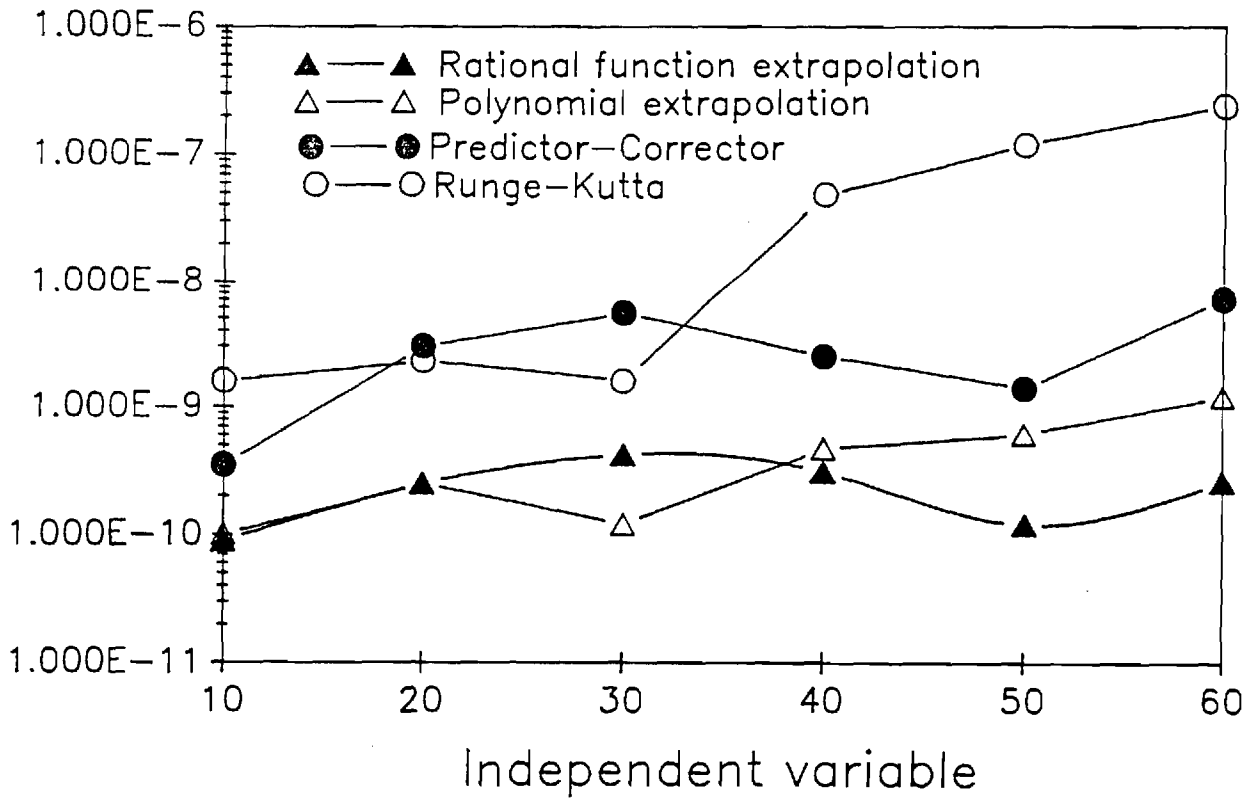

Fig. 8a-Absolute Error for Euler's Equation

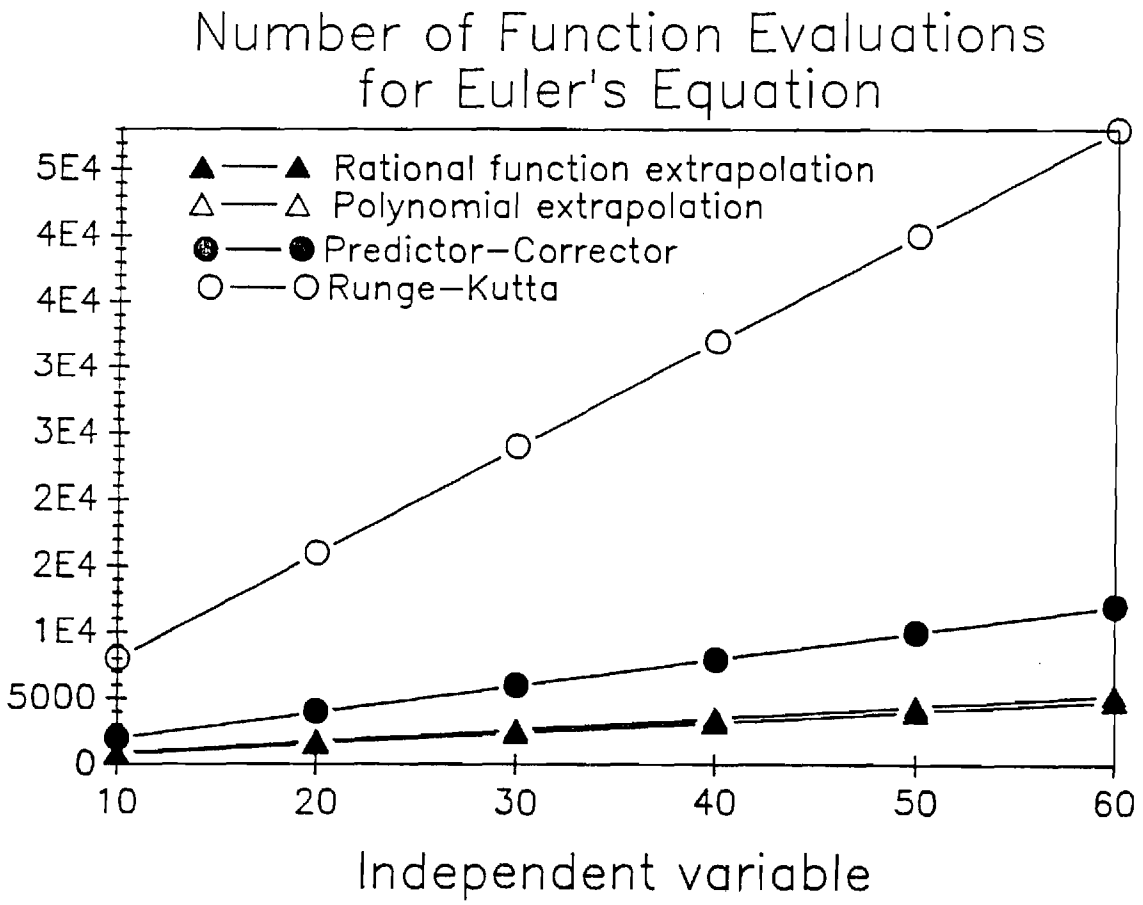

Fig. 8b-Number of Function Evaluations for Euler's Equation

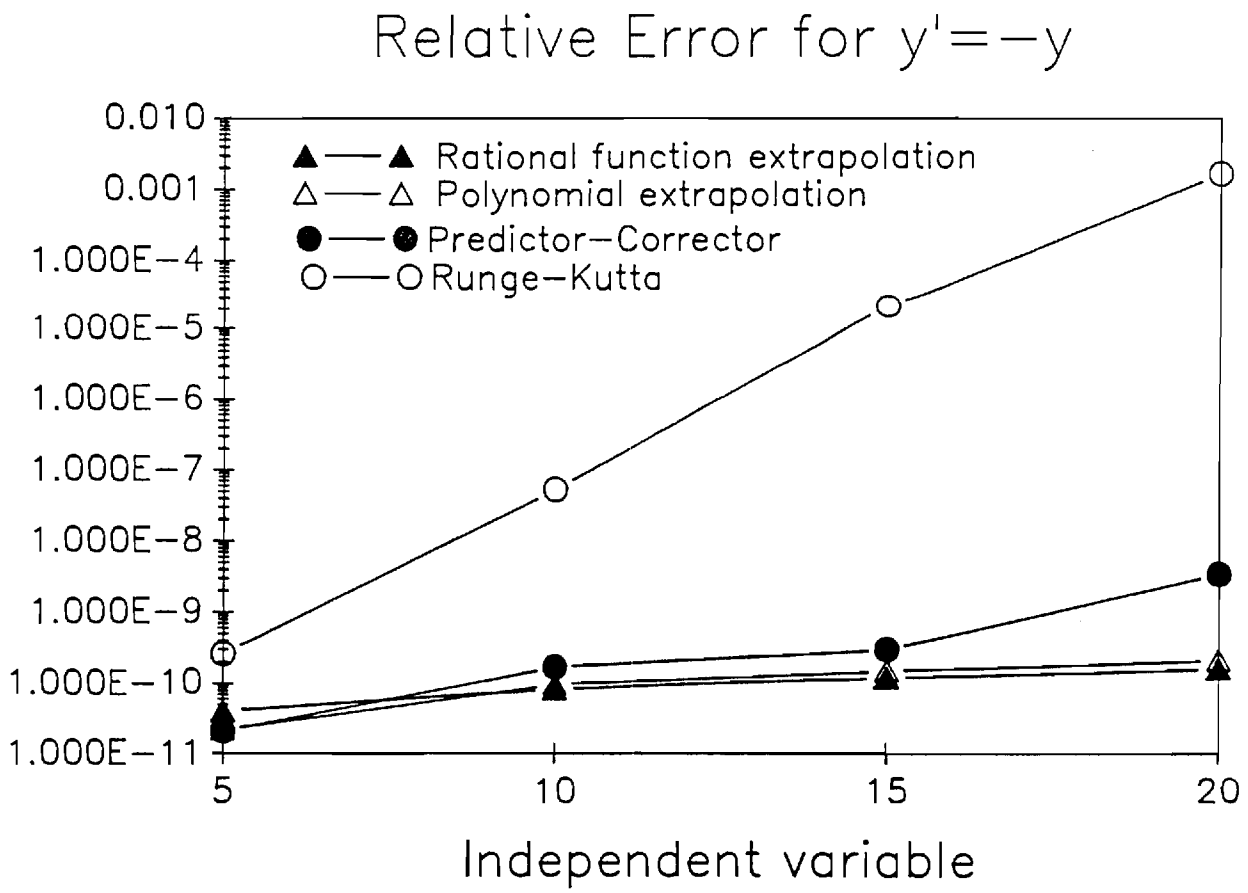

Fig. 9a-Relative Error for y' = -y

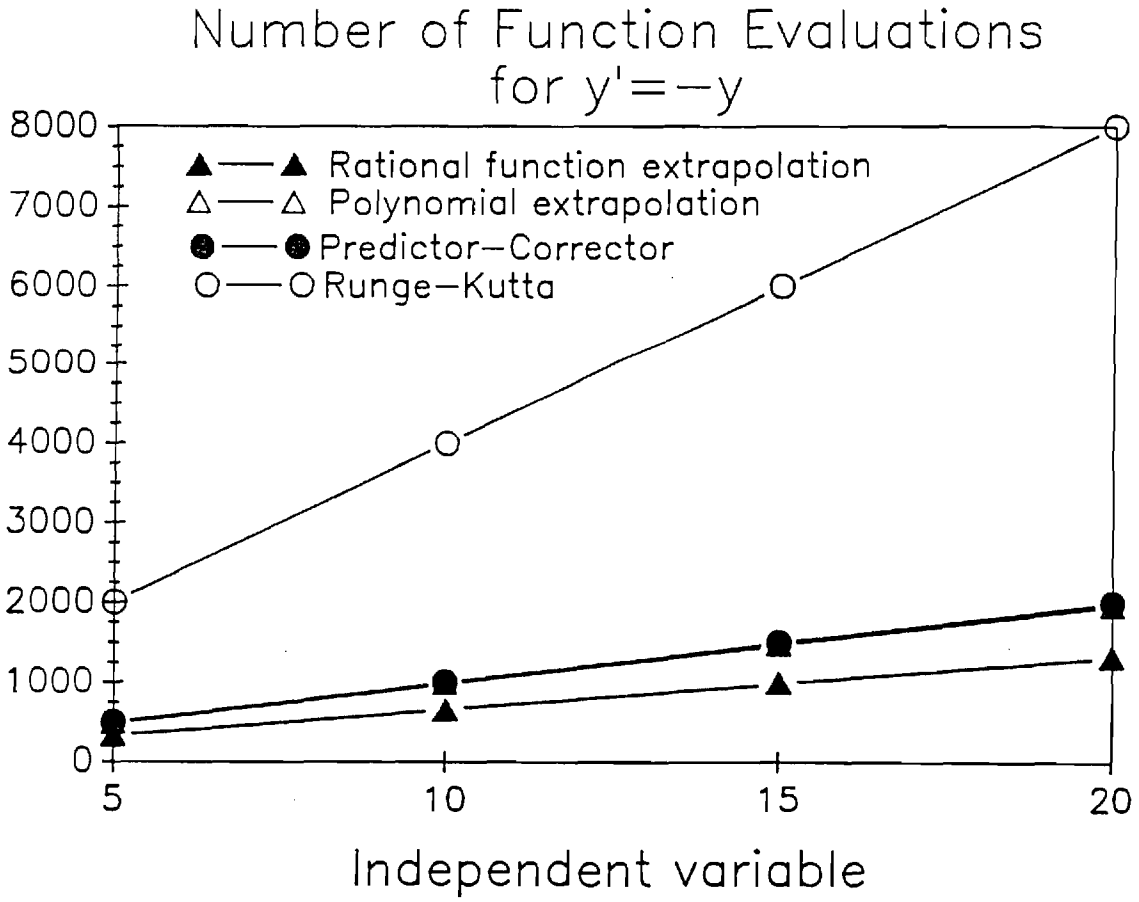

Fig. 9b-Number of Function Evaluations for y' = -y

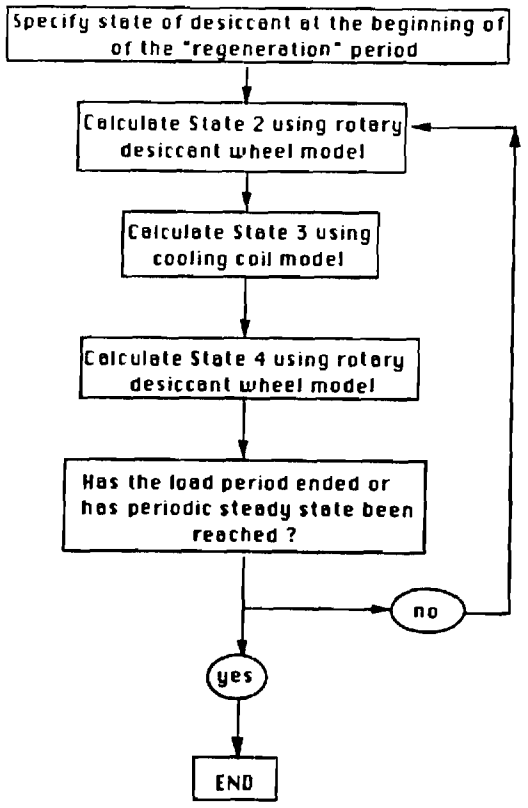

Fig. 10a-Illustration of the Transient Model Solution Process for each constant load period

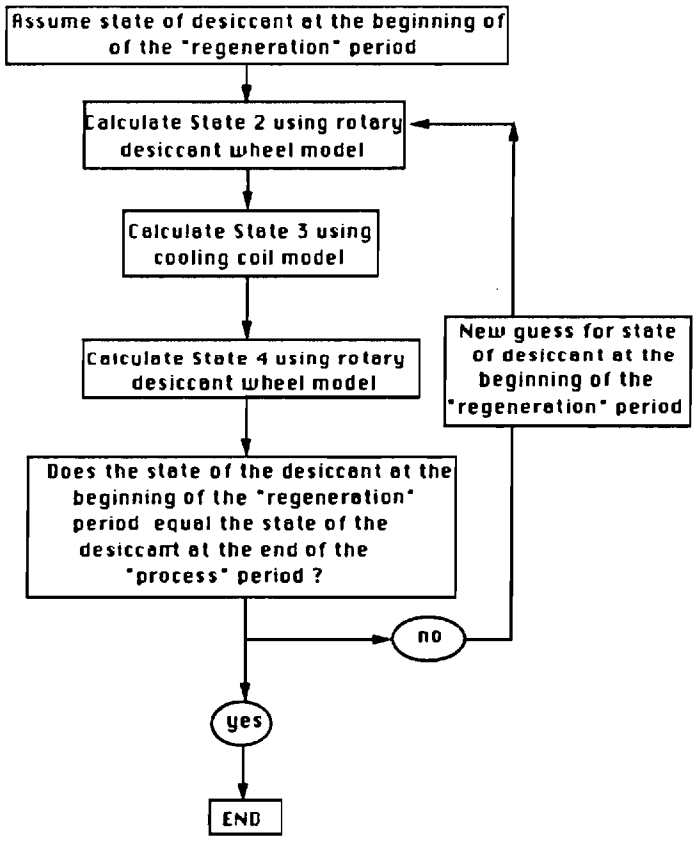

Fig. 10b-Illustration of the Periodic Steady State Solution Process for each constant load period

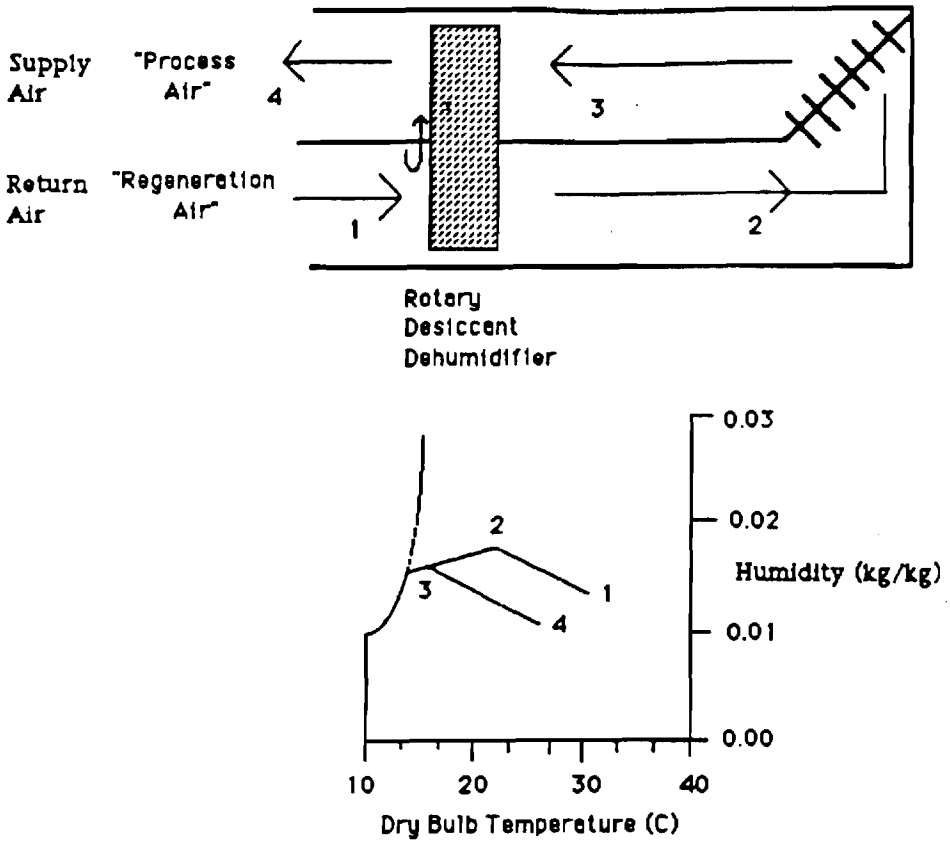

Fig. 11-Desiccant Enhanced Cooling

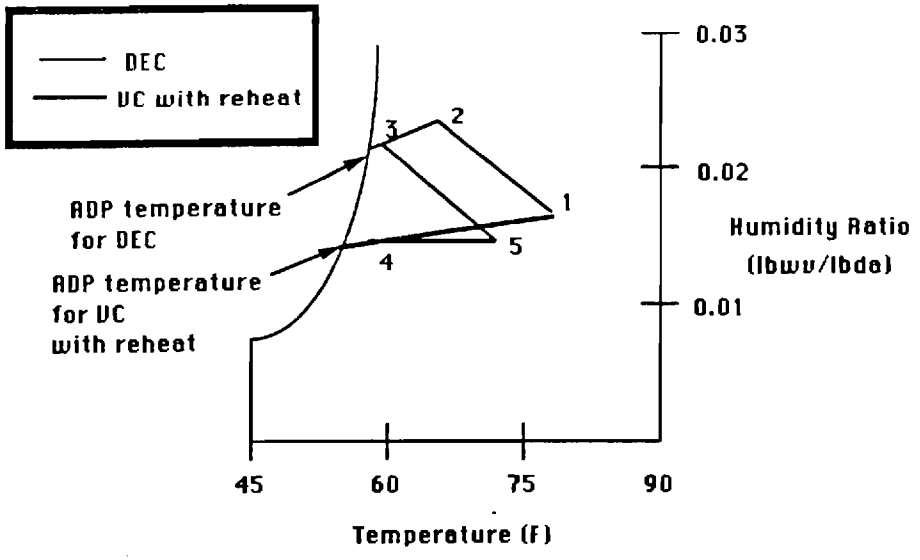

Fig. 12-Illustration of the Desiccant Enhanced Cooling System Process Versus Conventional Vapor Compression with Reheat Process on a Psychrometric Chart

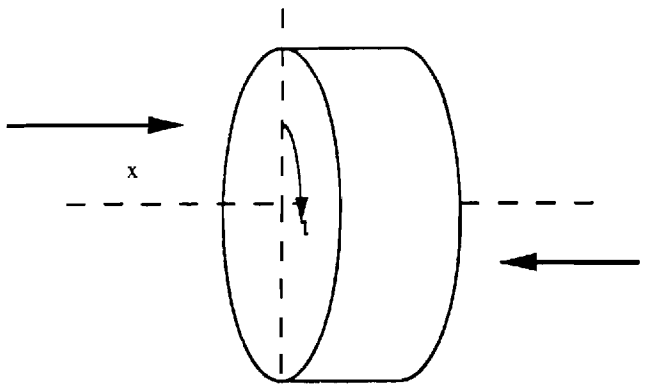

Fig. 13-Illustration of a Rotary Heat Exchanger

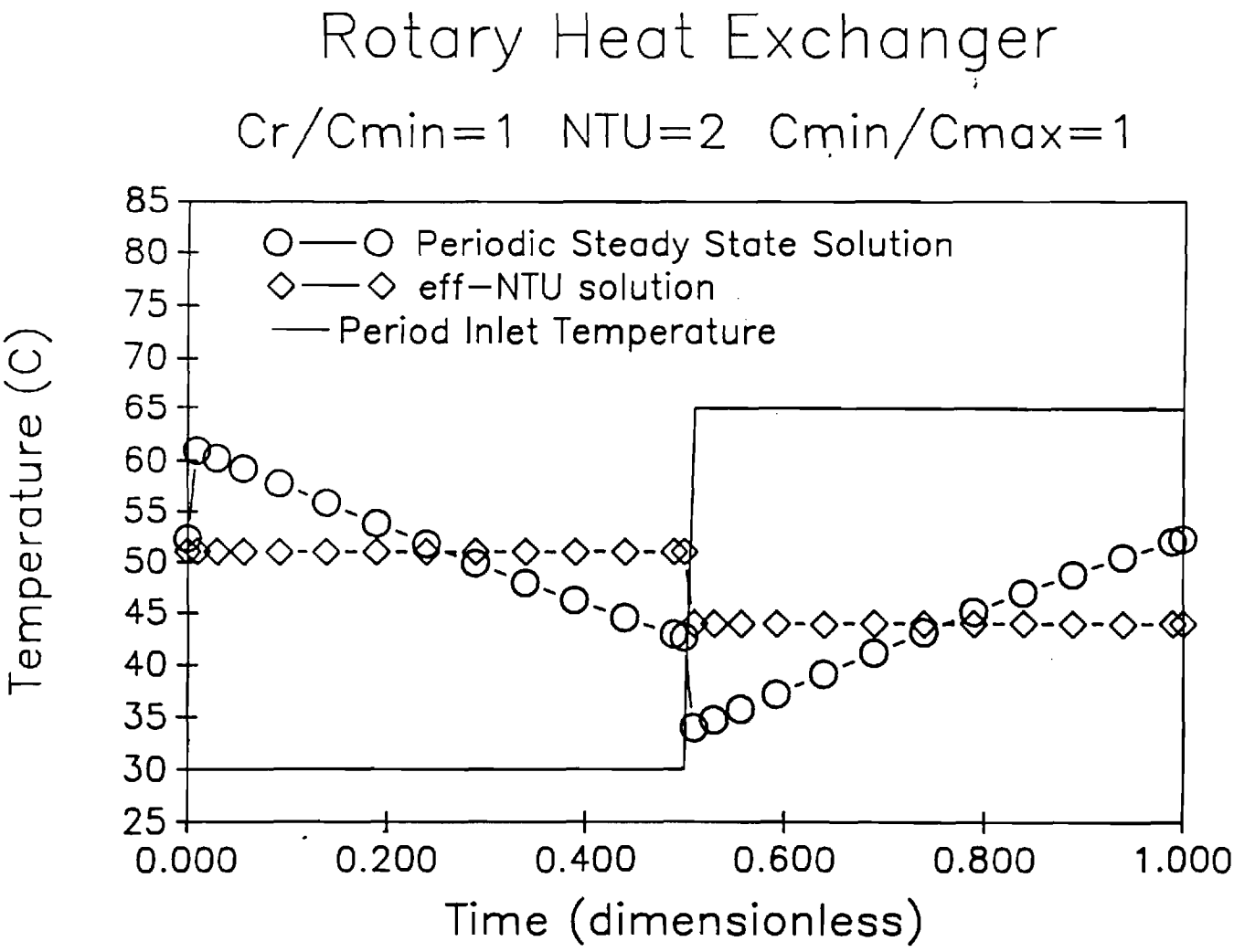

Fig. 14-Comparison of Model with Rotary Heat Exchanger: Case 1

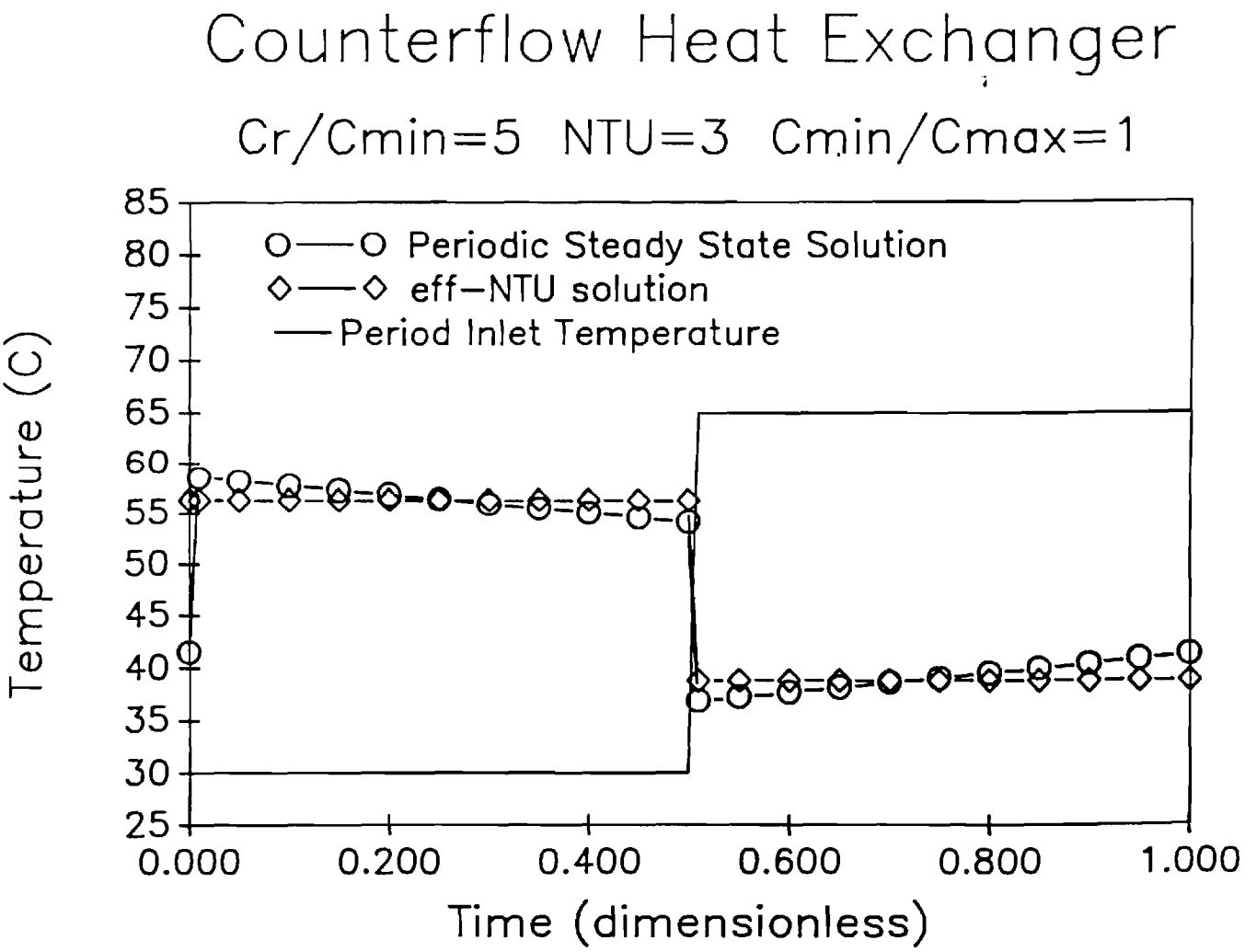

Fig. 15-Comparison of Model with Rotary Heat Exchanger: Case 2

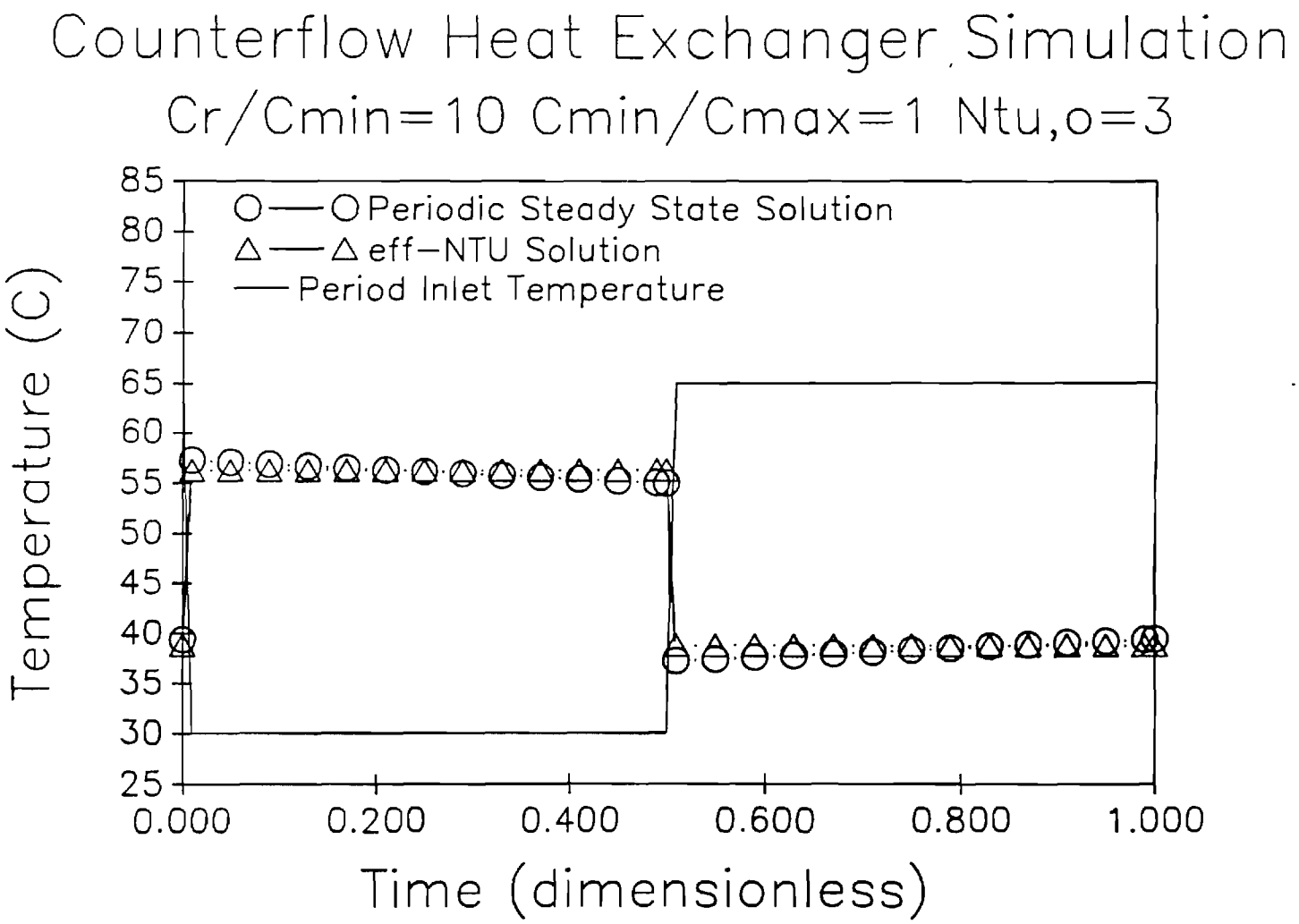

Fig. 16-Comparison of Model with Counterflow Heat Exchanger: Case 3

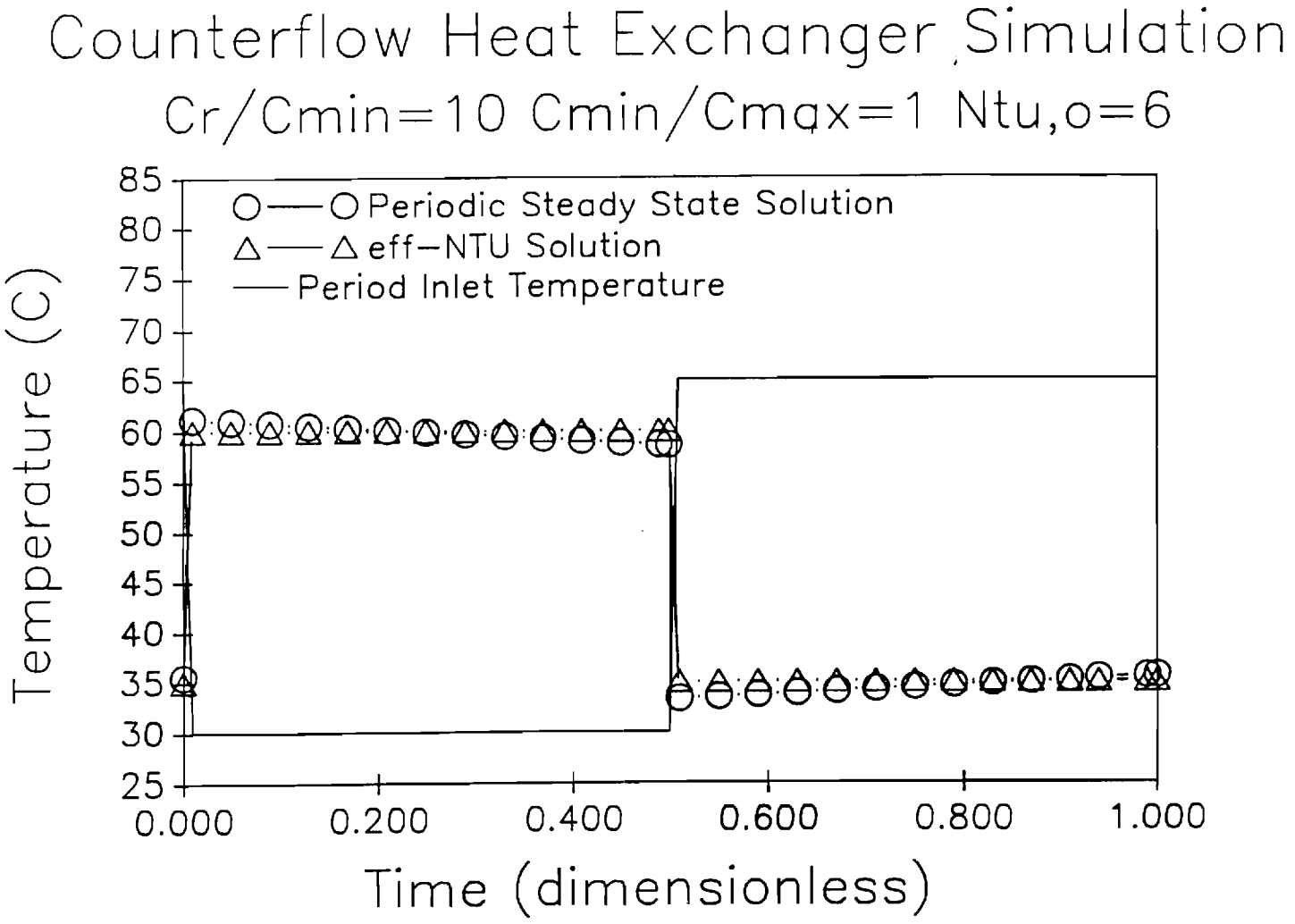

Fig. 17-Comparison of Model with Counterflow Heat Exchanger: Case 4

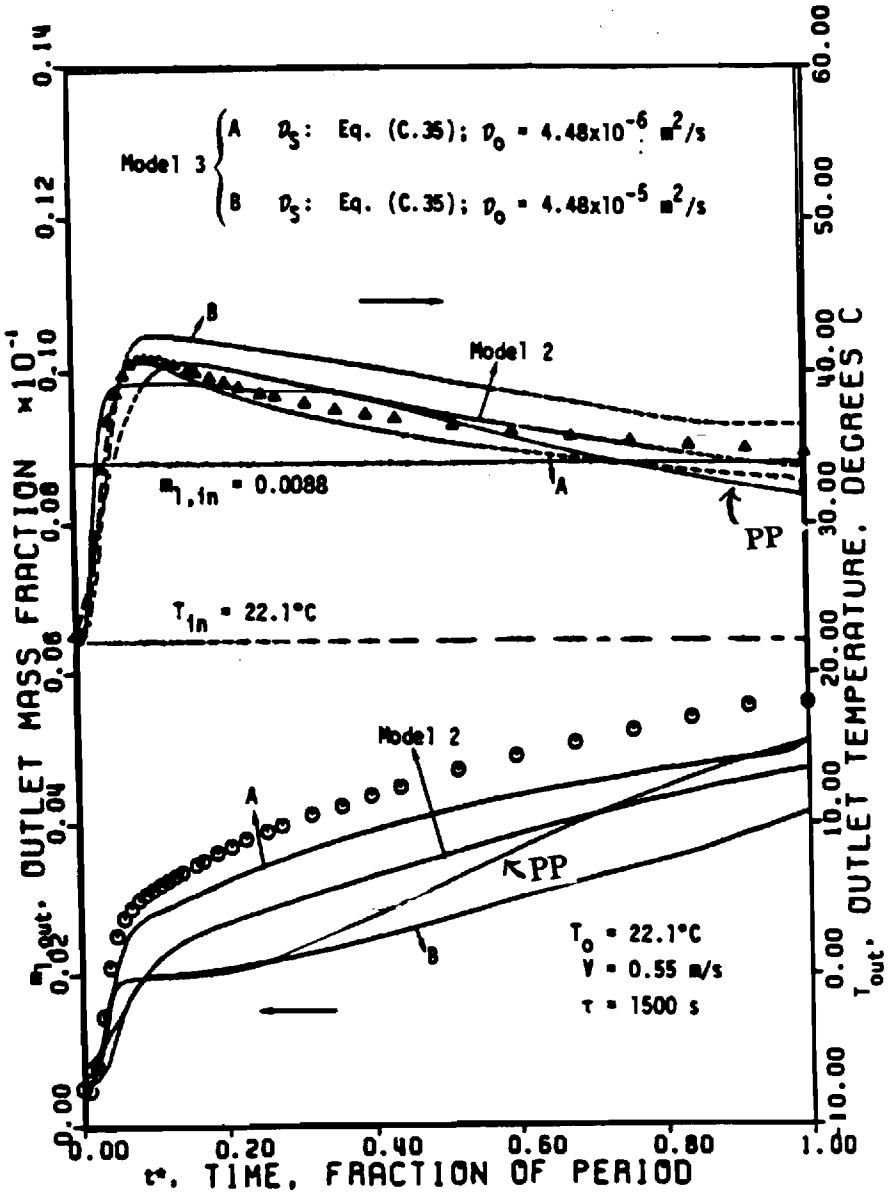

Fig. 18-Comparison of Model with Fixed Bed Adsorption, PGS model and Diffusion Resistance Model: Example 1

Model 2 refers to PSG controlled model

Model 3 refers to diffusion resistance model

PP = parabolic profile model

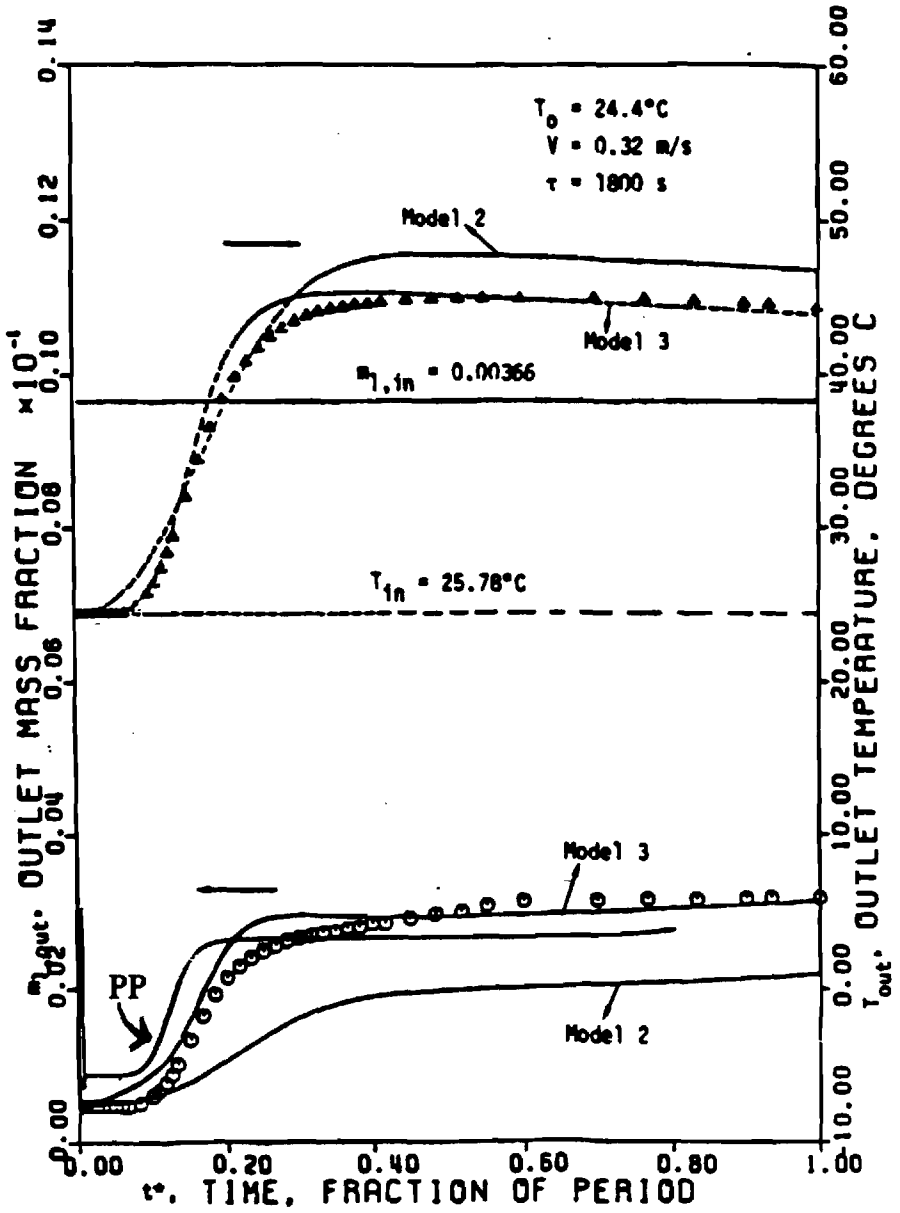

Fig. 19-Comparison of Model with Fixed Bed Adsorption Data, PGS model and Diffusion Resistance Model: Example 2

Model 2 refers to PSG controlled model

Model 3 refers to diffusion resistance model

note that 2 different diffusivities were used for the two runs of model 3

PP = parabolic profile model

Model Comparison with Experiment

Run # 11-13-85 1A

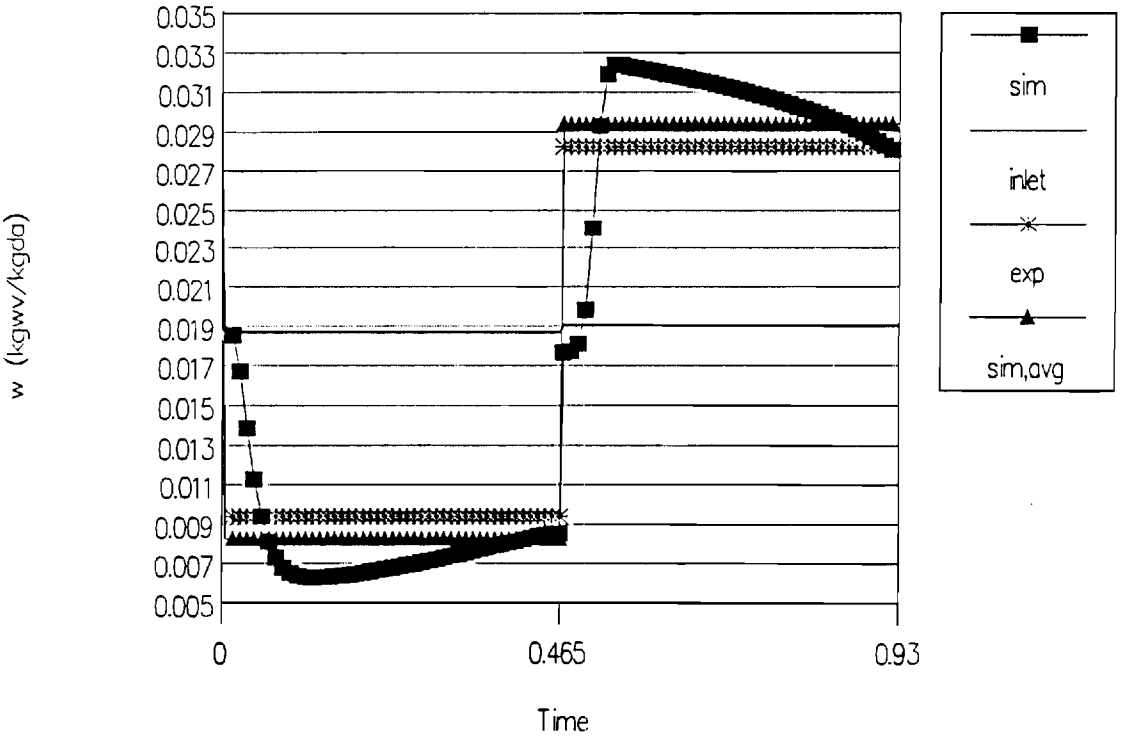

Fig. 20a-Comparison of Model with Rotary Desiccant Wheel Experimental Data
Outlet Humidity Ratio for Example 1

Model Comparison with Experiment

Run # 11-13-85 1A

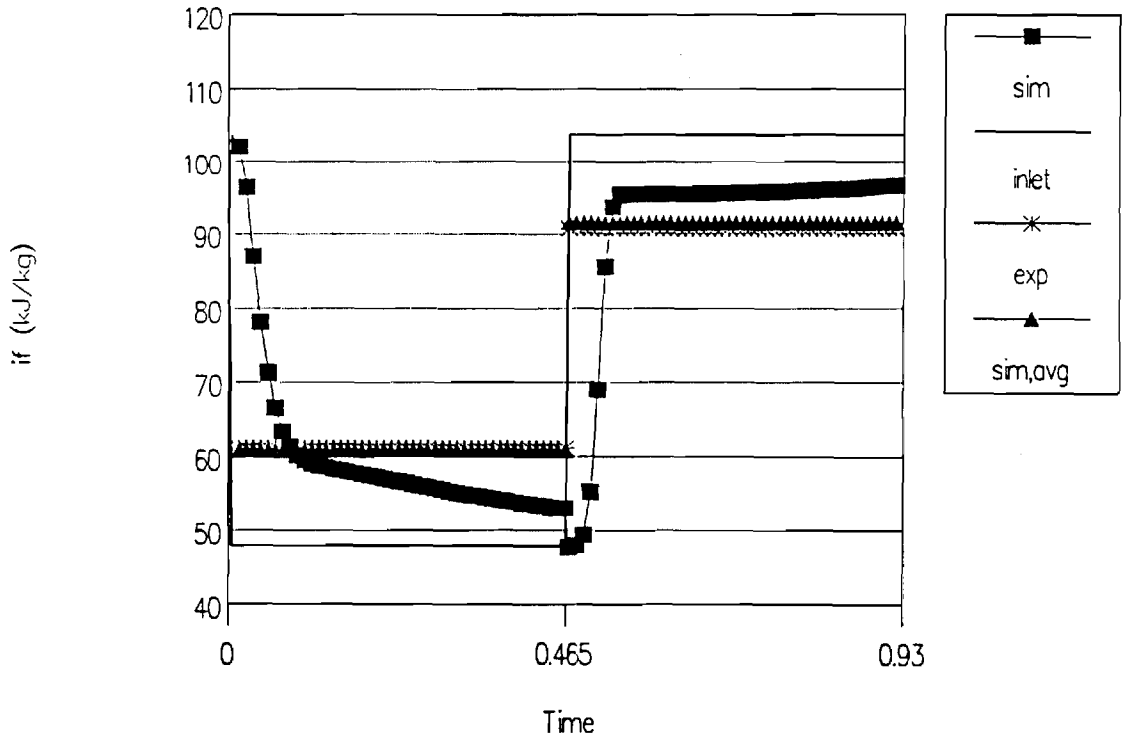

Fig. 20b-Comparison of Model with Rotary Desiccant Wheel Experimental Data Outlet Enthalpy for Example 1

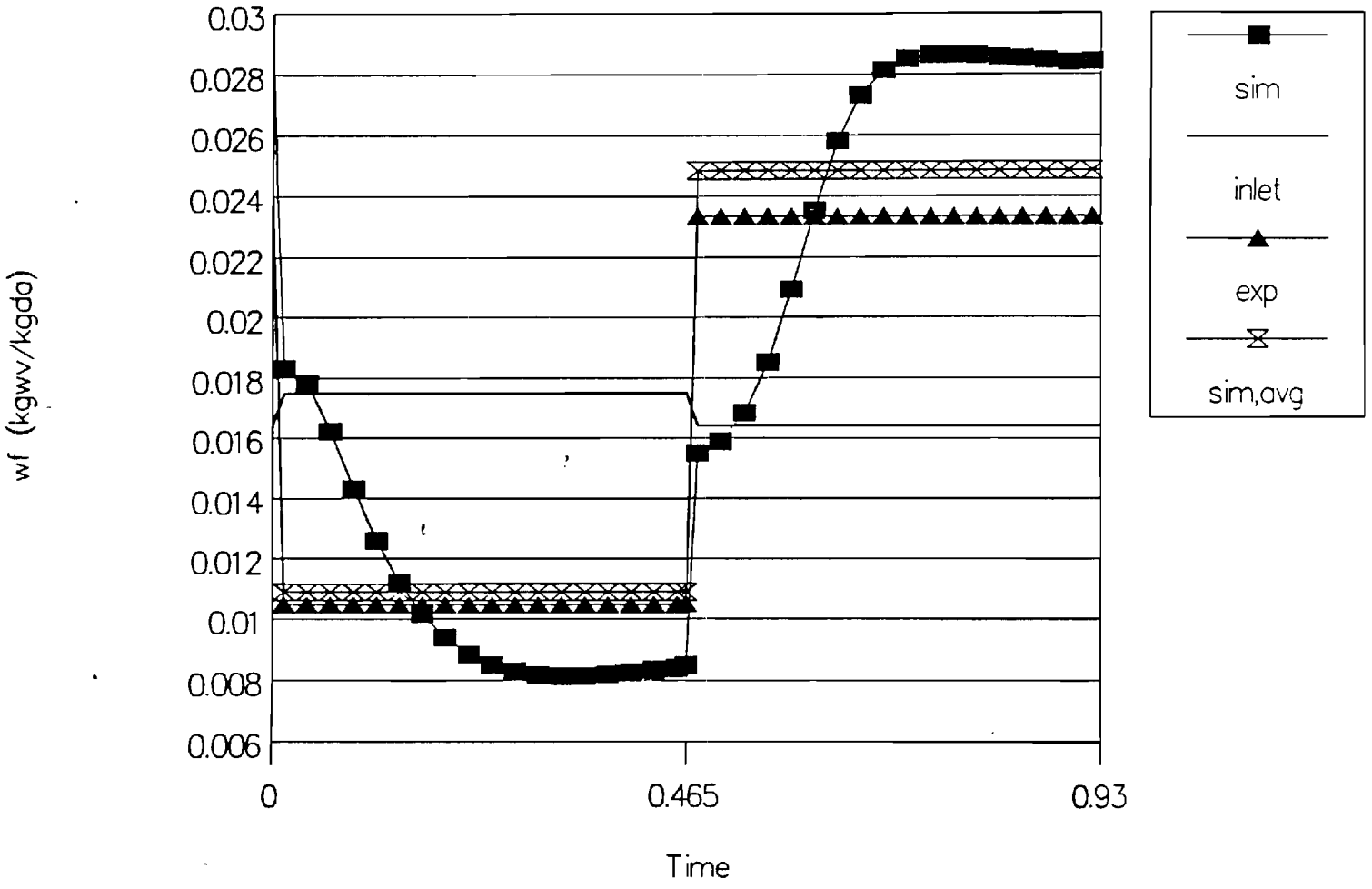

Fig. 21a-Comparison of Model with Rotary Desiccant Wheel Experimental Data
Outlet Humidity Ratio for Example 2

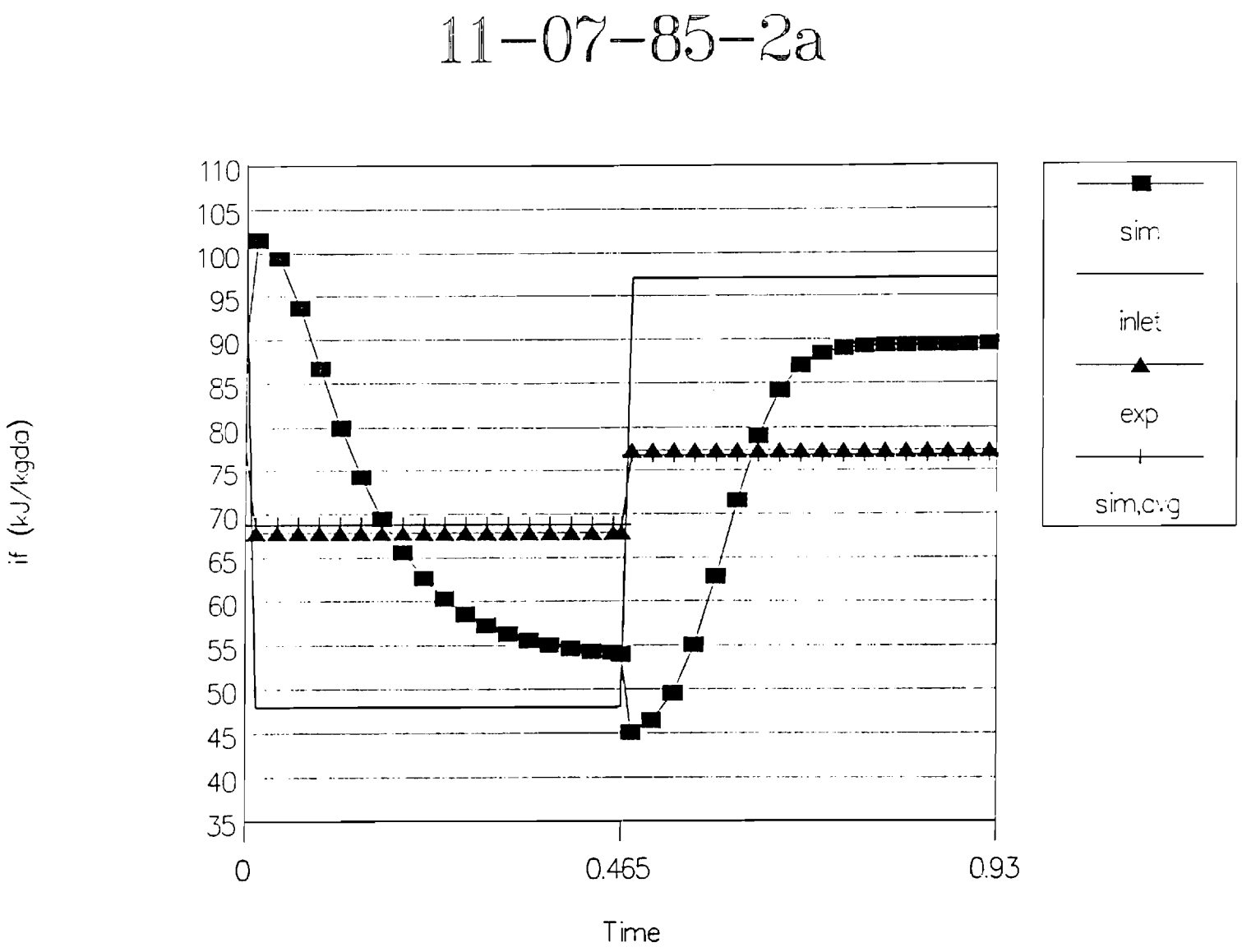

Fig. 21b-Comparison of Model with Rotary Desiccant Wheel Experimental Data
Outlet Enthalpy for Example 2

APPENDIX A-DEVELOPMENT OF GOVERNING EQUATIONS FOR THE ROTARY DESICCANT WHEEL

See Table A1 for nomenclature description

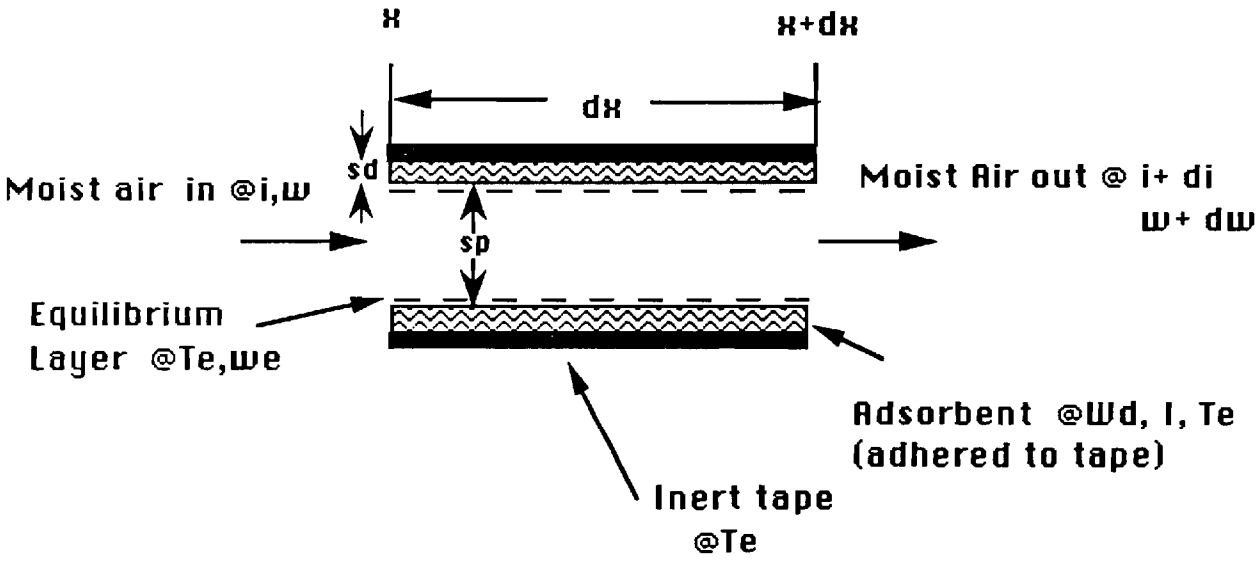

Fig. A1-Illustration of Parallel Passage Control Volume

i. Conservation of Mass:

$$\partial(dM_{sw})/\partial t = \dot{m}_{wv,x} - \dot{m}_{wv,x+dx}$$

$$= \dot{m}_{wv,x} - (\dot{m}_{wv,x} + \partial\dot{m}_{wv}/\partial x\, dx)$$

Canceling terms and rearranging:

$$\partial(dM_{sw})/\partial t + \partial\dot{m}_{wv}/\partial x\, dx = 0$$

Let:

$$\dot{m}_{wv} = (\dot{m}_{da,j}/N)\, w \qquad \text{and} \qquad dM_{sw} = W_d\, dM_{dd}$$

Where N, $\dot{m}_{da}$, dM_{dd} are constant. The conservation of mass becomes:

$$dM_{dd}\, \partial W_d/\partial t + (\dot{m}_{da,j}/N)\, \partial w/\partial x\, dx = 0$$

The mass of dry desiccant inside the control volume can be written as:

$$dM_{dd} = \rho_b \; A_c \, dx \quad (1)$$

Where the bulk density of dry desiccant is related to the true density of the desiccant as:

$$\rho_b = \{2 \, s_d/(s_p+2s_d)\} \, \rho_p$$

Substituting this into the conservation equation and canceling the dx term:

$$\rho_b \; A_c \, \partial W_d/\partial t + (\dot{m}_{da,j}/N) \, \partial w/\partial x = 0$$

Rearranging:

$$\partial w/\partial x + (\rho_{dd} \, A_c \, N/ \, \dot{m}_{da,j}) \, \partial W_d/\partial t = 0$$

Scale the independent variables as follows:

$$z = x/L \qquad \tau = t/\theta$$

The conservation equation becomes:

$$\partial w/\partial z + (\rho_{dd} \; A_c \, L \, N/ \, \dot{m}_{da} \, \Gamma) \, \partial W_d/\partial \tau = 0$$

The term $\rho_{dd} \; A_c \, L \, N = M_{dd,j} = \beta_j \, M_{dd}$, the active mass of the dry desiccant in period j, which is the total mass of the dry desiccant in the wheel times the period fraction β_j. The final form of the conservation of mass partial differential equation is:

$$\frac{\partial w}{\partial z} + \beta_j \frac{M_{dd}/\theta}{\dot{m}_{da,j}} \frac{\partial W_d}{\partial \tau} = 0$$

ii. Conservation of Energy:

$$\partial(dU_{wd})/\partial t = \dot{I}_{ma,x} - \dot{I}_{ma,x+dx}$$

$$= \dot{I}_{ma,x} - (\dot{I}_{ma,x} + \partial \dot{I}_{ma}/\partial x \, dx)$$

Canceling terms and rearranging:

$$\partial(dU_{wd})/\partial t + \partial \dot{I}_{ma}/\partial x \, dx = 0$$

Let:

$$\dot{I}_{ma} = (\dot{m}_{da,j}/N)\, i \qquad \text{and} \qquad U_{wd} = u_{wd}\, dM_{dd}$$

Conservation of energy becomes:

$$dM_{dd}\, \partial u_{wd}/\partial t + (\dot{m}_{da,j}/N)\, \partial i/\partial x\, dx = 0$$

The internal energy of the wet desiccant u_{wd}, can be written as:

$$u_{wd} = I - P\, v_{wd}$$

Inserting this expression into the conservation of energy:

$$dM_{dd}\, \partial\{I - (P\, v)_{wd}\}/\partial t + (\dot{m}_{da,j}/N)\, \partial i/\partial x\, dx = 0$$

Distributing the derivative:

$$dM_{dd}\, \{\partial I/\partial t - \partial(P\, v)_{wd}/\partial t\} + (\dot{m}_{da,j}/N)\, \partial i/\partial x\, dx = 0$$

and expanding the $P\, v_{wd}$ derivative:

$$dM_{dd}\, \{\partial I/\partial t - P\, \partial v_{wd}/\partial t - v_{wd}\, \partial P/\partial t\} + \dot{m}_{da,j}/N\, \partial i/\partial x\, dx = 0$$

The derivative $\partial v_{wd}/\partial t$ in the above equation is zero since the derivative of the specific volume of the wet desiccant with respect to time is negligible. The dry desiccant and the sorbed water can be considered to be incompressible substances. The derivative $\partial P/\partial t$ also disappears since the pressure drop with respect to time is zero for the desiccant bed as it is open to the atmosphere. The conservation of energy is:

$$dM_{dd}\, \partial I/\partial t + (\dot{m}_{da,j}/N)\, \partial i/\partial x\, dx = 0$$

Inserting Equation (1), scaling the independent variables as before and rearranging, the final expression for the conservation of mass is:

$$\frac{\partial i}{\partial z} + \beta_j\, \Gamma_j\, \frac{\partial I}{\partial \tau} = 0$$

iii. Heat Transfer Rate Equation

The control volume for development of the heat transfer rate equation is shown. The energy balance can be stated as follows:

Rate of change of moist air enthalpy	=	Rate of convective heat transfer	+	Rate of energy release due to heat of vaporization

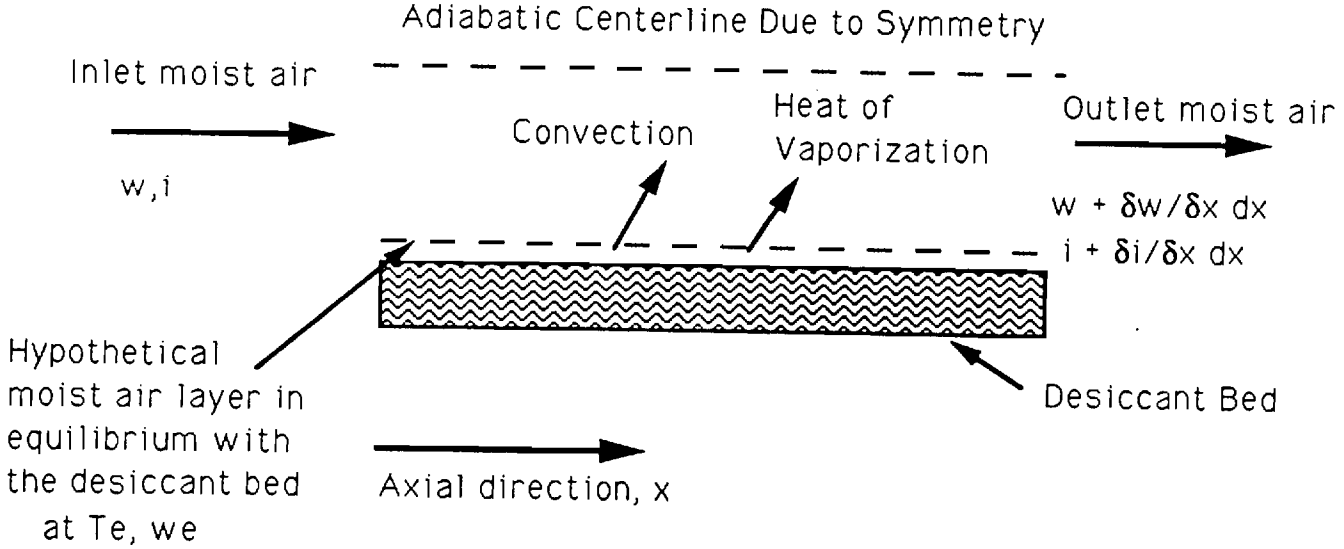

Fig. A2 Control Volume for Development of Heat Transfer Rate Equation

The energy balance statement can be written in equation form as:

$$(\dot{I}_{ma,x+\Delta x} - \dot{I}_{ma,x}) = h_q\, \alpha\, \Delta x\, (T_e - T) + i_{fg}[T_e]\, (\dot{m}_{w,x+\Delta x} - \dot{m}_w) \qquad (1)$$

Assuming that the surface area per unit length of the bed, α_s, is constant, and using the following relations:

$$\dot{m}_w = \dot{m}_{da,j}\, w$$

$$\dot{I}_{ma} = \dot{m}_{da,j}\, i$$

where the mass flow rate of the moist air, m_{da}, is constant, Equation (1) becomes:

$$\dot{m}_{da,j}\,(i_{x+\Delta x} - i_x)/\Delta x = h_q\,\alpha\,(T_e - T) + \dot{m}_{da,j}\; i_{fg}[T_e]\,(w_{x+\Delta x} - w_x)/\Delta x \qquad (2)$$

Rearranging Equation (2) and taking the limit as $\Delta x \to 0$:

$$\partial i/\partial x = h_q\;\alpha/m_{da,j}\,(T_e - T) + i_{fg}[T_e]\,\partial w/\partial x \qquad (3)$$

Let $z = x/L$ be the non-dimensionalized axial position, and noting that for α = constant, we have $\alpha L = A_s$, the final form of the heat transfer rate equation becomes:

$$\partial i/\partial z = NTU_{q,j}\;(T_e - T) + i_{fg}[T_e]\,NTU_{m,j}\,(w_e - w) \qquad (4)$$

where $NTU_{q,j} = h_{q,j}\;A_s/\dot{m}_{da,j}$ and the relationship $\partial w/\partial z = NTU_{m,j}\,(w_e - w)$ was developed in chapter 3.

for the given temperature and moisture content arrived at. The adsorption isotherm was determined by through a regression analysis of the data fitted to Equation (16).

Table A1. Nomenclature Used in Appendices

A = Adsorbed surface area
A_s = Surface area
A_c = Cross sectional area of passage
c_m = Heat capacity of matrix
c_{lw} = Heat capacity of liquid water
c_{wv} = Heat capacity of water vapor
c_{da} = Heat capacity of dry air
dM_{dd} = Differential mass of dry desiccant in control volume
G = Total Gibbs free energy
h_q = Convective heat transfer coefficient
i_{da} = Specific enthalpy of dry air
i_{wv} = Specific enthalpy of water vapor
i = Specific enthalpy of moist air fluid (per unit mass dry air)
i_{fg} = Enthalpy of vaporization of liquid water
I = Specific enthalpy of wet desiccant (per unit mass dry desiccant)
I_m = Specific enthalpy of mixture
$\dot{I}_{ma}$ = Total enthalpy rate of moist air
L = Length of desiccant bed
M_{dd} = Total mass of dry desiccant
$M_{dd,j} = (\beta_j M_{dd})$ = Active mass of dry desiccant in period j
m_s = Mass of sorbed water
$\dot{m}_{da}$ = Total mass flow rate of dry air through the dehumidifier
$\dot{m}_{da,j}$ = Total mass flow rate of dry air through the dehumidifier
M_{sw} = Mass of sorbed water in control volume
$\dot{m}_{wv}$ = Mass flow of water vapor through control volume passage
$NTU_{q,j}$ = Number of transfer units for heat transfer for period j
N = Number of passages
n = Number of moles
n_s = Number of moles adsorbed
P_{wv} = Partial pressure of water vapor
$P_{wv,sat}$ = Saturation pressure of water vapor
P = Total pressure
q_{st} = Isosteric heat of adsorption
RH = Relative humidity
R = Gas constant
S = Total enthalpy
s = specific enthalpy
s_p = Height of passage
s_d = Thickness of desiccant sheet
T = Temperature of fluid
T_e = Temperature of desiccant and moist air in equilibrium with desiccant
T_{ref} = Reference temperature where enthalpy of dry air and liquid water is taken to be zero

t = Real time coordinate
U = Total internal energy
U_{wd} = Total internal energy of wet desiccant
u_{wd} = Specific internal energy of wet desiccant (per unit mass dry desiccant)
V = Total volume
v = Specific volume
v_{wd} = Specific volume of wet desiccant
v_g = Specific volume of vapor
v_f = Specific volume of liquid
$v_{fg} = (v_f - v_g)$ = Volume of vaporization of liquid water
W_d = Volumetric average moisture content of desiccant per unit mass dry desiccant
w = Humidity ratio of moist air = (mass of water vapor/mass of dry air)
w_e = Humidity ratio of moist air in equilibrium with the desiccant
x = Real axial position
z = Nondimensional axial position

Greek:

α = Surface area per unit length
$\beta_j = (\theta_j/\theta)$ = Period fraction
ϕ = Surface tension of adsorbed phase
μ_s = Chemical potential of adsorbed phase
μ_g = Chemical potential of vapor phase
ρ_b = Bulk density of dry desiccant = Mass of dry desiccant per unit volume of dehumidifier
ρ_p = Particle density of dry desiccant = Mass of dry desiccant per unit volume of dry desiccant
τ = Nondimensional time coordinate
θ = Time for wheel to complete 1 revolution
θ_j = Duration of period j
$\Gamma_j = (M_{dd}/(\theta\, \dot{m}_{da,j}))$ = Mass capacity ratio for period j

APPENDIX B-THERMODYNAMIC PROPERTIES MOIST AIR

It is necessary to develop a consistent theory for the thermodynamic properties of moist air. Moist air can be treated as an ideal gas mixture at atmospheric pressure for water vapor pressure less than 2 psia [53]. The property development uses the Gibbs-Dalton mixture model for the mixture for the mixture of dry air and water vapor. The Gibbs-Dalton model considers the properties as if each component existed separately at the temperature and volume of the mixture. In this model, each component has an individual component pressure. For an ideal gas mixture, the component pressure is the partial pressure.

i. Enthalpy

The enthalpy of an ideal gas mixture, which depends on composition and temperature is:

$$I_m = \Sigma\, m_j\, i_j$$

For moist air, it will be assumed that the two components are water vapor and dry air; therefore,

$$I_m = m_{da}\, i_{da} + m_{wv}\, i_{wv}$$

$$i = I_m/m_{da} = i_{da} + (m_{wv}/m_{da})\, i_{wv} = i_{da} + w\, i_{wv}$$

If at the arbitrary reference temperature the enthalpy of liquid water and the enthalpy of dry air are chosen to be zero, then the enthalpy for the mixture is as follows:

$$i = i_{da} + w\, i_{wv}$$

$$= c_{p,da}\,(T - T_{ref}) + w\, c_{p,wv}\,(T - T_{ref}) + i_{fg}[T_{ref}] + i_{lw}[T_{ref}]$$

where $i_{lw}[T_{ref}]$ is chosen to be zero.

ii. Relative Humidity

The relative humidity of moist air is defined as:

$$RH\ (\%) = P_{wv}[w]/P_{wv,sat}[T]\ (100\%)$$

where:

$$P_{wv}[w] = w\,P_{total} / (0.62198 + w)$$

The expression used for the saturation pressure of water vapor at the temperature of the mixture is the Goff correlation for the saturation pressure of water vapor over liquid water:

$$\log_{10}(P) = a\,(1-\theta) + b\,\log_{10}(\theta) + c\,(1- 10^{d(1/\theta-1)}) + e(10^{f(1-\theta)} -1) + g$$

where:

$\theta = 273.15/T(K)$	a=10.79586	b=5.02808
c=1.50474E-4	d=-8.29692	e=.42873E-3
f=4.76955	g=-2.2195983	

iii. Enthalpy of Vaporization

The Clapeyron equation is employed for the enthalpy of vaporization:

$$i_{fg} = T\,v_{fg}\,dP/dT\ \big|_{sat} = T\,\{RT/P_{sat} - v\}\,dP/dT\big|_{sat}$$

The derivative of the Goff correlation is taken to evaluate the slope of the saturation curve for use in the Clapeyron equation. These property relations allow evaluations of the thermodynamic properties of moist air using only a saturation curve correlation and heat capacity data.

Appendix C - Thermodynamics of Desiccant Materials

i. Adsorption Isotherm

A desiccant is a material with a high affinity for water vapor. When water vapor at a moderate temperature is brought into contact with the desiccant, the water vapor "condenses" and adheres to the surface of the pores. This phenomena is called physical adsorption. Internal energy is released as a consequence of the adsorption process. The heat of sorption is similar in magnitude to the heat of vaporization of liquid water. The adsorbed phase is two dimensional and has less internal energy than a three dimensional liquid. Therefore the heat effect associated with adsorption is higher than that of pure condensation. Solution of the rotary desiccant wheel problem requires a relationship for the enthalpy of the wet desiccant as a function of temperature and moisture content. This enthalpy expression must correctly account for the heat effect associated with adsorption. Solution of the rotary desiccant wheel problem also requires an expression for the equilibrium adsorption isotherm. The adsorption isotherm is an expression for the moisture loading of the wet desiccant as a function of temperature and the vapor pressure of the water vapor air in contact with the desiccant. One method of developing the expression for the adsorption isotherm follows.

For the case of an adsorbate in equilibrium with the adsorbed phase, we have:

$$\mu_g = \mu_s$$

Therefore, for an infinitesimal change in conditions:

$$d\mu_g = d\mu_s \tag{1}$$

The chemical potential for a one component adsorbate is defined as:

$$\mu_s = \partial G/\partial n\big|_{T,A,P} \tag{2}$$

For the gaseous phase, water vapor in our case it is:

$$\mu_g = \partial G/\partial n\big|_{T,P} \tag{3}$$

Expanding both sides of Equation (1) for the case of constant number of moles adsorbed:

$$(\partial\mu_g/\partial T)_P\, dT + (\partial\mu_g/\partial P)_T\, dP = (\partial\mu_s/\partial T)_{P,A}\, dT + (\partial\mu_s/\partial P)_{T,A}\, dP + (\partial\mu_s/\partial A)_{T,P}\, dA$$

and inserting the definitions (2) and (3):

$$(\partial^2 G_g/\partial n\, \partial T)_P\, dT + (\partial^2 G_g/\partial n\, \partial P)_T\, dP$$

$$= (\partial^2 G_s/\partial n \partial T)_{P,A}\, dT + (\partial^2 G_s/\partial n \partial P)_{T,A}\, dP + (\partial^2 G_s/\partial n \partial A)_{T,P}\, dA \tag{4}$$

The first law of thermodynamics of the adsorbed phase is:

$$dU_s = T\, dS_s - \phi_s\, dA - P\, dV_s + \mu_s\, dn_s \tag{5}$$

The Gibbs free energy is:

$$G_s = U_s - T\, S_s + P\, V_s \tag{6}$$

The differential of the Gibbs free energy is found by differentiating Equation (6) and by inserting Equation (5) to eliminate some of the terms:

$$dG_s = -S_s\, dT + V_s\, dP + \mu_s\, dn_s - \phi_s\, dA \tag{7}$$

The differential of the Gibbs free energy for the water vapor phase is derived from the Maxwell relations and is:

$$dG_g = -S_g\, dT + V_g\, dP + \mu_g\, dn_s \tag{8}$$

Noting that the partials of Equation (4) are independent of the order of differentiation and inserting (7) and (8) into (4):

$$-\partial S_g/\partial n\, dT + \partial V_g/\partial n\, dP = -\partial S_s/\partial n\, dT + \partial V_s/\partial n\, dT + \partial V_s/\partial n\, dP - \partial\phi_s/\partial n\, dA \tag{9}$$

Rewriting this equation as:

$$-s_g\ dT + v_g\ dP = -\ s_s\ dT + v_s\ dP - \partial\phi_s/\partial n\ dA \qquad (10)$$

Where the partial molar notation is used for extensive quantities only. ϕ is not an extensive quantity so the derivative is kept on this term. The area of the absorbate is held constant, which is natural for a constant number of moles adsorbed on a desiccant of constant mass. Rearranging (10) we get:

$$(\partial P/\partial T)_{A,ns} = (s_g - s_s)/(v_g - v_s) \qquad (11)$$

The chemical potential for the gas phase is:

$$\mu_g = i_g - T_g\ s_g \qquad (12)$$

and for the adsorbed phase:

$$\mu_s = i_s - T_s\ s_s \qquad (13)$$

We can eliminate the entropies from (11) using (12) and (13) and noting that at equilibrium we have $\mu_s = \mu_g$:

$$(\partial P/\partial T)_{A,ns} = (i_g - i_s)/\{\ T\ (v_g - v_s)\ \} \qquad (14)$$

Assuming that the adsorbed phase is liquid-like, $V_g >> V_s$ and treating the water vapor as an ideal gas, which is valid for moist air at atmospheric pressure:

$$(\partial P/\partial T)_{A,ns} = P\ (i_g - i_s)/\ \{R\ T^2\} \qquad (15)$$

Rearranging (15):

$$(\partial \ln P/\partial T)_{A,ns} = (i_g - i_s)/\ \{R\ T^2\} \qquad (16)$$

Dropping the superscripts, the expression $(i_g - i_s)$, is the difference between the partial molar enthalpy in the adsorbed phase and in the gaseous phase. This is called the enthalpy of adsorption. The negative of this term is defined in the literature as the isosteric (constant number of moles adsorbed) heat of adsorption, as this is the heat effect associated with the change in vapor pressure with temperature with the number of moles adsorbed held constant. Equation (16) is developed in [47] and [19]. White [54] developed the same expression using

collision theory. This expression is the equilibrium adsorption isotherm. The isosteric heat of adsorption can be obtained from plotting experimental data of vapor pressure versus temperature at constant moisture content. The isosteric heat of adsorption is then the slope of this curve.

ii. Enthalpy

The enthalpy is a function of temperature and the mass of sorbed water: $I = I[T,m_s]$.

Therefore:

$$dI = (\partial I/\partial T)_{ms}\, dT + (\partial I/\partial m_s)_T\, dm_s \qquad (17)$$

But $(\partial I/\partial T)_{ms}$ is the heat capacity of the wet desiccant and assuming that the adsorbed phase behaves like liquid water:

$$(\partial I/\partial T)_{ms} = c_m + m_s\, c_{lw} \qquad (18)$$

Where c_m, the lumped heat capacity of the matrix:

$$c_m = \Sigma\, (c_i\, dm_i)/M$$

While the other partial derivative needs to be evaluated. As previously developed, the expression for the isosteric heat of adsorption is:

$$q_{st}' = -\,(\,\partial I_s/\partial n - \partial I_g/\partial n\,)$$

Where the prime notation indicates a per unit mole basis. Rearranging:

$$\partial I_s/\partial n = \partial i_g/\partial n - q_{st}'$$

The mass of sorbed water is $m_s = n_s\, M$, and the mass of the water vapor is $m_g = n_g\, M$ we get the following expression:

$$\partial I/\partial m_s = \partial i_g/\partial m - q_{st}$$

The term $\partial i/\partial m_g$ is the enthalpy of vaporization of liquid water. Therefore the partial derivative becomes:

$$\partial I/\partial m_s = i_{fg} - q_{st}$$

Assuming that the heat capacities are linear in the temperature range of interest, and integrating Equation (17) from $I[T_{ref},m_s=0] = 0$ to the state of interest $I[T,m_s=m]$, the following form of the enthalpy of the wet desiccant as a function of temperature and pressure results:

$$I[T,m_s] = (M_{dd}\, c_m + m_s\, c_{lw})\,(T - T_{ref}) + \int_0^m (i_{fg} - q_{st})\, dm_s \qquad (18)$$

Equation (18) can be expressed per unit mass of dry desiccant:

$$I[T,W_d] = (\, c_m + W_d\, c_{lw})\,(T - T_{ref}) + \int_0^{W_d} (i_{fg} - q_{st})\, dW \qquad (19)$$

Where $W_d = m_s/M_{dd}$.

a. Example Calculation for Regular Density Silica Gel

The ratio q_{st}/i_{fg} for regular density silica-gel was investigated by Close and Banks [4]. It was observed from examination of three sets of data from Hubard, Ewing and Bauer, and Hougen, Watson and Ragatz [22] that although the isosteric heat of adsorption and the enthalpy of vaporization are functions of temperature, the ratio between the two are independent of temperature, i.e. $q_{st}/i_{fg} = g(W_d)$. Now the expression $(i_{fg} - q_{st})$ in the integral of Equation (19) can be written as:

$$i_{fg} - q_{st} = i_{fg}\,(1 - q_{st}/i_{fg}) = i_{fg}\,(1 - f(W_d))$$

Rearranging Equation (19), we have the following final expression for the enthalpy of the wet desiccant:

$$I[T,W_d] = (\, c_m + W_d\, c_{lw})\,(T - T_{ref}) + i_{fg} \int_0^{W_d} (\, 1 - f(W)\,)\, dW \qquad (20)$$

The expressions for q_{st}/i_{fg} is a piecewise polynomials and are of the form:

$$f(W) = a\, W^3 - b\, W^2 + c\, W + d$$

This expression can be inserted into the integral of Equation (20) and the resulting enthalpy

APPENDIX D-PROGRAM LISTINGS

```
      program BSDES
C Controls the Bulirsch Stoer algorithm for solution of the
C parallel passage type rotary dessicant wheel
      implicit double precision (a-h,o-z)
      common /finalx/ xf
      common /finalt/ taufp,taufr
      common /max/ dxmax,dtmax
C xtry - first B-S step deltax
      data xs/0./
      data res,ip,tdid/1D-6,0,0./
C Call subroutine to open data files and calculate wheel parameters
      call SYSPAR(ip)
      call ODF
      xtry=dxmax
 10   continue
C  Call Bulirsch-Stoer algorithm which takes one temporal
C  step and one axial direction step using the B-S method.
C  Input is xs- axial positional position
C  xtry-step size to try  eps-accuracy required
C  Returned values are axial position, next suggested
C  step size, step size achieved and temporal position
      call XBSSTEP(xs,xtry,tau,tdid,ipss)
C if periodic steady state has been reached then end
      if(ipss.eq.1) goto 40
C Increment axial location
      xs = xs+xtry
C If final time coordinate and final axial coordinate
C have been reached then reset time and axial position
      if(tau.ge.(taufr-res).and.xs.ge.(xf-res)) then
      tau=0.
      xs=0.
      xtry=dxmax
C Start new rotation
      goto 10
      endif
C test for reaching outlet face of wheel
      if(xs.ge.(xf-res)) then
      xs = 0.
      xtry=dxmax
      endif
C test if next step size integrates past outlet face
      if (xs.lt.xf.and.(xs+xtry).ge.(xf-res)) xtry=xf-xs
C Restart B-S method
      goto 10
 40   continue
      close(1)
      close(2)
      stop
      end

      subroutine ODF
C opens data files
      open(1,file='des.prn')
      open(2,file='bc.prn')
      return
      end

      subroutine SYSPAR(ip)
C Subroutine prompts for input air stream states and
C calculates system parameters
```

```
      implicit double precision (a-h,o-z)
      common /totP/ Ptotal
      common /finalx/ xf
      common /finalt/ taufp,taufr
      common /htcap/ cpda,cpwv
      common /htcp2/ cplw,cd
      common /xfer/ rNTUqm,rNTUmm,rhqfd
      common /ref/ Tref
      common /mcap/ tmcap
      common /parp/ Rad,Deff,rhop
      common /calc/ Tempd,rmda,Asurf,RNrev,RMdd
      common /bcbed/ wf,rif
      common /thprop/ Re,Pr,Dh,rkf,rleng
      common /max/ dxmax,dtmax
C Physical parameters of the wheel and inlet air states are read
C in from input.dat: Rad - radius of desiccant particle
c Deff - effective diffusivity  rhop - density of particle
C rNrev - # of revolutions per hour  rmda - mass flow rate of dry air
C rMdd - total mass of dry desiccant
      if(icc.eq.0) then
      icc=1
      open(1,file='input.dat')
      read(1,*) cpda,cpwv,Tref,cplw,cd,Ptotal,Rad
     *  ,Deff,rhop,rmdap,rmdar,Asurf,rNrev,rMdd,taufp
     *  ,taufr,xf,wfp,Tfp,wfr,Tfr,Ac,Pr,Dh,rkf,rleng
     *  ,rmuair,rNufd
      close(1)
C calculate enthalpy of inlet process air stream
      Rifp = (Cpda+wfp*Cpwv)*(Tfp-Tref)+enthvap(Tref)*wfp
      wf=wfp
      rif=rifp
C Calculate enthalpy of inlet regeneration stream
      Rifr = (Cpda+wfr*Cpwv)*(Tfr-Tref)+enthvap(Tref)*wfr
      endif
      if(ip.eq.0) then
      rmda=rmdap
      beta = taufp
      wf=wfp
      rif=rifp
      else
      rmda=rmdar
      beta = taufr-taufp
      wf=wfr
      rif=rifr
      endif
      Re = rmda*Dh/(rmuair*Ac)
      rNTUqm= Asurf/rmda
      rNTUmm = beta*rMdd/(rmda*rhop*2.*Rad)
      Tmcap = beta*RMdd*RNrev/(3600.*rmda)
      rhqfd = rNufd*rkf/Dh
      if(ist.eq.0) then
      ist=1
      rNTUq = rhqfd*rNTUqm
      rNTUm = rhqfd/(Cpda+wfp*cpwv)*rNTUmm
      a = 1.0/(rNTUq**2.+rNTUm**2.)**0.5
      b = 1.0/rNTUm
      dxmax = 2.*dmin1(a,b)
      dtmax = tmcap*dxmax
      write(*,*) ' dtmax =',dtmax,' dxmax=',dxmax
      write(*,*) 'dtmax dxmax ?'
```

```
      read(*,*) dtmax,dxmax
      write(*,10) dtmax,dxmax
      endif
      return
 10    format(1x,' dtstable=',f8.6,' dxstable=',f8.6)
      end

      subroutine XBSSTEP(xs,xtry,tau,tdid,ipss)
C program description in main program
      implicit double precision (a-h,o-z)
      dimension rmast(2,20),dstate(2,20),dloc(3,200),dst(2,40)
      dimension rmasav(2,20),dstsav(2,20),yerr(2,20),dlocs(3,200)
      integer nseq(9)
      external enthvap
      common /finalx/ xf
      common /bcbed/ wf,rif
      common /finalt/ taufp,taufr
      common /htcp2/ cplw,cd
      common /max/ dxmax,dtmax
      data nuse,res,eps/7,1D-6,0.01/
      data nseq(1),nseq(2),nseq(3),nseq(4),nseq(5),nseq(6)
     *  ,nseq(7),nseq(8),nseq(9)/2,4,6,8,12,16,24,32,48/
C Boundary conditions of moist air depend on temporal position
C At the axial position x=0, perform B-S step in temporal direction
      if(xs.eq.0) then
C tstart returns the desiccant state at the inlet to the
C bed (dstsav) as well as the time step that was achieved (tdid)
C and the number of steps it took (nst). Tau is the initial
C time position. Save desiccant states at prior to integration
      if(tdid.eq.0.and.ncyc.eq.0) then
      j=1
      open(7,file='icbed.dat')
 26    continue
      read(7,*,end=29) dloc(1,j),dloc(2,j),Td
      dloc(3,j) = (cd+dloc(2,j)*cplw)*(Td-273.15)+
     *  (0.2843/10.28)*(exp(-10.28*dloc(2,j))-1.0)*enthvap(Td)
      j=j+1
      goto 26
 29    continue
      dstsav(1,1)=dloc(2,1)
      dstsav(2,1)=dloc(3,1)
      kllast=j-1
      close(7)
      else
C kllast is the number of B-S steps in the axial position
C taken last time period
      do 31 j=1,kllast
      dloc(1,j)=dlocs(1,j)
      dloc(2,j)=dlocs(2,j)
      dloc(3,j)=dlocs(3,j)
 31    continue
      endif
      call tstart(dstsav,nst,tau,tdid,eps)
      write(*,500) nst,tdid,tau
C  Save moist air state at inlet to bed
      do 24 j=1,nst
      rmasav(1,j) = wf
      rmasav(2,j) = rif
 24    continue
      dlocs(1,1)= xs
```

```
      dlocs(2,1)=dstsav(1,nst)
      dlocs(3,1)=dstsav(2,nst)
      kloc=1
      endif
35    continue
C Dstsav and rmasav are the starting points for the mmid routine
C Each time the solution is reintegrated
C the starting values of the desiccant and moist air states are
C needed. These values are stored as Dstsav and masav
      do 100 i=1,9
      do 39 j=1,nst
      do 37 k=1,2
      dstate(k,j) = dstsav(k,j)
      rmast(k,j) = rmasav(k,j)
37    continue
39    continue

C MMID performs modified midpoint steps in axial direction.
C The desiccant state at x=xs from tau to tdid is dstate.
C the moist air state at x=xs from tau to tdid is rmast.
C On output, these arrays are replaced by the moist air state
C and the desiccant states at x=xs+xtry. Integration in the
C temporal direction is achieved using nst modified midpoint
C  steps to go from tau to tau+tdid.
      call mmid(rmast,dstate,xs,xtry,nseq(i),tau,tdid,nst,dloc,dst)
C extrapolation method assumes even powered error function
      xest = (xtry/nseq(i))**2.
C Perform rational function extrapolation on the moist air
C state. On output, the error yerr is returned
      call rtextr(i,xest,rmast,yerr,nst,nuse)
      errmax=0.
C scale error and find the maximum
      do 41 k=1,nst
      do 40 j=1,2
      errmax=dmax1(errmax,dabs(yerr(j,k)/rmast(j,k)))
40    continue
41    continue
C scale error to desired accuracy
      errmax=errmax/eps
C if solution has converged, save values
     if(errmax.lt.1.) then
     write(*,600) xs+xtry,nseq(i)
C Desiccant state at tau+tdid is saved. This is needed for
C startup of the next time step
      do 42 j=1,nseq(i)
      kloc=kloc+1
      dlocs(1,kloc)=dlocs(1,kloc-1)+xtry/nseq(i)
      dlocs(2,kloc)=dst(1,j)
      dlocs(3,kloc)=dst(2,j)
42    continue
C if outlet face has been reached indice is kllast
      if((xs+xtry+res).ge.xf) then
      write(1,400) xs+xtry,real(ncyc)+tau,rmast(1,nst)
     *  ,rmast(2,nst)
      kllast=kloc
C test for end of process period
        if(dabs(tau-taufp).le.res) then
C change inlet air to regeneration stream
          ip=1
          call syspar(ip)
```

```
            tdid=dtmax
C Call subroutine which reverses direction
            call REV(dlocs,kllast)
            do 43 k=1,2
            dstate(k,1) = dlocs(k+1,1)
 43          continue
            endif
C test for end of regeneration period
          if(dabs(tau-taufr).le.res) then
C Reverse integration direction
          call REV(dlocs,kllast)
C store the calculated bed boundary condition
          do 48 j=1,kllast
          write(2,*) dlocs(1,j),dlocs(2,j),dlocs(3,j)
 48        continue
C change inlet air to process stream
            ip=0
            call SYSPAR(ip)
C Call subroutine to guess PSS boundary condition
            ncyc=ncyc+1
            call BCCONV(dlocs,dloc,kllast,relerr,ncyc)
C Store the guessed boundary condition
            do 50 j=1,kllast
            write(2,*) dlocs(1,j),dlocs(2,j),dlocs(3,j)
 50          continue
           if(relerr.lt.1.) ipss=1
            write(*,250) relerr,ncyc
            write(2,*) relerr,ncyc
            do 58 k=1,2
            dstate(k,1) = dlocs(k+1,1)
 58          continue
          endif
        endif
C save these values as they will be the new starting
C point for the mmid routine
        do 65 j=1,nst
        do 60 k=1,2
        dstsav(k,j) = dstate(k,j)
        rmasav(k,j) = rmast(k,j)
 60      continue
 65      continue
        goto 160
      endif
 100    continue
 110    continue
C if here, solution has not converged by nsteps=48
      write(*,*) ' xbsstep failure'
      ipss=1
      goto 35
 160    continue
      return
 250    format(1x,' pss error=',f8.3,' ncyc=',i3)
 300    format(1x,' x = ',f6.4,'  # steps=',i3)
 400    format(1x,f5.3,1x,f6.3,2(1x,f9.5))
 500    format(1x,' # of steps =',i3,' dtau =',
     *   f7.5,' time =',f7.5)
 600    format(1x,f7.5,1x,i3)
      end

      SUBROUTINE REV(dlocs,k)
```

```
      implicit double precision (a-h,o-z)
      common /finalx/ xf
      dimension dlocs(3,250),sw(3,250)
C Reverses integration direction
          do 55 j=1,k
          sw(1,j) = xf-dlocs(1,k-j+1)
          do 54 n=2,3
          sw(n,j) = dlocs(n,k-j+1)
 54        continue
 55        continue
          do 57 j=1,k
          do 56 n=1,3
          dlocs(n,j) = sw(n,j)
 56        continue
 57        continue
       return
       end

       subroutine TAUSTEP(rmast,taus,ttot,nst,dstate,dloc,x)
       implicit double precision (a-h,o-z)
C This subroutine performs modified midpoint steps to
C determine the desiccant state at positions
C in the temporal direction. The moist air state at
C all temporal positions is known, the desiccant state
C at time=taus is input as dstate(1,1) and dstate(2,1).
C the routine goes from taus to taus+ttot using nst steps.
C On output, the dstate array has been solved from
C dstate(i,1) through dstate(i,nst+1)
       dimension rmast(2,20),dstate(2,20),temp1(2,1)
       dimension eqst(2,1),dPdx(2,1),temp2(2,1),dloc(3,250)
       common /mcap/ tmcap
       data res /1E-6/
       dtau = ttot/(nst-1)
C find correct initial desiccant state
       i=2
 5     continue
       if(x.le.(dloc(1,i)+res).and.(x+res).ge.dloc(1,i-1)) then
       dstate(1,1) = (dloc(2,i)-dloc(2,i-1))/(dloc(1,i)-
     *   dloc(1,i-1))*(x-dloc(1,i))+dloc(2,i)
        dstate(2,1) = (dloc(3,i)-dloc(3,i-1))/(dloc(1,i)-
     *   dloc(1,i-1))*(x-dloc(1,i))+dloc(3,i)
       else
       i=i+1
       if(i.gt.250) then
       write(*,*) x,(dloc(1,j), j=1,i)
       endif
       goto 5
       endif
C the subroutine para finds the state of the
C hypothetical moist air layer in equilibrium with
C the desiccant. The desiccant state and the moist
C air state are inputs. Eqst is the output
       call para(dstate,rmast,1,eqst,x)
C Derivs evaluates the right hand side of the
C rate equations.
       call derivs(rmast,eqst,1,dPdx,x)
C mmm step
       dstate(1,2) = dstate(1,1) - dtau*dPdx(1,1)/tmcap
       dstate(2,2) = dstate(2,1) - dtau*dPdx(2,1)/tmcap
C the temporary variables are needed to pass to para and derivs
```

```
      do 15 i=1,2
      temp1(i,1) = dstate(i,2)
      temp2(i,1) = rmast(i,2)
 15    continue
      tau = taus+dtau
      call para(temp1,temp2,1,eqst,x)
      call derivs(temp2,eqst,1,dPdx,x)
      dt2 = 2.*dtau
C the second through nst-1 MMM steps
      do 30 j=2,nst-1
      dstate(1,j+1) = dstate(1,j) - dt2*dPdx(1,1)/tmcap
      dstate(2,j+1) = dstate(2,j) - dt2*dPdx(2,1)/tmcap
      do 25 i=1,2
      temp1(i,1) = dstate(i,j+1)
      temp2(i,1) = rmast(i,j+1)
 25    continue
      tau = tau+dtau
      call para(temp1,temp2,1,eqst,x)
      call derivs(temp2,eqst,1,dPdx,x)
 30    continue
C the last mmm step
      dstate(1,nst) = 0.5*(dstate(1,nst) +
     *           dstate(1,nst-1) - dtau*dPdx(1,1)/tmcap)
      dstate(2,nst) = 0.5*(dstate(2,nst) +
     *           dstate(2,nst-1) - dtau*dPdx(2,1)/tmcap)
 100   continue
      return
      end

      subroutine TBSSTEP(tau,ttry,dstate,nstmax,eps)
C Bulirsch-Stoer method for temporal direction at inlet to bed
C Inputs are tau-temporal position, ttry-time step to be
C attempted. Outputs are tdid-the time step which was achieved,
C tnext-the suggested next time step, dstate-the desiccant
C state at the inlet to the bed from tau to tau+tdid, and
C nstmax-the number of steps it took to achive this.
      implicit double precision (a-h,o-z)
      dimension dstate(2,20),temp(2,1),yerr(2,1)
      integer nseq(9)
      data nseq(1),nseq(2),nseq(3),nseq(4),nseq(5),nseq(6)
     * ,nseq(7),nseq(8),nseq(9) /2,4,6,8,12,16,24,32,48/
      data nuse /7/
 1     continue
      do 30 j=1,9
C perform modified midpoint steps from tau to tau+ttry
C using an increasing number of steps; nseq(j)
      call mmd(dstate,tau,ttry,nseq(j))
      xest = (ttry/nseq(j))**2.
      do 10 i=1,2
      temp(i,1) = dstate(i,nseq(j)+1)
 10    continue
C perform rational function extrapolation on the
C solution and assess its error based on the
C results of previous mmm steps
      call rtextr(j,xest,temp,yerr,1,nuse)
      errmax = 0.
C scale error and find its maximum
      do 12 i=1,2
      errmax = dmax1(errmax,dabs(yerr(i,1)/temp(i,1)))
 12    continue
```

```
C scale error according to desired accuracy
      errmax = errmax/eps
C test for convergence
      if(errmax.lt.1.) then
      nstmax = nseq(j)
      goto 40
      endif
 25    continue
 30    continue
      write(*,*) 'Tau BSSTEP failure'
      goto 1
 40    continue
      return
      end

      subroutine TSTART(dstate,nstmax,tau,ttry,eps)
C Tstart is the routine which controls the B-S routine
C in the time direction at the inlet to the bed. Tau is
C the input. dstate is the output array of the bed state
C from dstate(i,1) to dstate(i,nstmax+1) at x=0.
C which corresponds to
C time=tau to tau+ttry. The number of
C steps the algorithm needed for convergence is nstmax
      implicit double precision (a-h,o-z)
      dimension dstate(2,20),dstsav(2,1)
      common /icbed/ Wd,rId
      common /finalt/ taufp,taufr
      common /max/ dxmax,dtmax
      data res/1E-6/
C the first time through, the desiccant state is the initial
C             assumed bed state
C if regeneration or process period has just begun,
C        dstate is the proper input
C and if new rotation has begun, tau finish=tauprocess period
      if((tau-res).lt.0.0.and.(tau+res).gt.0.0) then
      tfin=taufp
      ttry=dtmax/2.
      goto 11
      endif
      if((tau-res).lt.taufp.and.(tau+res).gt.taufp) then
      ttry=dtmax/2.
      goto 11
      endif
C otherwise dstsav is the initial desiccant state
      do 10 i=1,2
      dstate(i,1) = dstsav(i,1)
 10    continue
 11    continue
C call the B-S routine for the temporal direction. Input is
C tau-starting position. ttry-time step to ttry. eps-rel accuracy
C dstate(1,1) and dstate(2,1) which are the initial conditions
C output is the desiccant state at positions from tau to
C tau+ttry using nstmax steps.
      call TBSSTEP(tau,ttry,dstate,nstmax,eps)
      tau=tau+ttry
C Save the converged desiccant state at x=0 and tau=tau+ttry
C as dstsav will be the initial condition next time.
      do 15 i=1,2
      dstsav(i,1) = dstate(i,nstmax+1)
 15    continue
```

```
      nstmax = nstmax+1
C do not integrate past tauf, change final time
C to end of regeneration period if process period has ended
      if((tau+ttry).ge.tfin) then
      ttry = tfin-tau
      tfin=taufr
      else
      ttry=dtmax
      endif
      return
      end

      subroutine MMD(dstate,taus,dttot,nstep)
C modified midpoint method for temporal direction
C at inlet to desiccant bed
C Inputs are dstate(1,1), dstate(2,1),
C taus-starting time position, dttot-total time
C step to be taken, and nstep-number of steps to take
C Output is dstate - the desiccant state at each position
C from taus to taus+dttot
      implicit double precision (a-h,o-z)
      common /bcbed/ wf,rif
      common /mcap/ tmcap
      dimension dstate(2,20),rmast(2,1),temp(2,1),dPdx(2,1)
      dimension eqst(2,1)
      data xst/0./
      nst=1
C moist air state is inlet moist air state
      rmast(1,1) = wf
      rmast(2,1) = rif
C find equilibrium state
      call para(dstate,rmast,1,eqst,xst)
C find right hand side of rate equations
      call derivs(rmast,eqst,1,dPdx,xst)
      dtau = dttot/nstep
      dstate(1,nst+1) = dstate(1,nst) - dtau*dPdx(1,1)/tmcap
      dstate(2,nst+1) = dstate(2,nst) - dtau*dPdx(2,1)/tmcap
      do 30 i=1,2
      temp(i,1) = dstate(i,nst+1)
30    continue
      nst=nst+1
      tau = taus + dtau
      call para(temp,rmast,1,eqst,xst)
      call derivs(rmast,eqst,1,dPdx,xst)
      dt2 = 2.*dtau
      do 40 j=2,nstep
      dstate(1,nst+1) = dstate(1,nst) - dt2*dPdx(1,1)/tmcap
      dstate(2,nst+1) = dstate(2,nst) - dt2*dPdx(2,1)/tmcap
      do 35 i= 1,2
      temp(i,1) = dstate(i,nst+1)
35    continue
      nst = nst + 1
      tau = tau + dtau
      call para(temp,rmast,1,eqst,xst)
      call derivs(rmast,eqst,1,dPdx,xst)
40    continue
      dstate(1,nst) = 0.5*(dstate(1,nst) + dstate(1,nst-1)
     *              - dtau*dPdx(1,1)/tmcap)
      dstate(2,nst) = 0.5*(dstate(2,nst) + dstate(2,nst-1)
     *              - dtau*dPdx(2,1)/tmcap)
```

```
      return
      end

      subroutine MMID(ym,dstate,xs,xtot,nstep,tau,tdid,knt,dloc
     * ,dst)
C MMID takes modified midpoint steps in the axial direction.
C Inputs are xs-axial starting position, xtot-total axial
C distance, nstep-number of steps to take
C ym-moist air state at x=xs from tau to tau+tdid,
C dstate-desiccant state at x=xs from tau to tau+tdid,
C (corresponds to ym)
C tau-starting time position, tdid-ending time position
C knt-number of time steps. Output is ym-moist air state
C at x=xs+xtot from tau to tau+tdid and dstate-desiccant state
C at x=xs+xtot from tau to tau+tdid.
      implicit double precision (a-h,o-z)
      dimension dstate(2,20),ym(2,20),yn(2,20),dloc(3,250)
      dimension eqst(2,20),dpdx(2,20),dst(2,40)
      dx = xtot/nstep
C find hypothetical moist air state in equilibrium with
C the desiccant
      call para(dstate,ym,knt,eqst,xs)
C  evaluate right hand side of rate equations
      call derivs(ym,eqst,knt,dpdx,xs)
      x=xs+dx
C MMM step
      do 20 j=1,knt
      do 10 i=1,2
      yn(i,j) = dx*dpdx(i,j) + ym(i,j)
 10    continue
 20    continue
 22    continue
C take time steps at x=xs+dx from time=tau to tau+tdid
C using knt steps to find desiccant state at this axial
C location.
      call taustep(yn,tau,tdid,knt,dstate,dloc,x)
      do 23 i=1,2
      dst(i,1) = dstate(i,knt)
 23    continue
      call para(dstate,yn,knt,eqst,x)
      call derivs(yn,eqst,knt,dpdx,x)
      dx2=2.*dx
C MMM step #2 though nstep-1
      do 30 n=2,nstep
      do 27 j=1,knt
      do 25 i=1,2
      sw = dx2*dpdx(i,j) + ym(i,j)
      ym(i,j) = yn(i,j)
      yn(i,j) = sw
 25    continue
 27    continue
      x = x + dx
      call taustep(yn,tau,tdid,knt,dstate,dloc,x)
      do 28 i=1,2
      dst(i,n) = dstate(i,knt)
 28    continue
      call para(dstate,yn,knt,eqst,x)
      call derivs(yn,eqst,knt,dpdx,x)
 30    continue
C Last MMM step
```

```
      do 45 j=1,knt
      do 40 i=1,2
      ym(i,j) = 0.5*(dx*dpdx(i,j) + ym(i,j) + yn(i,j))
40     continue
45     continue
      return
      end
```

```
      subroutine DERIVS(rmast,reqst,kno,dPdx,x)
      implicit double precision (a-h,o-z)
C Property subroutines- Contains heat transfer
C coefficient for spherical particles in a packed bed
C
C Programs DERIVS, PWVSAT, ENTHVAP, RTEXTR, RHQEL
C           contained in psubs.for
C
C Subroutine computes right hand side of rate equation
C given the moist air state (rmast) and the hypothetical
C equilibrium state (eqst), kno is the size of the input
C arrays. dPdx(i,1) through dPdx(i,kno) is the output.
      dimension rmast(2,20),reqst(2,20),dpdx(2,20)
      external enthvap
      external rhqel
      common /htcap/ cpda,cpwv
      common /xfer/ rNTUqm,rNTUmm,rhqfd
      common /ref/ Tref
      common /mcap/ tmcap
      do 10 j=1,kno
C find tf given wf and if
      cpm = cpda+rmast(1,j)*cpwv
      tf = (rmast(2,j)-rmast(1,j)*enthvap(Tref))/cpm + Tref
      dPdx(1,j) = (1.7/1.6)*rhqfd*rNTUmm/Cpm*(reqst(1,j)-rmast(1,j))
      dPdx(2,j) = rhqfd*rNTUqm*(reqst(2,j)-tf)
     *   + dPdx(1,j)*enthvap(tf)
 10    continue
      return
      end

      subroutine RTEXTR(iest,xest,yest,dy,kno,nuse)
      implicit double precision (a-h,o-z)
C Diagonal rational function extrapolation
      dimension x(11),yest(2,20),yz(2,20),dy(2,20),d(20,20,7)
      dimension fx(7)
      x(iest)=xest
      if(iest.eq.1) then
      do 10 j=1,kno
      do 5 i=1,2
      yz(i,j) = yest(i,j)
      d(i,j,1)=yest(i,j)
      dy(i,j)=yest(i,j)
 5     continue
 10    continue
      else
      m1=min(iest,nuse)
      do 11 k=1,m1-1
      fx(k+1) = x(iest-k)/xest
 11    continue
      do 15 j=1,kno
      do 14 i=1,2
      yy=yest(i,j)
      v=d(i,j,1)
      c=yy
      d(i,j,1)=yy
      do 13 k=2,m1
      b1=fx(k)*v
      b=b1-c
      if(b.ne.0) then
      b=(c-v)/b
```

```
      ddy=c*b
      c=b1*b
      else
      ddy=v
      endif
      if(k.ne.m1) v=d(i,j,k)
      d(i,j,k) = ddy
      yy=yy+ddy
 13    continue
      dy(i,j) = ddy
      yz(i,j) = yy
 14    continue
 15    continue
      endif
      do 20 j=1,kno
      do 17 i=1,2
      yest(i,j) = yz(i,j)
 17    continue
 20    continue
      return
      end

      function PWVSAT(temp)
      implicit double precision (a-h,o-z)

C Finds the saturation pressure of water vapor given temp.
C Goff correlation: good for -50C to 100C
C Pwvsat is in atmospheres
      real a,b,c,d,e,f,g,gz,thet
      data a,b,c,d,e,f,g /10.79586,5.02808,1.50474E-4,
     * -8.29692,0.42873E-3,4.76955,-2.2195983/
C test to see if error will occur here
      thet = 273.15/temp
      gz = a*(1.0-thet)+b*log10(thet)+c*(1.0-10.**(d*(1./thet
     *-1.)))+e*(10.**(f*(1.-thet))-1.0)+g
      pwvsat = exp(gz*log(10.))
      return
      end

      function ENTHVAP(Temp)
      implicit double precision (a-h,o-z)

C Function to compute the enthalpy of vaporization
C at saturation
      external pwvsat
      data Rmwv,vf1,vf2,vf3/0.46152,3.90638E-9,0.562034E-8,
     * 0.999406E-4/
       data a,b,c,d,e,f,g/10.79586,5.02808,1.50474E-4,
     *  -8.29692,0.42873E-3,4.76955,-2.2195983/
      thet = 273.15/temp
      dthdT = -273.15*(Temp)**(-2.0)
      ac = -a*dthdt
      bc = (b/log(10.))*(dthdT/thet)
      cc = c*d*log(10.0)*(dthdT/thet**(2.0))*10.0**(d*(1.0/thet-1.0))
      ec = -e*f*log(10.0)*thet*dthdT*10.0**(f*(1.0-thet))
      dlnpsdT = log(10.0)*(ac+bc+cc+ec)
      dPwsdt = dlnpsdT*pwvsat(temp)
      vf = vf1*(Temp-273.15)**2 + vf2*(Temp-273.15) + vf3
      enthvap = Rmwv*dlnpsdT*(Temp)**(2.0)+(Temp)*vf*dpwsdT
      return
```

```
      end

        function RHQEL(xs)
        implicit double precision (a-h,o-z)

C calculates convective heat transfer coefficient
C based thermal entry length for parallel plates
        common /thprop/ Re,Pr,Dh,rkf,rleng
        xbar=(xs*rleng)/(Dh*Re*Pr)
        if(xbar.le.2.5E-4) rNu=19.72
        if(xbar.gt.2.5E-4.and.xbar.le.2.5E-3) rNu=-4.34178E+03
     * *(xbar-2.5E-3)+9.951
        if(xbar.gt.2.5E-3.and.xbar.le.0.01) rNu=-294.667*(xbar-.01)
     * +7.741
        if(xbar.gt.0.01.and.xbar.le.0.015) rNu=-31.8*(xbar-.015)
     * +7.582
        if(xbar.gt.0.015.and.xbar.le.0.025) rNu=-3.9*(xbar-.025)
     * +7.543
        if(xbar.gt.0.025.and.xbar.lt.0.05) rNu=-.08*(xbar-.05)
     * +7.541
        if(xbar.ge.0.05) rNu=7.54072
        rhqel=rNu*rkf/Dh
        return
        end
```

```
      subroutine PARA(dstate,rmast,neval,eqst,xs)
      implicit double precision (a-h,o-z)
C
C Subroutines in this program contain properties of regular
C density silica gel grade 01. Desiccant diffusivity is not constant
C and the adsorption isotherm and heat of adsorption as fitted to
C             available data by Peseran
C
C This subroutine finds (we,Te) given Wd,Id, and wf for
C regular density silica gel using the
C parabolic profile assumption model
      dimension dstate(2,20),eqst(2,20),rmast(2,20)
      external rtsec
      external rhqel
      common /totp/ Ptotal
      common /parp/ Rad,Deff,rhop
      common /htcap/ cpda,cpwv
      common /xfer/ rNTUqm,rNTUmm,rhqfd
      common /ppr/ a2
      data xacc1,xacc2,eqstl/0.1,1E-5,.02/
      data A,B,C,D,F /.0078,.05759,24.16554,124.478,204.226/
C secant method is used to find the temperature
      do 10 j=1,neval
      niter=1
      eqst(2,j) = rtsec(dstate(1,j),dstate(2,j),xacc1)
C First guess
      if(j.gt.1) eqstl = eqst(1,j-1)
C Resubstitution loop to solve for a2
      if(dstate(1,j).lt.0.05) rHads=-12400*dstate(1,j)+3500
      if(dstate(1,j).ge.0.05) rHads=-1400*dstate(1,j)+2950
      Dseff= 4.48E-6*exp(-0.974E-3*rHads/eqst(2,j))/2.8
 5    continue
C once a2 is known, the humidity ratio of the moist
C air in equilibrium with the desiccant is found explicitly
C from the adsorption isotherm relationship.
      cpm = cpda+eqstl*cpwv
C Spherical Case
      rcoeff= -(1.7/1.6)*(rhqfd/cpm)*Rad/(2*rhop*Dseff)
C Planar Case
C      rcoeff= -(rhqfd/cpm)*Rad/(rhop*Dseff)
      a2 = rcoeff*(eqstl-rmast(1,j))
C Planar Case
C      y0 = dstate(1,j)+2.*a2/3.
C Spherical Case
      y0 = dstate(1,j)+0.4*a2
      RHE = A - B*y0 + C*y0**2 - D*y0**3 + F*y0**4
      pwv = pwvsat(eqst(2,j))*RHE
      eqst(1,j) = 0.62198*pwv/(Ptotal-Pwv)
      relerr = abs(eqstl-eqst(1,j))
      if(relerr.lt.xacc2) then
      goto 10
      else
      eqstl = eqst(1,j)
      niter=niter+1
      endif
      goto 5
 10   continue
      return
      end
```

```
      function rtsec(Wd,rid,xacc)
      implicit double precision (a-h,o-z)
C Root secant method
      common /htcp2/ cplw,cd
      data niter,tm1,tm2 /30,283.15,373.15/
      rK1 = cd + Wd*cplw
      if(Wd.lt.0.05) rK2 = -12400*Wd**2/2.+3500*Wd
      if(Wd.ge.0.05) rK2 = -1400*Wd**2/2.+2950*Wd
      rhfg1 = enthvap(Tm1)
      rhfg2 = enthvap(Tm2)
      fl = rid - rK1*(Tm1-273.15)- Wd*rhfg1+rK2
      f = rid - rK1*(Tm2-273.15)- Wd*rhfg2+rK2
      if(abs(fl).lt.abs(f)) then
      rtsec=tm1
      tml=tm2
      sw=fl
      fl=f
      f=sw
      else
      tml=tm1
      rtsec=tm2
      endif
      do 10 j=1,niter
      dtemp = (Tml-rtsec)*f/(f-fl)
      tml=rtsec
      fl=f
      rtsec=rtsec+dtemp
      rhfg = enthvap(rtsec)
      f = rid - rK1*(rtsec-273.15) - Wd*rhfg+rK2
      if(abs(dtemp).lt.xacc.or.f.eq.0) goto 20
10    continue
      write(*,*) 'no. of iterations exceeded'
20    continue
      tm1=rtsec
      return
      end
```

```
      subroutine PARA(dstate,rmast,neval,eqst,xs)
      implicit double precision (a-h,o-z)
C Subroutines in this program contain properties of regular
C density silica gel. Constant desiccant diffusivity is assumed
C Close and Banks heat of adsorption is used
C Clausius-Clayperon is used for adsorption isotherm
C
C This subroutine finds (we,Te) given Wd,Id, and wf for
C regular density silica gel using the
C parabolic profile assumption model
      dimension dstate(2,20),eqst(2,20),rmast(2,20)
      external rtsec
      external rhqel
      common /totp/ Ptotal
      common /parp/ Rad,Deff,rhop
      common /htcap/ cpda,cpwv
      common /xfer/ rNTUqm,rNTUmm,rhqfd
      common /ppr/ a2
      data xacc1,xacc2,eqstl/0.1,1D-3,.02/
C secant method is used to find the temperature
      do 10 j=1,neval
      niter=1
      eqst(2,j) = rtsec(dstate(1,j),dstate(2,j),xacc1)
C First guess
      if(j.gt.1) eqstl = eqst(1,j-1)
C Resubstitution loop to solve for a2
 5    continue
C once a2 is known, the humidity ratio of the moist
C air in equilibrium with the desiccant is found explicitly
C from the adsorption isotherm relationship.
      cpm = cpda+eqstl*cpwv
C Spherical Case
C      rcoeff= -(rhqfd/cpm)*Rad/(2.*rhop*Deff)
C Planar Case
      rcoeff= -(rhqfd/cpm)*Rad/(rhop*Deff)
      a2 = rcoeff*(eqstl-rmast(1,j))
C Planar Case
      y0 = dstate(1,j)+2.*a2/3.
C Spherical Case
C      y0 = dstate(1,j)+0.4*a2
      rhstar = 1.0+0.2843*dexp(-10.28*y0)
      y1 = (2.112*y0)**rhstar
      y2 = (29.91*pwvsat(eqst(2,j)))**(rhstar-1)
      pwv = pwvsat(eqst(2,j))*y1*y2
      eqst(1,j) = 0.62198*pwv/(Ptotal-Pwv)
      relerr = 2.*abs(eqstl-eqst(1,j))/(eqstl+eqst(1,j))
      if(relerr.lt.xacc2) then
      goto 10
      else
      eqstl = eqst(1,j)
      niter=niter+1
      endif
      goto 5
 10   continue
      return
      end

      function rtsec(Wd,rid,xacc)
      implicit double precision (a-h,o-z)
C Root secant method
```

```
      common /htcp2/ cplw,cd
      data niter,tm1,tm2 /30,283.15,373.15/
      rK1 = cd + Wd*cplw
      rK2 = (0.2843/10.28)*(dexp(-10.28*Wd)-1.)
      rhfg1 = enthvap(Tm1)
      rhfg2 = enthvap(Tm2)
      fl = rid - rK1*(Tm1-273.15)- rK2*rhfg1
      f = rid - rK1*(Tm2-273.15)- rK2*rhfg2
      if(dabs(fl).lt.dabs(f)) then
      rtsec=tm1
      tml=tm2
      sw=fl
      fl=f
      f=sw
      else
      tml=tm1
      rtsec=tm2
      endif
      do 10 j=1,niter
      dtemp = (Tml-rtsec)*f/(f-fl)
      tml=rtsec
      fl=f
      rtsec=rtsec+dtemp
      rhfg = enthvap(rtsec)
      f = rid - rK1*(rtsec-273.15) - rK2*rhfg
      if(dabs(dtemp).lt.xacc.or.f.eq.0) goto 20
10     continue
      write(*,*) 'no. of iterations exceeded'
20     continue
      tm1=rtsec
      return
      end
```

```
      subroutine BCCONV(dstc,dstg,k,relerr,ncyc)
C Calculates PSS relative error at end of each rotation
      implicit double precision (a-h,o-z)
      dimension dstc(3,150),bcc(2,150),bcg(2,150)
      data pssacc/1D-3/
      relerr = 0.0
      do 3 j=1,k
      do 2 i=2,3
      relerr = dmax1(relerr,dabs(2.*(dstc(i,j)-bcc(i-1,j))/
     *    (dstc(i,j)+bcc(i-1,j))))
 2    continue
 3    continue
      do 10, j=1,k
      do 5, i=1,2
      bcc(i,j) = dstc(i+1,j)
 5    continue
 10   continue
      relerr = relerr/pssacc
      return
      end
```

```
      subroutine BCCONV(dstc,dstg,k,relerr,ncyc)
      real dstc(3,50), bcc(2,50), bcc1(2,50), bcc2(2,50)
C Contains convergence routines to guess the periodic steady state
C boundary conditions
      real bcg(2,50), bcg1(2,50), bcg2(2,50), smg(2,50)
      real dstg(3,50)
      data pssacc/1E-2/
      relerr = 0.0
      do 3 j=1,k
      do 2 i=2,3
      relerr = max(relerr,abs(2*(dstc(i,j)-bcc(i-1,j))/
     *   (dstc(i,j)+bcc(i-1,j))))
 2    continue
 3    continue
      do 10, j=1,k
      do 5, i=1,2
      bcc(i,j) = dstc(i+1,j)
      if(ncyc.eq.1) bcg(i,j)=dstg(i+1,j)
C     call EXP(bcc(i,j),ncyc,bcc1(i,j),bcc2(i,j))
      dstc(i+1,j) = bcc(i,j)
 5    continue
 10   continue
C call smoothing routine
C     call smcurv(dstc,k)
      relerr = relerr/pssacc
      return
      end

      SUBROUTINE LAGEXT(XG,XC,ncyc,XG1,XC1,XG2,XC2)
      data thet,dampf/.785398,0.2/

C Convergence routine by Lagrange Interpolation Method
C variables:
C     XC-new calculated state          XG-New guess (output)
C     XC1-Last calculated state        XG1-Last guess
C     XC2-2nd to last calculated value   XG2-2nd to last guess
C     XG3-3rd to last calculated value   XG3-3rd to last guess
C     ncyc-Number of revolutions

C First three times, resubstitution is used
     if(ncyc.lt.3) then
      XG2=XG1
      XC2=XC1
      XG1=XG
      XC1=XC
      XG=XC
      return
     endif

C Transform X,Y coordinate system to Zeta,Xi coordinate system
     if(icc.eq.0) then
      icc=1
      f=cos(thet)
      g=sin(thet)
     endif
     if(ncyc.ge.12) dampf=.05
     if(ncyc.ge.20) dampf=0.0
     Zeta=XG*f-XC*g
     Zeta1=XG1*f-XC1*g
     Zeta2=XG2*f-XC2*g
```

```
      Xi=XG*g+XC*f
      Xi1=XG1*g+XC1*f
      Xi2=XG2*g+XC2*f
C Calculate new Xi
      Xi = Zeta1*Zeta2*Xi/((Zeta-Zeta1)*(Zeta-Zeta2)) +
     *     Zeta*Zeta2*Xi1/((Zeta1-Zeta)*(Zeta1-Zeta2)) +
     *     Zeta*Zeta1*Xi2/((Zeta2-Zeta)*(Zeta2-Zeta1))
C Transform back to X,Y
      XT = Xi*g
      XG2=XG1
      XC2=XC1
      XG1=XG
      XC1=XC
      XG=dampf*XT+(1-dampf)*XC
      if(xg.lt.0.0) xg=xc
      return
      end

      SUBROUTINE WEGST(XG,XC,ncyc,XG1,XC1,XG2,XC2)
       data dampf/0.1/
C
C...convergence by wegstein's method
C
C...summary dictionary
C   xc, xg on input:  calculated and guessed values
C       xg on output: new guess
C
C   ncyc:        number of revolutions
C
C   xc1, xg1:    last values
C
C...begin routine processing
C
C...on first call, resubstitution
C
      IF (ncyc.eq.1)  THEN
        XG1 = XG
        XC1 = XC
        XG = XC
        RETURN
      ENDIF
C
      XT = (XG1*XC-XC1*XG)/(XG1-XG+XC-XC1)
      XG1 = XG
      XC1 = XC
      XG = dampf*XT +(1-dampf)*XC
      if(xg.lt.0.0) XG=XC
      if((xg/xc).gt.20) XG=XC
      RETURN
      END

      SUBROUTINE LSELIN(XG,XC,ncyc,XG1,XC1,XG2,XC2)
       data dampf,npts/1.,3/

C Convergence routine by LSE line fit
C     XC-new calculated state            XG-New guess (output)
C     XC1-Last calculated state          XG1-Last guess
C     XC2-2nd to last calculated value     XG2-2nd to last guess
C     ncyc-Number of revolutions
      if(ncyc.ge.35) dampf=0.
```

```
C First two times, resubstitution is used
      if(ncyc.lt.npts) then
       XG2=XG1
       XC2=XC1
       XG1=XG
       XC1=XC
       XG=XC
       return
      endif

      Xgbar=(xg+xg1+xg2)/npts
      Xcbar=(xc+xc1+xc2)/npts
      Bnum = xg*xc + xg1*xc1 + xg2*xc2 - npts*xgbar*xcbar
      Bden = xg**2 + xg1**2 + xg2**2 - npts*xgbar**2
      B = Bnum/Bden
      A = Xcbar-B*Xgbar
      XT = A/(1-B)
      XG2=XG1
      XC2=XC1
      XG1=XG
      XC1=XC
      XG=dampf*XT+(1-dampf)*XC
      if(xg.lt.0.0) xg=xc
      if(((xg-xg1)/(xg1-xg2)).gt.10) xg=xg1+(xg1-xg2)
      return
      end

      SUBROUTINE NRAPH(XG,XC,ncyc,XG1,XC1,XG2,XC2)
C Newton Raphson in one dimension
      if(ncyc.eq.1) then
       F = 2*(XG-XC)/(XG+XC)
       XG1=XG
       XC1=XC
       XG=XC
       return
       endif
C Newton Raphson method in one dimension
       F1 = 2*(XG1-XC1)/(XG1+XC1)
       F = 2*(XG-XC)/(XG+XC)
       DFDX = (F1-F)/(XG1-XG)
       DX = F/DFDX
       XT = XG - DX
       XG2=XG1
       XG1=XG
       XC1=XC
       XG=XT
       if(xg.lt.0.0) xg=xc
       if(((xg-xg1)/(xg1-xg2)).gt.10) xg=xg1+(xg1-xg2)
       return
       end

       subroutine QUADR(X,NCYC,X1,X2)
C Fits the last three points to a quadratic as a
C function of N
       if(ncyc.lt.15) then
       X2=X1
       X1=X
       return
      endif
```

```
      Ncyc1=Ncyc-1
      Ncyc2=Ncyc-2
      D = Ncyc*Ncyc2+Ncyc1*Ncyc2-Ncyc*Ncyc1-Ncyc2**2
      C =  ((X-X2) + (X1-X)*(Ncyc2-Ncyc)/(Ncyc1-Ncyc))/D
      B =  (X1-X)/(Ncyc1-Ncyc)-C*(Ncyc+Ncyc1)
      A = X - B*Ncyc - C*Ncyc**2
      XT = A - B**2/(2*C)
      X2=X1
      X1=X
      if(XT.lt.0) return
      X = XT
      return
      end

      subroutine EXP(X3,Ncyc,X2,X1)
C Exponential curve fit
      rn1 = real(ncyc)/2.0
      rn2 = real(ncyc/2)
      if(ncyc.lt.8.or.(rn1-rn2).gt.0.1) then
      X1=X2
      X2=X3
      Return
      endif
      X0 = (X1*X3-X2**2)/(X1+X3-2*X2)
      X1=X2
      X2=X3
      X3=X0
      return
      end
```

```
      subroutine smcurv(dstg,k)
C Subroutine smooths the guessed bed condition
      real dstg(3,50)
      do 100 j=3,k-2
      do 50 i=2,3
      iavg1=0
      iavg2=0
      iavg3=0
      d1 = (dstg(i,j-2)-dstg(i,j-1))/(dstg(1,j-2)-dstg(1,j-1)
     * )*(dstg(1,j)-dstg(1,j-1))+dstg(i,j-1)
      d2 = (dstg(i,j-1)-dstg(i,j+1))/(dstg(1,j-1)-dstg(1,j+1)
     * )*(dstg(1,j)-dstg(1,j-1))+dstg(i,j-1)
      d3 = (dstg(i,j+2)-dstg(i,j+1))/(dstg(1,j+2)-dstg(1,j+1)
     * )*(dstg(1,j)-dstg(1,j+1))+dstg(i,j+1)
      if((d1/dstg(i,j)).lt.0.85.or.(d1/dstg(i,j)).gt.1.15)
     * iavg1=1
      if((d2/dstg(i,j)).lt.0.85.or.(d2/dstg(i,j)).gt.1.15)
     * iavg2=1
      if((d3/dstg(i,j)).lt.0.85.or.(d3/dstg(i,j)).gt.1.15)
     * iavg3=1
      if(iavg1.eq.1.and.iavg2.eq.1.and.iavg3.eq.1) dstg(i,j) = D2
50     continue
100    continue
      return
      end
```